

Models of Dysbiosis to Investigate the Role of SOCS3 in Intestinal Inflammation



Ciarra McGoran

Submitted for the degree of Research Masters

August 2021

Acknowledgements

First and foremost, I would like to extend my gratitude to Dr Rachael Rigby for the opportunity to work alongside her and for being a friend to me, as well as a supervisor. I would also like to acknowledge Jayde Whittingham-Dowd and Elisabeth Shaw for their help and guidance in the laboratory, and the Rosemere Cancer Foundation for funding this project. Thank you to Fion Lo for the fantastic company and amazing memories both in and out of the lab. Although we met under unusual circumstances, I know I have found a friend for life. Finally, my most sincere gratitude goes to my best friend, Alice; my boyfriend, James; my brother, Conall; and my parents for their continued support and belief in me. I could not have done this without you.

Abstract

Suppressor of cytokine signalling 3 is an important protein in the maintenance and homeostasis of the intestinal epithelium. Its dysregulation is associated with severe disease including inflammatory bowel disease and colorectal cancer. It is therefore a tightly regulated protein, its oscillatory nature thought to be regulated by both transcriptional and post-translational mechanisms such as proteasomal degradation and autophagy. The intestinal microbiota has been implicated in intestinal inflammation, inflammatory bowel disease and inflammation-associated cancer. We used two models of dysbiosis in both human resection specimens and cultured human intestinal epithelial cells. Both models are used to investigate the impact of dysbiosis on inflammatory signalling pathways and autophagy. In addition, we used transgenic cells to investigate the impact of SOCS3 expression upon these pathways. Our results suggest that dysbiosis may stimulate autophagy, but not chronic inflammation. Meanwhile, SOCS3 modulation did not impact inflammatory signalling pathways, but may be playing a role in the modulation of autophagy.

Declaration

I, Ciarra McGoran, confirm that the work presented in this thesis is my own and has not been submitted in substantially the same form for the award of a higher degree elsewhere. Where information has been derived from other sources, I confirm this has been indicated in the thesis.

Contents

1. Introduction.....	1
1.1. Colorectal Cancer.....	1
1.1.1. Aetiology.....	2
1.1.2. Diagnosis.....	4
1.2. Inflammatory Bowel Disease.....	7
1.2.1. Genetics.....	7
1.2.2. The Intestinal Microbiota.....	8
1.3. The intestine.....	10
1.3.1. Intestinal Stem Cells.....	11
1.3.2. Crypt Base Columnar Cells.....	11
1.3.3. +4 Cells.....	13
1.3.4. Intestinal Stem Cells and Cancer.....	14
1.3.5. Regulation of Intestinal Stem Cell Populations.....	15
1.4. Cell Signalling in the Intestinal Epithelium.....	17
1.4.1. Cytokines.....	17
1.4.2. The JAK/STAT Pathway.....	17
1.4.3. Regulation of JAK/STAT Signalling.....	18
1.4.4. STAT3 and Intestinal Homeostasis.....	19
1.4.5. SOCS3 and Intestinal Homeostasis.....	20
1.4.6. IRF3 in Viral Infection.....	22
1.4.7. STING in Defence Against Microbes.....	25
1.4.8. Autophagy.....	29
1.5. Project Aims.....	34

2. Materials and Methods.....	35
2.1. Cell Lines.....	35
2.1.1. Maintenance.....	35
2.1.2. Plating Cells.....	35
2.1.3. Transfecting Cells.....	36
2.1.4. Cell Lysis.....	37
2.2. Western Blot.....	38
2.3. qPCR Analysis.....	39
2.3.1. mRNA Extraction.....	39
2.3.2. Reverse Transcription.....	39
2.3.3. qPCR.....	40
2.4. Intestinal Tissue Homogenisation.....	41
2.5. Bradford Assay.....	41
2.6. Measurement of Villous Height.....	42
3. The Impact of Microbiome Manipulation on Signalling in the Human Intestine.....	43
3.1. Results.....	43
4. The Impact of SOCS3 on Microbiome Signalling in Human Intestinal Epithelial Cells.....	47
4.1. Results.....	47
5. Discussion.....	54
5.1. Summary of Findings.....	54

5.2. Clinical Relevance.....	54
5.3. Defunctioned Bowel Shows no Biochemical Signs of Inflammation.....	55
5.4. Autophagy is Implicated in Atrophy of the Defunctioned Bowel.....	56
5.5. The link between STING and SOCS3 expression.....	57
5.6. Limitations.....	59
5.6.1. The Reliability of LC3B as a Measure of Autophagic Flux.....	59
5.6.2. The Impact of SOCS3 Regulation by Autophagy.....	60
5.7. Future Direction.....	62
5.8. Conclusion.....	63
6. Appendix.....	64
7. References.....	57

List of tables and figures

Table 1.1. Newly diagnosed cancer cases in 2018, ranked by incidence.....	1
Figure 1.1. Most common cancers amongst UK men and women in 2016.....	2
Figure 1.2. Organisation of the intestinal epithelium.....	10
Figure 1.3. The maturation of pluripotent CBC cells to form mature post-mitotic columnar and mucous cells.....	12
Figure 1.4. The JAK/STAT pathway.....	18
Figure 1.5. The structure of SOCS3.....	21
Figure 1.6. Activation of the cGAS-STING pathway in response to cytosolic dsDNA.....	26
Figure 1.7. Type 1 IFN signalling culminating in upregulation of antiviral genes via the JAK/STAT pathway.....	28
Figure 1.8. Degradation of cytosolic components by micro- and macroautophagy.....	31
Table 2.1. Antibodies used in western blot and their product numbers.....	38
Figure 2.1. Measurement of villous height.....	42
Figure 3.1. Villous height in functioning and defunctioned intestine of two patients.....	43
Figure 3.2. western blot analysis of pSTAT3, STAT3, STING and SOCS3 in functioning (F) and defunctioned (D) intestinal tissue of 13 patients.....	44
Figure 3.3. Percentage change in Activated STAT3, STING and SOCS3 in defunctioned bowel, relative to functioning tissue.....	45

Figure 3.4. Western blot analysis of the autophagy marker beclin-1 in functioning and defunctioned intestinal tissue of 13 patients.....	46
Figure 3.5. beclin-1 expression in functioning and defunctioned bowel.....	46
Figure 4.1. Western blot analysis of STING, SOCS3, pSTAT3 and STAT3 in control empty vector (SOCS3 ^{EV}) HIEC.....	47
Figure 4.2. Percentage change in SOCS3, STING and activated STAT3 in cells stimulated with DNA, relative to unstimulated controls.....	48
Figure 4.3a. RPLPO and hSOCS3 mRNA were amplified by qPCR.....	50
Figure 4.3b. Δ Ct values for SOCS3 ^{EV} , SOCS3 ^{low} and SOCS3 ^{high}	50
Figure 4.3c. Transgenic cells showed variation in SOCS3 protein levels despite sustaining genetic modifications.....	50
Figure 4.4. Western blot analysis of autophagy markers in under-expressing (SOCS3 ^{low}), normal (SOCS3 ^{EV}) and overexpressing (SOCS3 ^{high}) untreated HIEC.....	51
Figure 4.5. Percentage change in beclin-1 and LC3B-I in untreated SOCS3 ^{low} and SOCS3 ^{high} cells, relative to SOCS3 ^{EV} controls	52
Figure 4.6. Western blot analysis of pSTAT3, STAT3 and STING in under-expressing (SOCS3 ^{low}), normally expressing (SOCS3 ^{EV}) and over-expressing (SOCS3 ^{high}) HIEC transfected with DNA.....	53
Figure 4.7. Percentage change in the expression of activated STAT3 and STING in under-expressing (SOCS3 ^{low}) and overexpressing (SOCS3 ^{high}) cells, relative to empty vector controls (SOCS3 ^{EV}) following transfection with DNA.....	53

1. Introduction

1.1. Colorectal Cancer

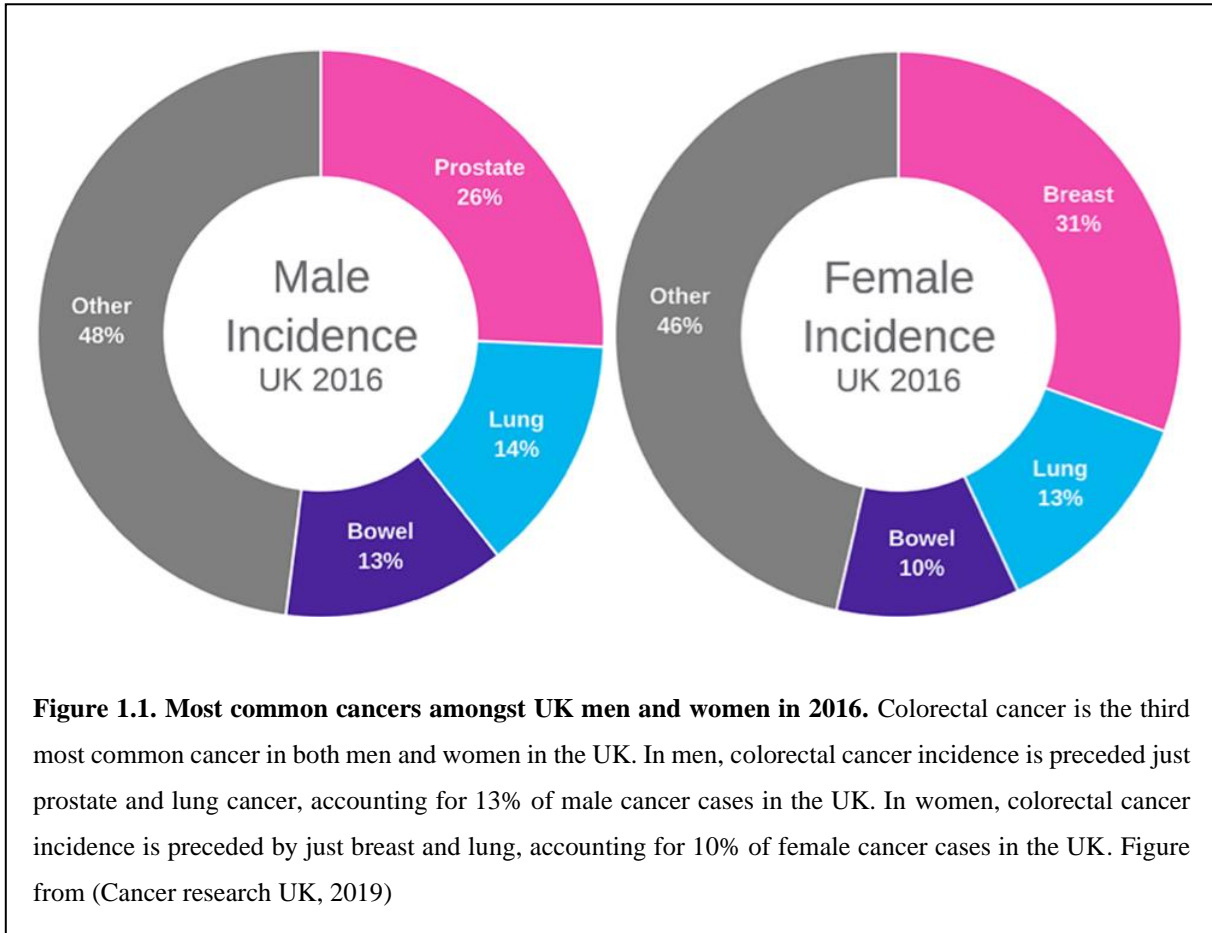
In 2018, around 18 million cancer diagnoses were made worldwide. Of these new cases, almost 2 million were colorectal cancer (CRC), making it the third most common cancer worldwide in both men and women (Table 1.1) (World Health Organization, 2018).

Cancer	Number of diagnoses	% of all new cases	Crude rate per 100,000
All cancers	18 078 957	N/A	236.9
Lung	2 093 876	11.58	27.4
Breast	2 088 849	11.55	55.2
Colorectum	1 849 518	10.23	24.2
Prostate	1 276 106	7.06	33.1
Stomach	1 033 701	5.72	13.5
Liver	841 080	4.65	11

Table 1.1. Newly diagnosed cancer cases in 2018, ranked by incidence. Of 17,036,901 newly diagnosed cases, over 10% (1,849,518 cases) were colorectal cancer. Colorectal cancer incidence was preceded only by lung and breast cancer, which accounted for 2,093,876 and 2,088,849 cases (or around 12% each), respectively. Data from WHO (World Health Organization, 2018)

Mirroring the global patterns of cancer incidence, colorectal cancer was the 3rd most common cancer in men and women in the UK in 2016 (Figure 1.1) and is currently the second most common cancer death worldwide (Cancer research UK, 2019). Of the 9.6 million cancer deaths reported in 2018, colorectal cancer was responsible for 862,000 deaths, second only to lung cancer, which caused 1,760,000 deaths (World Health Organization, 2018). Five-year survival rates suggest that earlier diagnoses of CRC are critical to reducing mortality and promise a better prognosis for many sufferers (World Cancer Research Fund and American

institute for cancer research, 2017). In fact, 5-year survival rates surge from just 13% in late-stage diagnoses to 90% in early-stage diagnoses – an increase just short of 600%.



1.1.1. Aetiology

Lifestyle and environmental factors weigh heavily on the aetiology of colorectal cancer. For instance, sub-populations living within the same community are subject to different degrees of risk of developing CRC, despite being exposed to comparable environmental factors (Boyle and Langman, 2000). On the other hand, studies have demonstrated that, as well as dissociating from the CRC risk patterns associated with their home country, groups of migrants quickly adopt those associated with host countries, demonstrating a strong environmental influence on risk factors (Boyle and Langman, 2000). Specifically, data has shown CRC incidence increased

by as much as four-fold in Japanese populations who migrated to the USA, relative to control populations who remained in Japan. Furthermore, this increase saw the incidence amongst migratory Japanese populations roughly match the incidence seen in the host country (Boyle and Langman, 2000). Such findings have branded CRC an ‘environmental’ disease – 70-80% of colorectal cancer cases may be attributed to cultural, social and lifestyle practices, with genetic factors being far less influential than in many other cancers (Boyle and Langman, 2000). As well as this, CRC is viewed as a disease of the westernised and developed world, although its prevalence is rising in economically developing countries (Bishehsari et al., 2014).

Arguably the most potent environmental factor influencing CRC is diet and nutrition. In 1990, Willett et al observed a strong and significant positive correlation between animal fat consumption by women and colon cancer risk, demonstrating that the relative risk to women who reported eating red meat at least once per day was 2.49 times that to women who consumed red meat less than once per month (Willett et al., 1990). Meanwhile, the relative risk of developing CRC is negatively correlated with physical activity. A major study illustrating this association measured the physical activity of 100 recently diagnosed CRC patients in Iran and compared it with that of unaffected companions who were not first or second-degree relatives. Occupational physical activity, household physical activity, and leisure activity were measured using a questionnaire. The results demonstrated that whilst there was no significant difference in occupational or household physical activity between the female case and control groups, there were statistically significant differences in levels of leisure activity between the two groups. The group concluded that risk of developing CRC is significantly reduced by moderate activity levels (Golshiri et al., 2016).

The impact of diet and nutrition on CRC risk extends far beyond simple correlations. Diet directly impacts nuclear receptor function as well as the intestinal microbiota, the pro-inflammatory capacities of which can be exacerbated by diet. Specifically, diets high in animal products and deficient in complex carbohydrates have been reported as major offenders (Bishehsari et al., 2014, Greer and O'Keefe, 2011). Nuclear receptors facilitate responses to environmental alterations by binding compounds from the diet and activating the appropriate metabolic pathways (Francis et al., 2003). It is now understood that nuclear receptors play key roles in both cancer development and progression (Dhiman et al., 2018). The involvement of the nuclear hormone receptor peroxisome proliferator-activated receptor delta (PPAR δ) in the development and progression of CRC was long hypothesized after Park et al demonstrated that generation and inoculation of a PPAR δ null cell line (simulating disruption of both alleles) in murine models inhibited the tumorigenic potential of affected cells (Park et al., 2001). Today, it is understood that although PPAR δ is normally expressed by epithelial cells of the colon, it is upregulated in the vast majority of human colorectal carcinomas (Gupta et al., 2000, Takayama et al., 2006). Furthermore, its upregulation is most notable in malignant cells, demonstrating a role of PPAR δ in both the development and progression of CRC (Takayama et al., 2006).

1.1.2. Diagnosis

First-line screening methods for CRC are stool-based and detect the presence of blood in patient faecal samples. The tests are readily available in two forms: the guaiac faecal occult blood test (g-FOBT) and the faecal immunochemical test (FIT).

There are numerous studies backing the use of g-FOBT in the reduction of CRC mortality. Annual g-FOBT screening is associated with a 33% decrease in 13-year cumulative

mortality, and even less frequent biennial screening still reduces mortality by 18% (Mandel et al., 1993, Kronborg et al., 1996). In addition to the abundant evidence rationalising the use of g-FOBT for first-line CRC screening, there are a number of advantages which make it an appealing strategy. Not only does the non-invasive nature of the procedure make g-FOBT a popular option amongst patients, but its cost effectiveness and high specificity make it equally favourable among healthcare professionals as well (Hassan et al., 2012, Mousavinezhad et al., 2016, Dancourt et al., 2008). Of course, g-FOBT is not without its drawbacks, the most notable being its low sensitivity which makes it susceptible to producing false positive results. Although such results are often due to the detection of non-human blood from the patient's diet, studies implementing dietary restrictions to negate the effect of animal haem found that the rates of false positives were not significantly reduced by such efforts (Schreuders et al., 2016, Coughlin and Friend, 1987, Pignone et al., 2001). In fact, the restrictions were associated with lower patient adherence, which is essential for effective testing (Konrad, 2010).

The FIT method possesses a similarly impressive specificity to g-FOBT but boasts a higher sensitivity due to the use of antibodies which selectively bind human haemoglobin (Allison et al., 1996). Despite this, the efficacy of FIT in reducing CRC incidence and mortality relative to gFOBT is poorly studied, meaning the data to support its preferential use is still perhaps insufficient. However, its improved sensitivity and patient compliance often brand FIT the superior first-line screening test (Parra-Blanco et al., 2010).

Although g-FOBT and FIT are undoubtedly useful tools, their low capacity for the detection of premalignant lesions means that screening must be conducted biennially or ideally annually to effectively reduce CRC mortality (Hassan et al., 2012). Should a g-FOBT or FIT return a positive result, then patients are referred for a colonoscopy or flexible sigmoidoscopy (FS). These screening methods can detect pre-malignant lesions but are highly invasive and so not used without sufficient concern. The ability to screen the colon in its entirety means that

colonoscopy is widely regarded as the most effective CRC screening method, whilst FS is able to examine just the rectum and sigmoid colon (Bénard et al., 2018). In spite of this, FS is often favoured due to its less-invasive nature and proven effectiveness; in one study FS alone reduced CRC incidence and mortality by 32% and 50% respectively (Elmunzer et al., 2012).

1.2. Inflammatory Bowel Disease

Inflammatory bowel disease (IBD) is characterised by non-infectious, recurring inflammation of the gastrointestinal tract and affects almost 7 million people worldwide (Inflammatory Bowel Disease Collaborators, 2019). The term IBD is used to describe multiple idiopathic diseases, but Ulcerative Colitis (Wilks 1859) and Crohn's Disease (Crohn et al., 1952) are most prominent. Ulcerative Colitis (UC) describes inflammation specific to the colonic mucosa, whilst Crohn's Disease (CD) refers to inflammation within any region of the gastrointestinal tract and throughout the wall (Xavier and Podolsky, 2007). Despite striking similarities in their symptoms, contributing factors and treatments, the extent to which these diseases are related is still up for debate, with much of this uncertainty on account of an incomplete understanding of the aetiology. What is understood is that IBD most often arises due to an immune response to the intestinal microbiota in a genetically predisposed individual.

1.2.1. Genetics

Family history is a major risk factor associated with IBD pathogenesis. First degree relatives of UC and CD patients are 10-fold more likely to develop the same disease themselves than first-degree relatives of unaffected controls. Furthermore, the risk to second-degree relatives of affected individuals is also increased (Orholm et al., 1991). In 2001, the first susceptibility gene for CD was identified by two separate research groups (Ogura et al., 2001, Hugot et al., 2001). Three polymorphisms at the carboxy terminal end of the nucleotide-binding oligomerization domain containing 2 (*NOD2*) gene are all linked with CD (Hugot et al., 2001). More recently, a meta-analysis of genome wide association studies (GWAS) of IBD identified 163 loci which were significantly associated with the disease. Of these loci, 110 are common to CD and UC, 30 are CD-specific and 23 are UC-specific (Jostins et al., 2012).

1.2.2. The Intestinal Microbiota

The gut microbiota is a population of tens to hundreds of trillions ($10^{13} - 10^{14}$) of symbionts residing in the within the gastrointestinal (GI) tract (Bishehsari et al., 2014). Their existence there is vital to numerous physiological processes including inflammation, intestinal and immune homeostasis, response to pathogens, and digestion (Halfvarson et al., 2017, Rakoff-Nahoum et al., 2004, Hooper et al., 2003, Lathrop et al., 2011, Tancredi, 1992, Gill et al., 2006).

The role of the microbiota in the development of IBD is a topic of great interest and murine studies have been indispensable in our current understanding of this relationship. For instance, an earlier study found that without the presence of resident gut bacteria, colitis cannot develop (Veltkamp et al., 2001). More recently, germ-free mice inoculated with the microbiota of IBD models had higher T helper cell counts, and lower regulatory T cell (Treg) counts than germ-free mice inoculated with healthy microbiotas (Britton et al., 2019). Furthermore, introduction of T cells to B and T lymphocyte-deficient mice induced IBD (Powrie et al., 1994). The healthy microbiota was therefore associated with a higher degree of immune tolerance, whilst the microbiota of IBD models is associated with a heightened immune response. In addition, a less diverse microbiome is associated with increased risk of IBD (Glassner et al., 2020).

Numerous studies in both animals and humans have demonstrated that the diversity of the microbiota is influenced by the host diet. Food quality, incorporation of both plant and animal products, as well as fat and fibre consumption have all been closely linked with microbiome diversity (Yu et al., 2021, Lau et al., 2018, Hildebrandt et al., 2009, Menni et al., 2017). Furthermore, nutrient deprivation in the intestinal lumen causes dysbiosis and, on account of the capacity of the microbiota to modulate intestinal inflammation, this may be

detrimental to the regulation of signalling pathways in the intestinal epithelium (Beamish et al., 2017, Yang et al., 2017, Buttó et al., 2015). Our understanding of the gut microbiota was long limited to its bacterial constituents, but more recently our comprehension of their viral cohabitants has advanced.

The virome is composed of both prokaryotic and eukaryotic viruses, which interact with both resident bacteria and host cells, respectively. Given the requirement for phages to infect bacteria, there is a well-established positive correlation between the diversity of these two populations (Breitbart et al., 2003). Numerous studies have now reported alterations in the intestinal viromes of individuals affected by a range of diseases, indicating a compelling link between the presence of exogenous DNA and modulation of the gut microbiome. Specifically, the abundance of *Caudovirales* increased significantly in the intestines of patients with ulcerative colitis and Crohn's disease (Norman et al., 2015), whilst virome has been found to increase significantly in colorectal cancer patients, relative to healthy controls (Nakatsu et al., 2018).

1.3. The Intestine

The human intestine is lined with villi which protrude into the lumen and aid digestion. Mechanical abrasion caused by movement of food through the intestine means that the epithelium must be turned over every 3 to 5 days (Karam, 1999). Around 10^7 colonic crypts known as the crypts of Lieberkühn are dedicated to maintaining the intestinal epithelium (Stamp et al., 2018). Each crypt is composed of approximately 2000 cells, around 100 of which are stem cells residing in the stem cell niche at the crypt base (Kang and Shibata, 2013) (Figure 1.2). The intestinal epithelium is made up of 6 mature cell types, which can be sub-divided into 2 categories: absorptive cells and secretory cells. Absorptive cells include enterocytes and M cells, whilst secretory cells include Paneth cells, goblet cells, enteroendocrine cells and tuft cells (Gehart and Clevers, 2019). High intestinal epithelial turnover drove the evolution of a complex system devoted to supplying the intestinal epithelium with new cells in specific quantities.

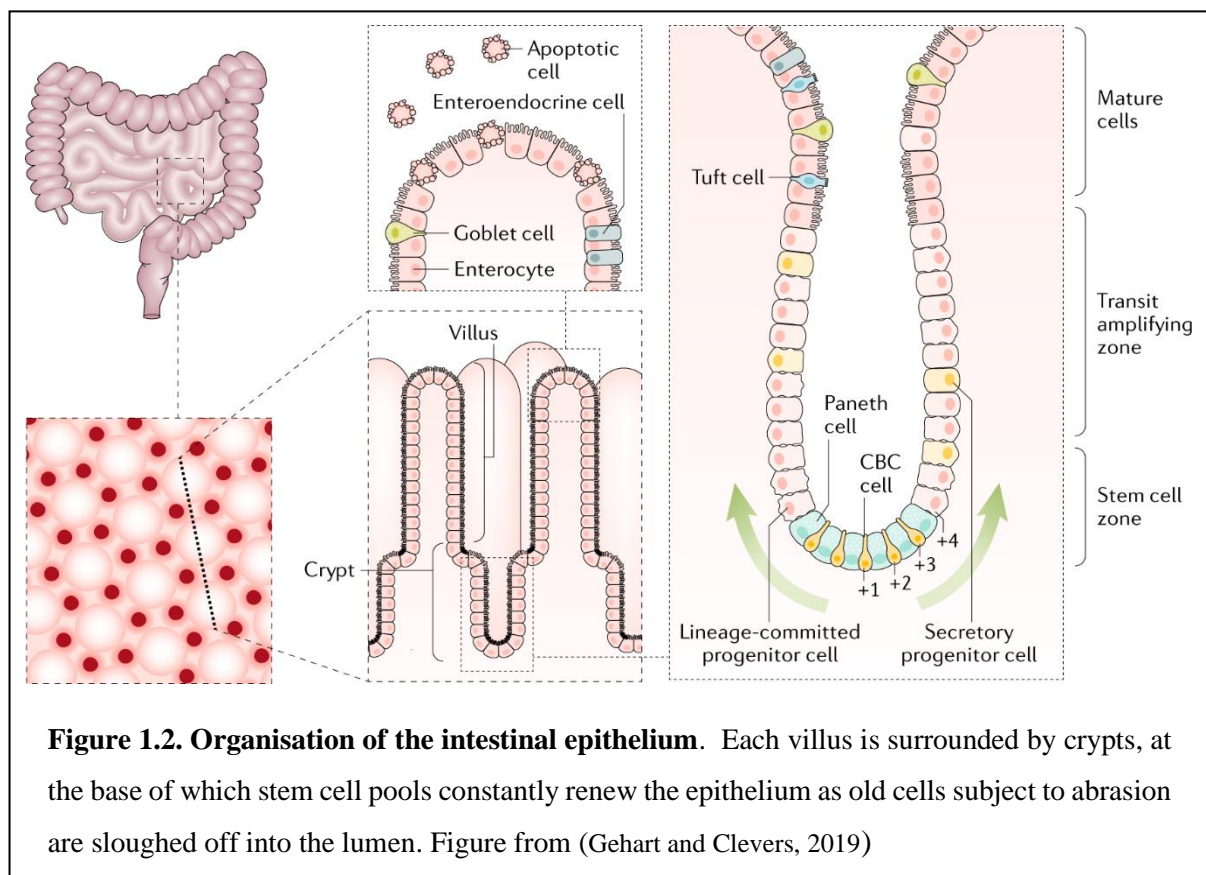


Figure 1.2. Organisation of the intestinal epithelium. Each villus is surrounded by crypts, at the base of which stem cell pools constantly renew the epithelium as old cells subject to abrasion are sloughed off into the lumen. Figure from (Gehart and Clevers, 2019)

1.3.1. Intestinal Stem Cells

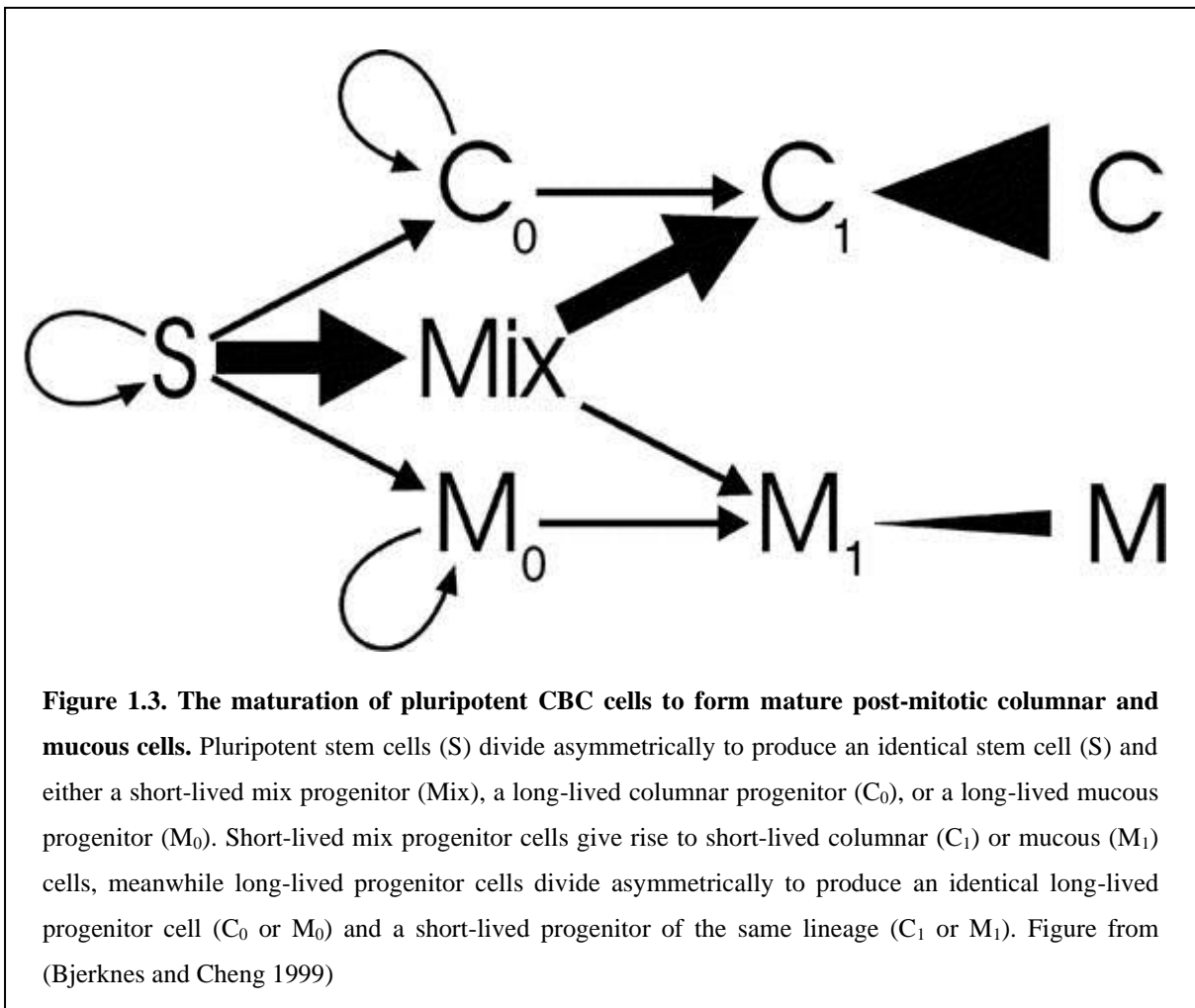
The constant requirement for intestinal epithelial replenishment is met by intestinal stem cells (ISCs) which divide asymmetrically to give rise to non-identical stem cell and progenitor cell daughters. Whilst stem cells remain in the niche, progenitor cells undergo around 5 divisions, during which they differentiate and migrate upwards (Cui and Chang, 2016). Eventually, mature cells reach the intestinal epithelium at the top of the crypt. After just 3-5 days they are shed into the lumen and must be replaced by new cells from the niche (Gehart and Clevers, 2019). There are thought to be 2 stem cell populations within the intestine: Crypt base columnar cells and +4 cells.

1.3.2. Crypt Base Columnar Cells

Crypt base columnar (CBC) cells were the first intestinal stem cells to be characterised, after Cheng and Leblond recognised that enteroendocrine cells were terminally differentiated yet phenotypically similar to CBC cells. They therefore proposed that CBC cells were the predecessors of enteroendocrine cells (Cheng and Leblond, 1974). Bjerknes and Cheng later identified short-lived and long-lived clones in the intestinal epithelium. The short-lived clones are now known as short-lived progenitor cells, whilst the long-lived clones may be categorised as long-lived progenitor cells or stem cells (Bjerknes and Cheng, 1999). Short-lived progenitor cells comprise lineage restricted columnar and mucous progenitors, as well mix progenitors which can differentiate into both columnar and mucous short-lived progenitors. Long-lived progenitor cells comprise pluripotent stem cells, long-lived mucous progenitors and long-lived columnar progenitors. Pluripotent stem cells give rise to mix short-lived progenitor cells, mucous long-lived progenitor cells and columnar long-lived progenitor cells. These in turn give rise to mucous and columnar short-lived progenitor cells which, when matured to post-mitotic

columnar and mucous cells, function in the intestinal epithelium. (Figure 1.3). Long-lived progenitors remain at the base of the crypt, whilst short-lived progenitors divide 2-3 times, migrate upwards and differentiate to form a post-mitotic cell (Bjerknes and Cheng, 1999).

CBC cells express the Wnt target gene Leucine-rich repeat-containing G protein-coupled receptor 5 (Lgr5) and are the only cell in the colon to do so (Barker et al., 2007). Since the identification of Lgr5 as an intestinal stem cell marker, it has been identified as a marker for adult stem cell populations in numerous other tissues, including the hair follicles, stomach and kidneys (Jaks et al., 2008, Barker et al., 2010, Barker et al., 2012). Furthermore, lineage tracing using an inducible Cre knock-in allele and the Rosa26-lacZ reporter revealed that the CBC cell is responsible for the production of all intestinal epithelial lineages. Lgr5 positive



(Lgr5⁺) CBC cells give rise to enterocytes, M cells, goblet cells, Paneth cells and tuft cells, as well as the previously proposed enteroendocrine cells (Barker et al., 2007).

1.3.3. +4 Cells

The +4 cell, named for its position in the crypt, is now recognised as a second intestinal stem cell. However, this concept was challenged for some time due to characteristics which brought the nature of these cells into question. Their label-retaining ability made +4 cells viable stem cell candidates and a number of studies identified a range of genetic markers for them. These include doublecortin-like kinase 1 (DCAMKL1), secreted Frizzled-related protein 5 (FRP-5) and B lymphoma Mo-MLV insertion region 1 (Bmi1) (Giannakis et al., 2006, Gregorieff et al., 2005, Sangiorgi and Capecchi, 2008). Bmi1 is perhaps the most widely recognised for this lineage; expressing cells were found to be capable of restoring the intestinal epithelium single-handedly, but they differed greatly in function and characteristics from Lgr5⁺ CBC cells. Upon their initial characterisation, the stem cells of the intestine were each designated a rank within a hierarchy (Potten, 1998). Ancestor stem cells (now recognised as mitotically active CBC cells) are primarily responsible for intestinal epithelial regeneration and sit at the bottom of the hierarchy due to their vulnerability to irradiation. In the event that this population is eradicated, reserve stem cells (now recognised as quiescent Bmi1⁺ +4 cells) repopulate the crypts due to their higher resilience to such insult (Yan et al., 2012). +4 cells are therefore regarded as a reserve stem cell population which serves primarily to replenish depleted CBC cell pools.

1.3.4. Intestinal Stem Cells and Cancer

The high abundance and proliferation rate of cells in the small intestine relative to the large should make it an obvious area of concern with regards to cancer predisposition. Remarkably, cancer of the small bowel is very rare. Between 2015 and 2017, 1,703 new cases were reported in the United Kingdom and these comprised below 1% of the total number of cancer cases reported in that time (Cancer Research UK, 2020). The reasons for this lie in the stem cell populations of the small and large intestine.

Apoptosis can occasionally be observed at the stem cell position in the healthy human small intestine, meanwhile it is almost inexistent in the large intestine. Furthermore, when apoptosis does occur in the large intestine, it can be seen throughout and is not limited to the stem cell position (Potten, 1998). Upon exposure to identical doses of radiation, cells of the small intestine undergo apoptosis at a higher rate than those of the colon. Furthermore, following irradiation, expression of the tumour suppressor gene *p53* by stem cells of the small intestine was high but remained low throughout the colon. Damage-induced apoptosis in the small intestine ceased upon *p53* knockout in mouse models (Merritt et al., 1994). This was an early indication that *p53* was involved in destroying damaged cells and circumventing neoplasia. Further investigation confirmed this and revealing that mutations in *p53* are common in colorectal carcinoma (Potten, 1998).

The differences in cancer incidence throughout the intestine cannot be solely attributed to expression of a tumour suppressor gene in the small bowel; the anti-apoptotic gene *bcl-2* is expressed exclusively in the large intestine, meaning that cells undergoing neoplastic transformation often will not be killed (Merritt et al., 1995). Furthermore, reciprocal expression of *bcl-2* and *p53* by carcinomas only widens the gap between the small and large intestine's vulnerability to cancer development.

1.3.5. Regulation of Intestinal Stem Cell Populations

The process of self-renewal for +4 and CBC cells in the intestinal crypt is highly dependent on signal transducer and activator of transcription 3 (STAT3) signalling (see 1.4.4). Studies which inactivated floxed STAT3 (STAT3^{fl}) alleles reported apoptosis and complete eradication of STAT3^{fl/-} cells from murine crypts, followed by replenishment of normal intestinal epithelial cell (IEC) pools (Matthews et al., 2011). As well as supporting ISC turnover under normal homeostatic conditions, STAT3 also stimulates proliferation in surviving cells following physical insult to the intestinal epithelium. Although this role has implicated STAT3 in tumourigenesis, organoid studies found that without STAT3 activation, insufficient interleukin-2 (IL-2) signals prevented organoids from maturing (Oshima et al., 2019, Jung et al., 2019).

In 2011, Takeda et al identified the homeodomain-only protein homeobox (HOPX) as a +4 cell marker. This novel gene is expressed specifically by +4 cells capable of generating CBC cells, and +4 cells generated from CBCs. This alluded to an unprecedented capability of +4 and CBC cells to ‘convert’ between lineages and facilitate regeneration of the intestinal epithelium regardless of the environment, which may favour one population (Takeda et al., 1998).

In a 2012 study which set out to deduce the molecular signature of the CBC cell, Javier Munoz and his colleagues observed the expression of +4 cell markers including HOPX, Bmi1, Tert, and Lrig1 by CBC cells (Muñoz et al., 2012). A later study led by Tara Srinivasan in 2016 went on to find that the key pathway underlying stem cell regulation by interconversion was the Notch signalling pathway. Murine organoids and pair cell assays were used to demonstrate that intestinal stem cells could divide both symmetrically and asymmetrically, to produce identical daughter pairs (Bmi⁺/Bmi⁺ or Lgr5⁺/Lgr5⁺ pairs) and non-identical Bmi⁺/Lgr5⁺

daughter pairs, respectively. Furthermore, the rate of asymmetric divisions fluctuated in accordance with Notch signalling levels, which occur in response to microenvironmental changes in the intestine. Whilst asymmetric divisions increased following activation of Notch signalling, Notch inhibition reduced asymmetric division frequency (Srinivasan et al., 2016). Tumour Necrosis Factor alpha (TNF- α) was used to stress organoid cells and caused an increased rate of asymmetric divisions. Addition of the γ -secretase inhibitor DAPT inhibited Notch signalling, resulting in the formation of more Bmi⁺/Bmi⁺ and Lgr5⁺/Lgr5⁺ pairs, relative to non-identical daughter pairs. The response of intestinal stem cells to similar stresses was tested *in vivo* by treating mice with dextran sulphate sodium (DSS) to induce intestinal inflammation. As expected, an increased rate of asymmetric divisions was observed, which fell again upon subsequent treatment with DAPT. However, it must be noted that although Notch-dependent asymmetric division was observed both *in vitro* and *ex vivo*, it was not so often the case *in vivo*. Regardless, the results demonstrated that intestinal inflammation induces Notch-dependent asymmetric division in ISCs in order to efficiently replenish both stem cell reserves (Srinivasan et al., 2016).

1.4. Cell Signalling in the Intestinal Epithelium

1.4.1. Cytokines

The cytokine protein superfamily plays a fundamental role in our innate immune system and intestinal epithelial barrier maintenance (Holdsworth and Gan, 2015). These small peptides are secreted most readily by immune cells and interact with membrane-bound receptors of the same cell, nearby cells or distant cells. The result is the initiation of autocrine, paracrine or endocrine responses which allow the host immune system to respond to stimuli such as infection and trauma (Zhang and An, 2007, Dinarello, 2000). The responses triggered by cytokine signalling are extensive but ultimately culminate in regulating the host immune response to invasion by pathogenic microorganisms (Holdsworth and Gan, 2015).

1.4.2. The JAK/STAT Pathway

Cytokine signalling is mediated by the Janus kinase (JAK) – STAT (JAK/STAT) pathway (Figure 1.4) (Harrison, 2012). Upon cytokine binding, receptors associated with tyrosine kinases known as Janus kinases (JAKs) dimerize. Formation of receptor homodimers allows JAKs to cross-phosphorylate each other and receptor cytoplasmic domain tyrosine residues, which create docking sites for SH2-containing proteins such as STAT (signal transducer and activator of transcription) proteins. STAT dimers translocate to the nucleus, where they act as transcriptional activators by binding to enhancer sequences in target genes (Yasukawa et al., 2000, Harrison, 2012).

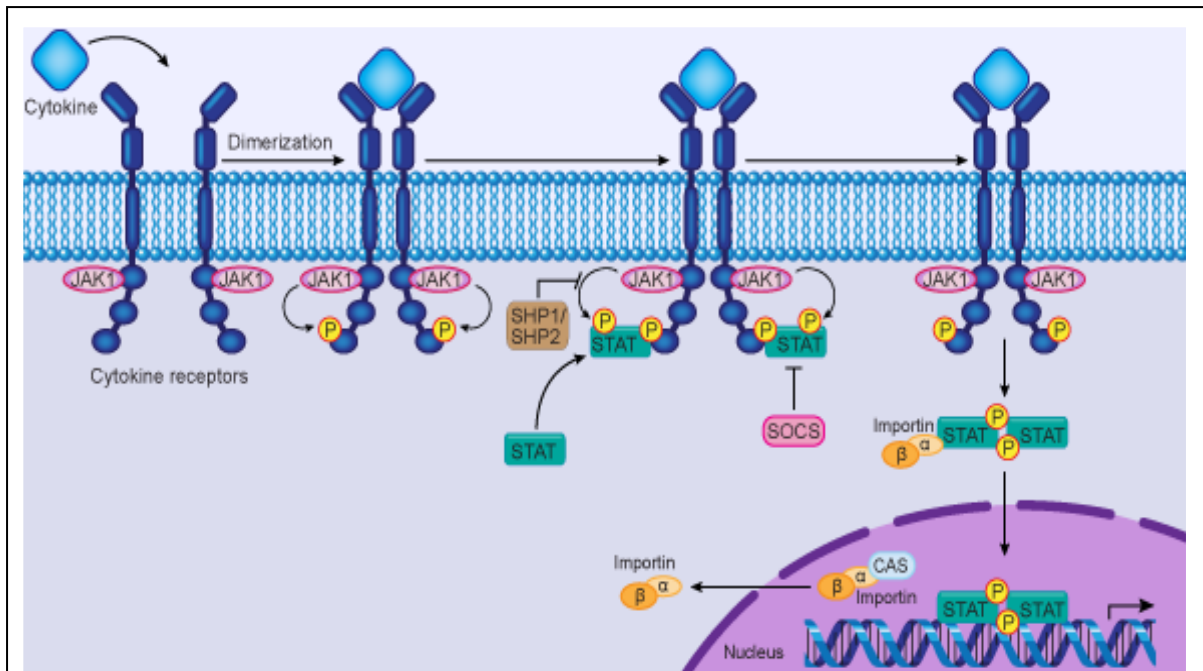


Figure 1.4. The Janus kinase / signal transducers and activators of transcription (JAK/STAT) pathway. Upon cytokine binding, JAKs form homodimers which create docking sites for STAT and its related proteins via cross-phosphorylation. STAT dimers act as transcriptional activators of genes in the nucleus by binding to enhancer sequences in target genes. Figure from (UT Southwestern Medical Centre, 2019)

1.4.3. Regulation of JAK/STAT Signalling

The JAK/STAT pathway is regulated by STATs, SOCS (suppressor of cytokine signalling) proteins, and PTPs (Protein tyrosine phosphatases) (Seif et al., 2017). SOCS protein dysregulation is thought to result in inappropriate STAT activation and account for the well-documented involvement of STATs in cancer (Inagaki-Ohara et al., 2014). The roles of SOCS1 and SOCS3 in cancer have also been particularly well studied. Both are powerful JAK inhibitors, capable of dysregulating essential cytokine-mediated processes such as proliferation, differentiation, maturation and apoptosis (Jiang et al., 2017, Inagaki-Ohara et al., 2014).

The SOCS family of proteins consists of 8 proteins: SOCS1 to SOCS7 and CIS (cytokine-inducible SH2 protein) (Krebs and Hilton, 2001). In response to cytokine signalling, SOCS1, SOCS2, SOCS3 and CIS transcripts are upregulated, causing inhibition of JAK/STAT signalling pathways via negative feedback. The proteins inactivate JAKs, block STAT binding sites and ubiquitinate signalling proteins, making them targets for proteasomal degradation (Krebs and Hilton, 2001).

1.4.4. STAT3 and Intestinal Homeostasis

STAT proteins are latent transcription factors activated by cytokines and growth factors (Darnell et al., 1994, Gadina et al., 2001). STAT3, one of the seven members of this protein family is a transcription factor capable of regulating the growth, apoptosis, survival and migration of a variety of cell types (Akira, 2000). In the intestine STAT3 regulates IEC homeostasis, and its dysregulation here has been linked with both the innate and acquired immune responses involved in IBD and CRC development (Lovato et al., 2003, Sugimoto, 2008, Corvinus et al., 2005)

The correlation between STAT3 dysregulation and IBD has been well studied in mice. Although the exact cause of IBD remains unclear, there is abundant evidence implicating an abnormal response of the intestinal immune system to the gut microflora (Strober et al., 2007). Furthermore, overexpression of Interleukin-6 and -22 (IL-6 and IL-22) has been linked with human IBD development (Reinecker et al., 1993, Brand et al., 2006). IECs are crucial in the innate immune defence of the intestine. In wild type mice, active phosphorylated STAT3 (pSTAT3) became detectable in 80% of IECs within 5 days of colitis development. Moreover, the effects of experimentally induced colitis in mice varied between those with IEC-specific STAT3 knockouts (STAT3^{IEC-KO}) and controls. STAT3^{IEC-KO} mice demonstrated reduced

expression of STAT3 transcriptional targets including SOCS3 (see 1.4.5). Furthermore, STAT3^{IEC-KO} mice were subject to increased tissue damage, crypt ablation, increased apoptosis, delayed intestinal healing and reduced proliferation (Pickert et al., 2009). The acquired immune response requires STAT3 activation to prevent T cell apoptosis and induce IL-6-dependent T cell proliferation. T cells subject to STAT3 deletions do not proliferate in response to IL-6 signals as apoptosis is not prevented (Takeda et al., 1998).

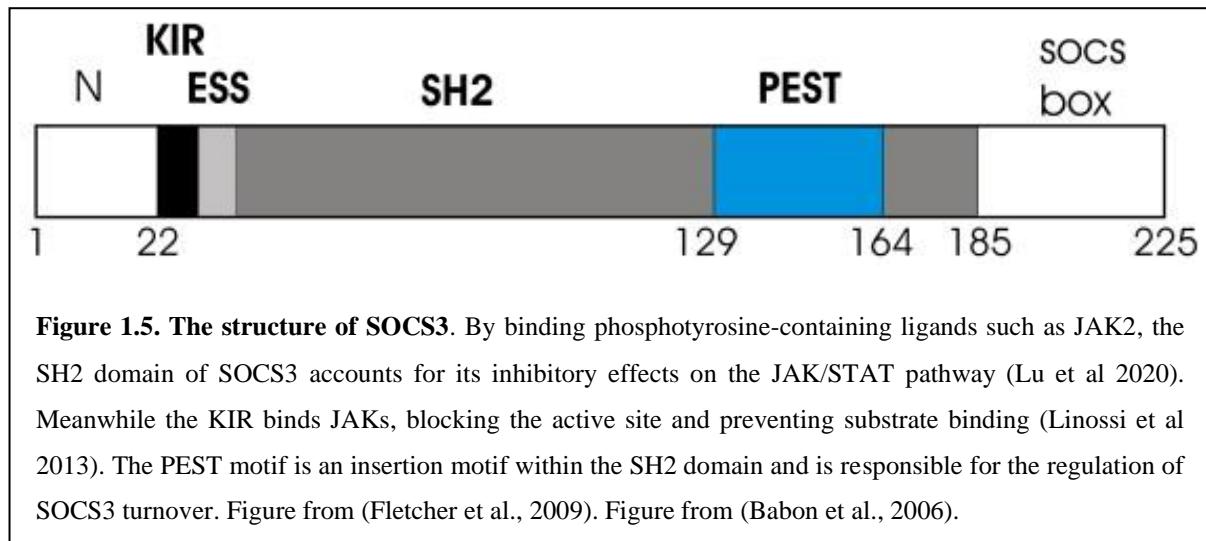
Following the recognition of constitutive STAT3 activation in various human malignancies, Corvinus and colleagues observed similar dysregulation in numerous CRC cases. Importantly, similar constitutive STAT3 activation to that observed in other human cancers was identified in neoplastic intestinal epithelial tissue, but not in normal adjacent tissue. This suggested a direct involvement of STAT3 in tumour development. CRC-derived cell lines were cultured, but critically lost their sustained STAT3 activity as a result (Corvinus et al., 2005). The indisputable inference here – that aberrant STAT3 activation relies on external stimuli – was poorly understood until recently, when Heichler and colleagues discovered that STAT3 is activated in cancer associated fibroblasts (CAFs), causing proliferation of cells responsible for shaping the CRC tumour microenvironment (Heichler et al., 2020).

1.4.5. SOCS3 and Intestinal Homeostasis

SOCS3 is a vital regulator of disease. Its expression is upregulated in myeloid, lymphoid and some non-haematopoietic cells in response to infection and inflammation, such that it may bind JAK kinases or cytokine receptors, inhibiting STAT3 activation (Carow and Rottenberg, 2014).

Like all SOCS proteins, SOCS3 contains an N terminal domain, a central SH2 domain and a SOCS box (Hilton et al 1998). Furthermore, SOCS3 possesses an extended SH2

subdomain (ESS), a kinase inhibitory region (KIR) and a proline, glutamine, serine, threonine (PEST) motif (Figure 1.5) (Babon et al., 2006).



Given the ability of SOCS3 to regulate JAK/STAT signalling, this essential protein also contributes to the maintenance of intestinal homeostasis by restricting IEC proliferation whilst permitting renewal and repair of dead and damaged IECs. Downregulation of SOCS3 in the intestinal epithelium is conducive to increased IEC turnover and hyperproliferation, which facilitates tumourigenesis (Rigby et al., 2007). This also alludes to a tumour suppressive role of SOCS3 (Shaw et al., 2017). However, complete knockout results in embryonic lethality due to overexpression of STAT3 and MAP kinase (Carow and Rottenberg, 2014). On the contrary, SOCS3 overexpression can be equally problematic, inhibiting JAK/STAT signalling and contributing to IBD development (Li et al., 2013).

The role of SOCS3 in the intestine has been studied using *Trichuris muris* in murine intestine as a model for the human gastrointestinal parasite *Trichuris trichiura* (Whipworm) (Shaw et al., 2017). Whilst high dose infection causes expulsion of the parasite, low doses

cause chronic infection and increased SOCS3 mRNA expression at the site of infection, compared to high dose subjects. Further investigation revealed that upregulation of SOCS3 inhibits IEC proliferation, rendering the host unable to expel the parasite. Meanwhile, downregulation resulted in increased IEC turnover and parasitic expulsion in infected mice but did not confer resistance to *T. muris* infection relative to uninfected controls (Shaw et al., 2017). This was thought to be due to an increased expression of the immunosuppressor enzyme indoleamine 2,3-dioxygenase (IDO) which is degraded by SOCS3 (Orabona et al., 2004).

IDO is upregulated in the gut in response to inflammation, although some studies have observed increases following chronic *T. muris* infection (Datta et al., 2005). Such results may be attributed to the increased number of IDO-expressing goblet cells associated with hyperplasia. SOCS3 inhibits IDO via proteasomal degradation and has been shown to induce *T. muris* resistance in models by facilitating migration of cells up crypts. This so-called “epithelial escalator” expels worms without reducing crypt depth. Furthermore, knockout mouse goblet cells express more IDO than those of controls (Bell and Else, 2011). Without the action of SOCS3, uninhibited IDO allows worm survival by impeding the epithelial escalator.

1.4.6. IRF3 in Viral Infection

The presence and threat of pathogens in the body is detected by highly specialised pattern recognition receptors (PRRs) which bind evolutionarily conserved pathogen-specific motifs known as pathogen associated molecular patterns (PAMPs) expressed by invading pathogens as well as damage associated molecular patterns (DAMPs) expressed by damaged self-cells (Mogensen, 2009, Tang et al., 2012). Multiple PRRs have been identified to date, with most belonging to one of 4 families: toll-like receptors (TLRs), retinoic acid-inducible gene-I-like receptors (RIG-I-like receptors or RLRs), nucleotide-binding oligomerization

domain-like receptors (NOD-like receptors or NLRs) and C-type lectin receptors (CLRs) (Takeuchi and Akira, 2010). In addition, the receptor for advanced glycation end products (RAGE) has also been identified as a PRR (Teissier and Boulanger, 2019). Association between PRRs and either PAMPs or DAMPs initiates intracellular signalling cascades which culminate in an immune response (Tang et al., 2012).

The discovery of the Interferon Regulatory Factor (IRF) protein family began in 1988, with the identification of the first of nine members. The so-called IRF-1 protein is a nuclear factor which regulates the transcription of IFN- β (Miyamoto et al., 1988). It was not until 1995 that Au and colleagues identified IRF3, which is now understood to be a key transcription factor in the response to viral infection (Au et al., 1995). IRF3 remains inactive in the cytoplasm until, upon stimulation, C terminus phosphorylation permits its dimerization and translocation into the nucleus (Yoneyama et al., 1998, Lin et al., 1998). Nuclear IRF3 binds DNA and induces the transcription of type 1 interferon (type I IFN) genes, then is degraded by the proteasome (Lin et al., 1998).

Viral infection may be detected due to the presence of viral DNA or double-stranded RNA (dsRNA) within the cell. The response relies on the phosphorylation of IRF3, mediated by one of three adapter proteins: Stimulator of interferon genes (STING), mitochondrial antiviral signalling (MAVS) or Toll/IL-1R resistance domain-containing adapter-inducing IFN- β (TRIF). Exactly which adapter protein is recruited is determined by the PAMP detected and signalling pathway induced. The STING signalling pathway, activated by the presence of viral RNA in the cytosol, is discussed later in detail (see 1.4.7) and will not be discussed here.

The presence of dsRNA in the cytosol is detected by RLRs (Yoneyama et al., 2004). RLRs contain C-terminal repressor domains (RDs) which prevent the N terminal caspase activation and recruitment domains (CARDs) from interacting with downstream signalling

pathway components in unstimulated cells (Saito et al., 2007). Ligand binding liberates CARDs, which are thereby free to facilitate the recruitment of MAVS (Cui et al., 2008, Kawai et al., 2005). Phosphorylation of MAVS by TANK-binding kinase 1 (TBK1) or I κ B kinase (IKK) creates a binding site for IRF3 which, once bound, is also phosphorylated by TBK1 (Liu et al., 2015). Phosphorylated IRF3 dimerizes and translocates to the nucleus, where it associates with the co-activators CREB-binding protein and p300 (CBP/p300) and drives the expression of type I IFN genes (Seth et al., 2005, Yoneyama et al., 1998, Lin et al., 1998). Phosphorylation of MAVS may mediate IRF7 and nuclear factor kappa B (NF- κ B) activation as well as IRF3 (Tang and Wang, 2009, Seth et al., 2005).

Whilst TLRs are a major subset of PRRs, IRF3 is activated in response to PAMP recognition by TLR3 and TLR4 only (Doyle et al., 2002). Intracellular TLR3 binds viral double stranded RNA, meanwhile cell surface TLR4 (initially identified as the signalling receptor for lipopolysaccharides of gram-negative bacteria) also binds some viral proteins (Alexopoulou et al., 2001, Kurt-Jones et al., 2000, Mogensen and Paludan, 2005, Hoshino et al., 1999). TLRs bind their respective ligands and recruit Toll/IL-1R resistance (TIR) domain-containing adapter proteins which in turn initiate the signalling pathways necessary to orchestrate a response. TLR3 and TLR4 activate IRF3 via the TRIF pathway. TRIF interacts directly with TLR3 following receptor phosphorylation by the epithelial growth factor receptor (ErbB1) or Bruton's tyrosine kinase (Btk) (Yamashita et al., 2012, Lee et al., 2012). Alternatively, indirect interaction between TRIF and TLR4 is facilitated via TIR-containing adapter molecule (TICAM)-2, also known as TRIF-related adapter molecule (TRAM) (Oshiumi et al., 2003). TRIF then activates TBK1 and IKK ϵ , which phosphorylate IRF3 (Jiang et al., 2004).

Through an independent signalling pathway, IRF3 also acts as an apoptotic factor in the virus-infected cell. Through its BH3 domain, IRF3 interacts with the Bcl-2 family member Bax, with which it then translocates to the mitochondria (Chattopadhyay et al., 2010). In the

mitochondria, Bax oligomers are inserted into the mitochondrial membrane, which make it permeable to the cytochrome complex and activates the mitochondrial apoptotic pathway (Antonsson et al., 2001, Lovell et al., 2008).

1.4.7. STING in Defence Against Microbes

STING is an endoplasmic reticulum (ER)-bound adaptor protein central to the response to viral infection (Ishikawa and Barber, 2008). Detection and binding of microbial or self-DNA by cyclic guanosine monophosphate-adenosine monophosphate synthase (cGAS) in the otherwise DNA-free cytoplasm is sufficient to activate the innate immune response. STING elicits anti-microbial responses by inducing Type I and III IFNs or activating autophagy (Figure 1.6) (Sun et al., 2013, Deb et al., 2020, Gui et al., 2019).

The cGAS-STING signalling cascade induces type I and III IFNs to regulate inflammation by activating the transcription factors IRF3 and NF- κ B. The STING-NF- κ B pathway is incompletely elucidated but is known to employ TBK1 and induce Type I IFN expression (Cerboni et al., 2017, Abe and Barber, 2014). The STING-IRF3 pathway, however, is well understood. Activated cGAS catalyses a reaction between adenosine triphosphate (ATP) and guanosine triphosphate (GTP) to form cyclic guanosine monophosphate-adenosine monophosphate (cGAMP) (Zhang et al., 2013, Ablasser et al., 2013). cGAMP binds STING to induce a conformational change which activates and displaces it from the ER (Wu et al., 2013). Activated STING oligomerizes and recruits TBK1, which creates binding sites for IRF3 (Zhang et al., 2019). Upon recruitment to these sites, IRF3 is phosphorylated by TBK1 before it dimerizes, translocates to the nucleus and mediates expression of target genes.

The cGAS-STING cascade can also activate autophagy to clear the cytosol of stimulatory DNA. The interaction between cGAMP and STING drives its translocation to the endoplasmic reticulum-Golgi intermediate compartment (ERGIC), where it facilitates LC3 lipidation to the autophagosome component LC3-II. cGAMP-induced autophagosome formation can occur both in addition to and independently of IFN induction (Gui et al., 2019).

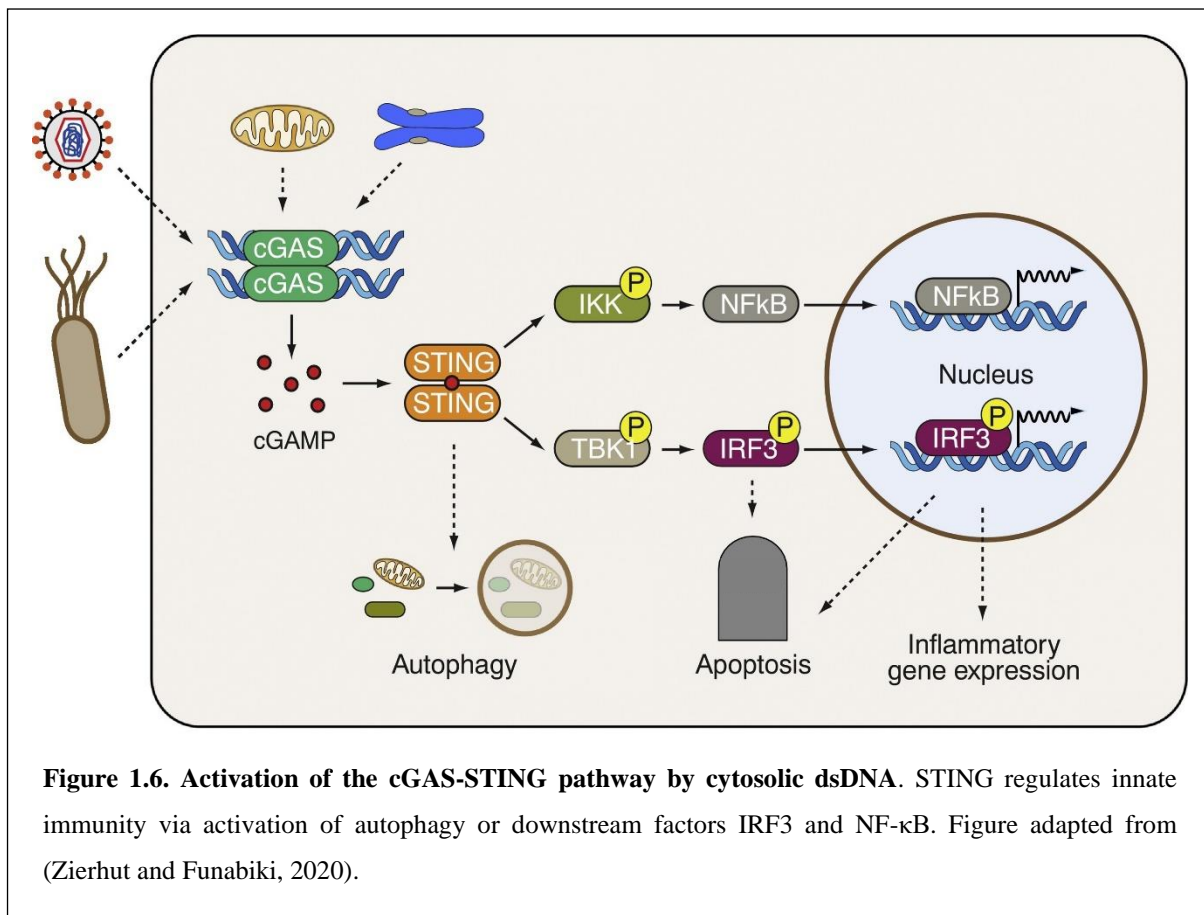


Figure 1.6. Activation of the cGAS-STING pathway by cytosolic dsDNA. STING regulates innate immunity via activation of autophagy or downstream factors IRF3 and NF-κB. Figure adapted from (Zierhut and Funabiki, 2020).

With regards to IFN induction, the cGAS-STING signal transduction cascade invokes the secretion of type I IFNs in most cells (Zhao et al., 2016). Type III IFNs are secreted by a smaller selection of cell types including plasmacytoid dendritic cells (pDCs) according to a recent study (Deb et al., 2020). Type I IFNs readily activate the JAK/STAT signalling pathway

by binding the IFN α receptor (IFNAR), which is composed of IFNAR1 and IFNAR2 subunits (Darnell et al., 1994, Uzé et al., 1990). Meanwhile, type III IFNs activate the JAK/STAT pathway through binding the interleukin-28 receptor (IL-28R), which is composed of IFN- λ R1 and IL-10R2 (Kotenko et al., 2003). Type I and III IFN binding to their respective receptor induces dimerization and phosphorylation of tyrosine kinase 2 (TYK2) and JAK1. STAT1 and STAT2 are phosphorylated by the JAKs and form a heterodimer. The STAT1-STAT2 dimer translocates to the nucleus and associates with IFN regulatory factor 9 (IRF9) to form the IFN-stimulated gene factor 3 (ISGF3) complex (Dale et al., 1989, Schindler et al., 1992). ISGF3 binds IFN-stimulated response elements (ISREs) in the promoter region of some IFN-stimulated genes (ISGs) and drives their transcription (Reich et al., 1987). Upregulation of ISGs creates a potent anti-viral environment within the cell (Figure 1.7) (Ivashkiv and Donlin, 2014, Schneider et al., 2014).

The STING-cGAS pathway has received positive publicity in the field regarding its proposed role in cancer protection. Its repression is reported in ovarian cancers, meanwhile its activation induces apoptosis in malignant cells, indicating a tumour suppressive role (de Queiroz et al., 2019, Tang et al., 2016). Specifically, STING signalling offers protection against the oncogenic effects of abnormal DNA (Kwon and Bakhom, 2020). Genomic instability is a hallmark of cancer and may manifest as fluctuations in chromosome number and structure (Hanahan and Weinberg, 2011, Geigl et al., 2008). This flux - known as chromosomal instability - eventually causes surplus DNA to erupt from micronuclei into the cytosol, where it can activate cGAS and initiate the STING signalling cascade (Bakhom et al., 2018). STING also stimulates immunogenic autophagy by interacting with LC3, before being degraded itself (Liu et al., 2019).

The virome must infect both prokaryotic and eukaryotic cells within the gut in order to persist. In host cells, such interactions cause activation of the cGAS-STING pathway, which raises the possibility that the microbiota is capable of influencing the body's response to cancer by modulating anticancer signalling cascades.

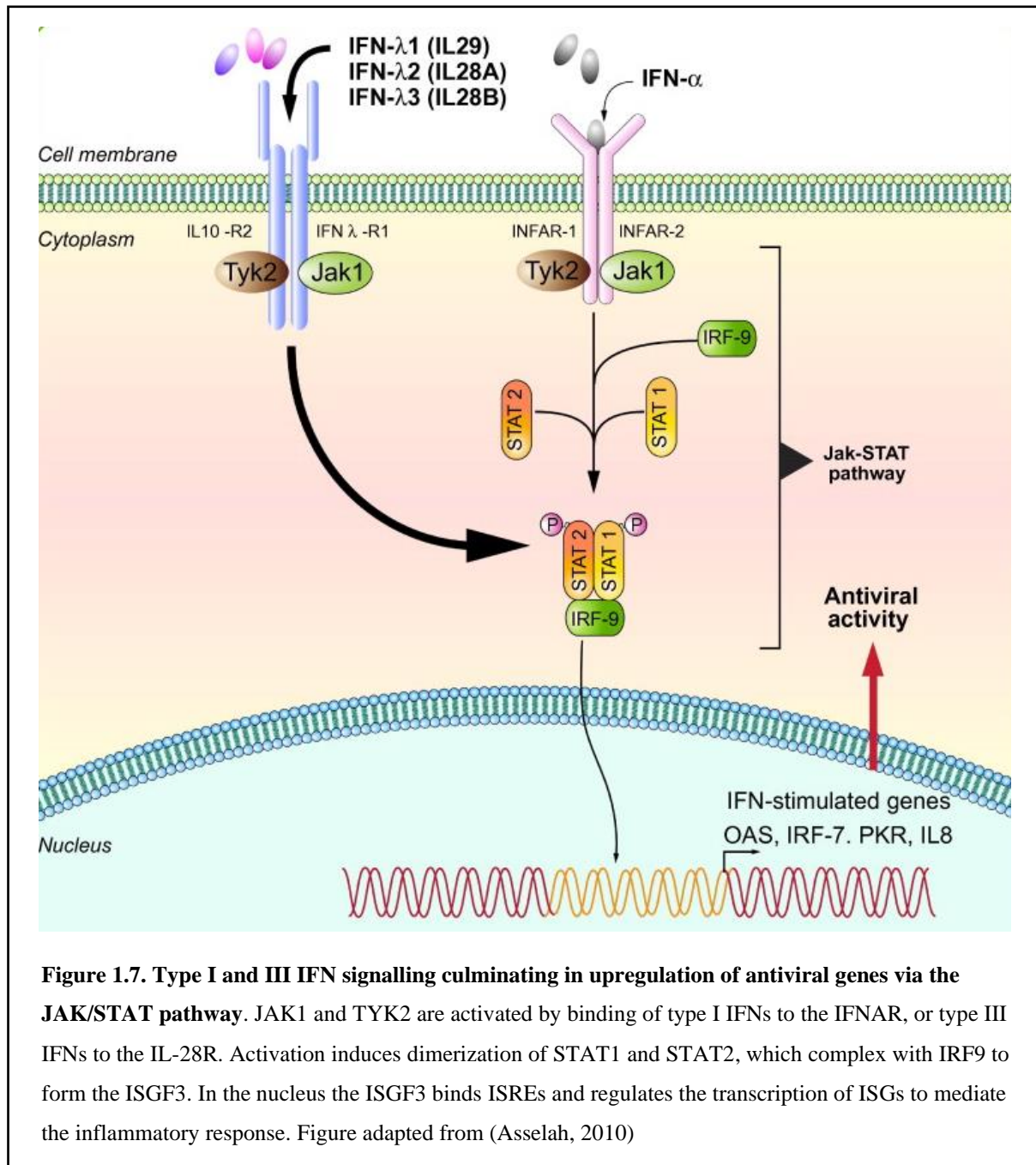


Figure 1.7. Type I and III IFN signalling culminating in upregulation of antiviral genes via the JAK/STAT pathway. JAK1 and TYK2 are activated by binding of type I IFNs to the IFNAR, or type III IFNs to the IL-28R. Activation induces dimerization of STAT1 and STAT2, which complex with IRF9 to form the ISGF3. In the nucleus the ISGF3 binds ISREs and regulates the transcription of ISGs to mediate the inflammatory response. Figure adapted from (Asselah, 2010)

1.4.8. Autophagy

Autophagy is the cellular mechanism responsible for the lysosomal degradation of cytoplasmic components including proteins and organelles (Mizushima et al., 2008). Conserved from yeast to humans, autophagy can be observed throughout eukaryotic cells, with 3 types identified in mammalian cells (Levine and Deretic, 2007, Parzych and Klionsky, 2014). These are known as macroautophagy, microautophagy and chaperone-mediated autophagy (CMA).

First described in 1966 by Christian De Duve and Robert Wattiaux, microautophagy involves deformation of the lysosomal membrane in order to trap a region of the cytosol which includes, but is not limited to, proteins and organelles (Cuervo and Dice, 1998). Cytoplasmic components therefore become trapped within invaginations, which eventually bud off into the lysosome, engulfing the cargo (Figure 1.8a.) (De Duve and Wattiaux, 1966).

Macroautophagy also involves sequestration of an entire portion of the cytosol and its constituents, however in this process cargo becomes trapped within a double-membraned autophagosome which is synthesised *de novo* (Cuervo and Dice, 1998). The so-called autophagic body – comprised of the inner membrane and the intra-autophagosomal components – is released into the lysosomal lumen upon fusion between the lysosome and autophagosome and degraded by lysosomal hydrolases (Figure 1.8b) (Yorimitsu and Klionsky, 2005, Tanida et al., 2008).

Chaperone-mediated autophagy involves a highly specific selection of cytosolic proteins, and their subsequent sequestration via translocation into the lysosome. CMA is activated when the 73kDa heat shock cognate protein Hsc73 or Hsc70 binds KFERQ-like sequences of substrate proteins in the cytosol (Terlecky and Dice, 1993) (Cuervo and Wong, 2014). Chaperone-bound proteins interact with monomeric lysosome-associated membrane

protein type 2A (LAMP-2A protein) at the surface membrane of the lysosome (Cuervo and Dice, 1996). This interaction initiates formation of a translocation complex consisting of LAMP-2A homotrimers which interact with Hsc70 chaperones (Cuervo and Wong, 2014); (Rout et al., 2014). LAMP-2A homotrimers are stabilised at the lysosomal surface and disassemble, meanwhile lysosomal Hsc70 drives KFERQ-like motifs of substrate proteins into the lysosomal lumen for degradation (Bandyopadhyay et al., 2008).

As the most common and well-studied form, the term ‘autophagy’ shall now refer to macroautophagy alone. Paradoxically, this process which is dedicated to self-destruction supports cell survival. Whilst autophagy is primarily activated in response to metabolic stresses in yeast and other unicellular organisms (Tsukada and Ohsumi, 1993), it is activated in many mammalian cells during periods of fasting. A 2003 study identified autophagy induction in skeletal muscle, liver, heart, kidney and other GFP-LC3 transgenic mouse tissues following 24-hour food deprivation (Mizushima et al., 2004). Furthermore, mammalian neonates induce autophagy immediately at birth for in order to compensate for the termination of nutrient supply from the placenta until the requirement can be met by milk (Kuma et al., 2004). This allows cells to maintain their metabolic functions. Degraded cargo is returned to the cytosol to create a pool of metabolites which can be utilised throughout periods of nutrient deprivation (Lum et al., 2005b).

Microtubule-associated protein 1A/1B-light chain 3 (LC3) is a soluble protein which is widely used to study autophagy in mammalian cells. Upon activation of autophagy, LC3 is cleaved to form cytosolic LC3-I, which is conjugated to phosphatidylethanolamine to form the autophagosome membrane component LC3-II (Tanida et al., 2008, Koukourakis et al., 2015). Fusion of autophagosomes with lysosomes releases intra-autophagosomal cargo, including membrane-bound LC3-II, into the lysosomal lumen. This LC3 flux has branded it a reliable

marker of autophagy, making it a popular target for immunoblotting using Anti-LC3 antibodies (Tanida et al., 2008).

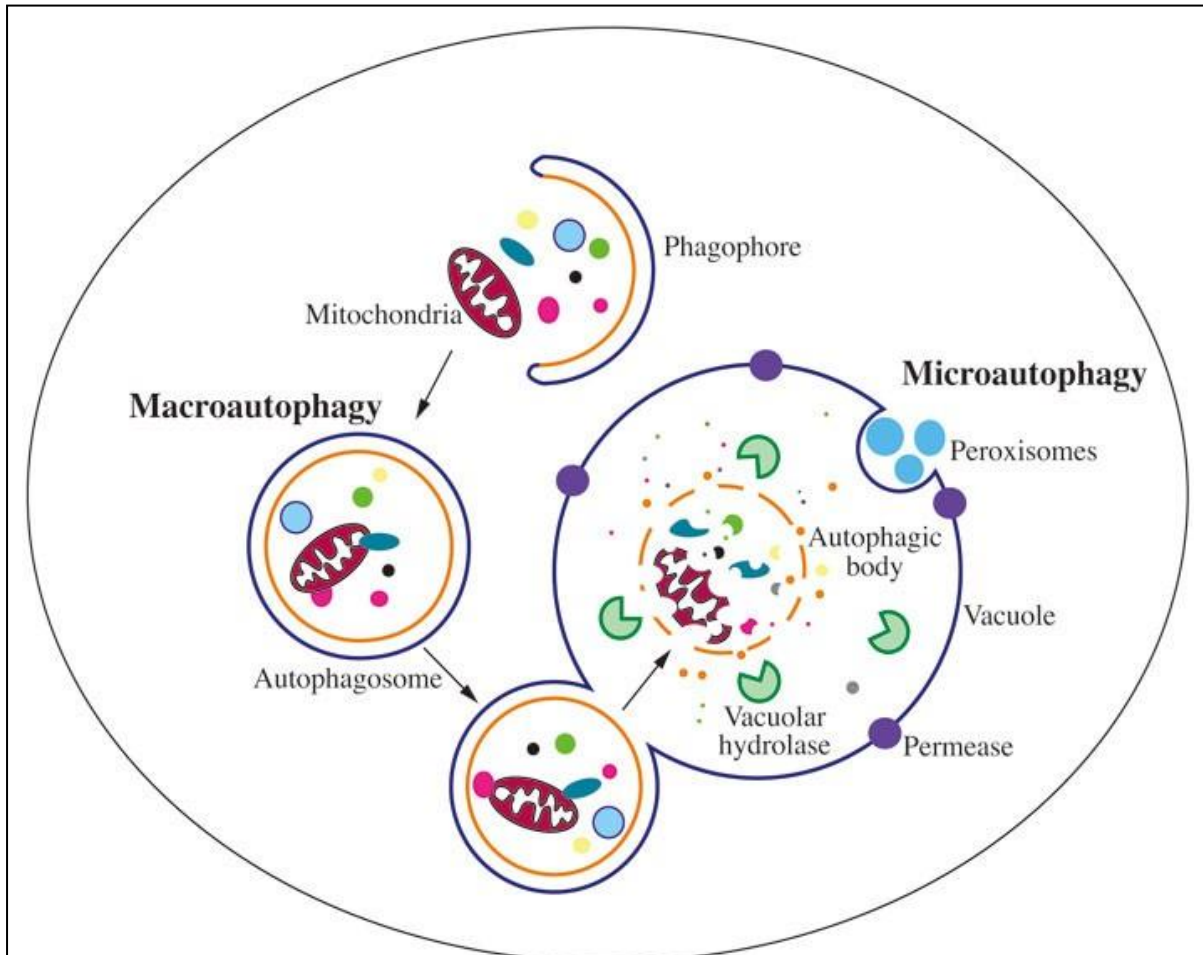


Figure 1.8. Degradation of cytosolic components by micro- and macroautophagy.

- a) During microautophagy cytosolic components become sequestered within invaginations in the lysosomal membrane and are subsequently degraded by lysosomal hydrolases.
- b) During macroautophagy cytosolic components become trapped within a double-membraned autophagosome, forming an autophagic body. Fusion of the autophagosome with the lysosome releases the autophagic body for degradation by lysosomal hydrolases.

Figure from (Feng et al., 2014)

There are three distinct human isoforms of the LC3 protein, known as LC3A, LC3B and LC3C (He et al., 2003). One study found LC3A and LC3C to co-localize in the nucleus of cancer cell lines. Meanwhile LC3B expression is poor throughout the nucleus, but common in the LC3A-negative nucleolus. Whilst cytoplasmic LC3A expression is restricted to the perinuclear space, LC3B and LC3C are expressed throughout, although it is important to note that co-localization has not been observed here (Koukourakis et al., 2015). Of the three human LC3 isoforms, LC3B is the best understood and is therefore widely recognised as the most dependable marker of autophagic flux in cells.

The haploinsufficient tumour suppressor protein beclin-1 is central to the regulation of autophagy and is often deleted in cancer (Yue et al., 2003, Aita et al., 1999). Under normal conditions, beclin-1 is inhibited by interactions with members of the anti-apoptotic B-cell lymphoma-2 (Bcl-2) protein family. When cells are subject to short periods of stress such as nutrient deprivation, beclin-1 dissociates from its inhibitory complex and induces autophagy (Pattingre et al., 2005). In humans, beclin-1 binds phosphatidylinositol 3-kinase (hVps34), UVRAG, hVps15, Atg14L and Rubicon to form three distinct complexes, at their core a beclin-1-hVps34-hVps15 complex (Kihara et al., 2001, Liang et al., 2006, Matsunaga et al., 2009). UVRAG (UV radiation resistance associated gene) and Atg14L (Autophagy-related 14-like) bind the same region of this complex under different conditions, to regulate beclin-1 mediated autophagy. Meanwhile Rubicon (Run domain beclin-1 interacting and cysteine-rich domain-containing protein) binds just a few pre-existing UVRAG complexes in order to negatively regulate autophagy (Matsunaga et al., 2009).

Autophagy dysfunction has been linked with a plethora of diseases (Mizushima et al., 2008). Among these are pathogenic infection, neurodegeneration, heart disease, ageing and cancer. The relationship between autophagy and cancer is complex. As mentioned, autophagy promotes survival by providing cells with the means to degrade organelles and proteins, recycle

nutrients and sustain metabolic reactions under stress. In healthy somatic cells, maintenance of cell viability under metabolic stress is of course beneficial to the host. However, in malignant cells this promotes tumourigenesis and can be detrimental. The early tumour microenvironment is poorly oxygenated due to compromised blood supply. Induction of angiogenesis is one of the hallmarks of cancer and has been found to be stimulated by autophagy (Liang et al., 2018, Hanahan and Weinberg, 2011). Furthermore, developing tumours are deprived of nutrients but require a surplus to grow. Autophagy-mediated recycling of cellular components can sustain starved cells for prolonged periods and provide tumours with the means to progress for many weeks (Lum et al., 2005a).

In light of the profound effects of autophagy activation on tumour survival, it is almost incomprehensible that it is beneficial to the host in the early stages of cancer. When autophagy is blocked at this stage, immunosuppressive T regulatory (Treg) cells infiltrate tumours and suppress immune responses to it (Rao et al., 2014). In contrast, upregulation of beclin-1 expression in colon cancer cells inhibits tumourigenesis (Koneri et al., 2007). Activation of autophagy is therefore initially necessary to prevent immune tolerance to, and growth of, cancers. Only once a tumour is malignant does autophagy become a threat.

1.5. Project Aims

Inflammatory signalling and autophagy are key pathways involved in intestinal epithelial homeostasis and maintenance. Dysregulation of these pathways can be detrimental to the host, leading to cancer and IBD. We hypothesise that SOCS3 in the intestinal epithelium is a regulator of microbial-mediated signalling pathways. To investigate this, we aim to create two models of dysbiosis using human intestine starved of enteral nutrition and cells transfected with exogenous DNA. We will use these models to investigate the impact of dysbiosis upon inflammatory signalling pathways and autophagy. Furthermore, we aim to use transgenic cell lines to investigate the role of SOCS3 in these pathways.

2. Materials and Methods

2.1. Cell Lines

2.1.1. Maintenance

Cells were transfected with empty vector or SOCS3 expression plasmids to create control (SOCS3^{EV}) and overexpressing (SOCS3^{high}) cell lines, respectively. SOCS3 and non-silencing shRNA GIPZ lentiviral constructs (Thermo Scientific) were used to produce a SOCS3 knockdown (SOCS3^{low}) cell line, as described in Shaw et al, 2017. Human intestinal epithelial cell (HIEC) medium was prepared using Opti-MEM, 5% foetal bovine serum, 5mM HEPES and 10µg/ml EGF. Cells were cultured in HIEC medium with either 0.5mg/ml G418 (SOCS3^{high}) or 0.4µg/µl puromycin (SOCS3^{EV} and SOCS3^{low}) added. Cells were maintained in T75 (75ml) culture flasks and passaged every second day, or at 70% confluence. Cells were passaged under sterile conditions using a laminar flow cabinet. Media from all flasks was discarded and cells were washed with 5ml of Dulbecco's Phosphate-Buffered Saline (DPBS) from ThermoFisher Scientific before being incubated with 1ml Trypsin-EDTA for 10 minutes. Trypsinised cells were diluted to approximately 2×10^5 cells/ml and incubated at 37°C for 48 hours, or until 70% confluence was reached.

2.1.2. Plating Cells

Media was discarded and HIECs were washed with DPBS and trypsinised. 5ml of HIEC medium was added to each flask and homogeneous flasks were mixed. 10µl of each suspension was removed and mixed with 10µl 0.4% trypan blue (Sigma T8154) in an Eppendorf tube. 10µl of stained suspension was loaded to a haemocytometer and observed at 100 x magnification using the brightfield microscope. Live, unstained cells within the 1mm² area in each corner of

the grid were counted and the mean of these values was multiplied by 10^4 to obtain the number of live cells per ml (cm^3) of solution. Finally, the concentration of live cells per ml was multiplied by 2 as the cells were diluted 1:1 with Trypan Blue.

Suspensions of each cell line at a concentration of 200,000 cells/ml in HIEC medium were used to prepare a 12-well plate for each cell line. Each well received 200,000 cells in 1ml of suspension and was incubated at 37°C overnight.

2.1.3. Transfecting Cells

Cells were either untreated controls, were transfected with Herring Sperm DNA using the K4 transfection system by Biontex (DNA-treated), were transfected with K4 transfection reagent only (K4 control) or were used for mRNA analysis (see 2.3) and this was done in triplicate. Herring sperm DNA ($8\mu\text{g}/\mu\text{l}$) and the K4 transfection system were brought to room temperature and agitated gently to ensure even mixing. Media was removed from all wells and $200\mu\text{l}$ complete growth medium was added to controls. Complete growth medium and K4 multiplier ($200\mu\text{l}$ and $2\mu\text{l}$, respectively) was added to all treated wells. Plates were incubated at 37°C for 30 minutes. Solutions of Herring sperm DNA and K4 transfection reagent were prepared according to the manufacturer protocol. In order for each well to receive $1\mu\text{g}$ of DNA, $1.2\mu\text{l}$ of $8\mu\text{g}/\mu\text{l}$ DNA stock was mixed with $135\mu\text{l}$ of serum-free medium and $15\mu\text{l}$ of this solution was pipetted into each K4-treated well. $18\mu\text{l}$ of K4 transfection reagent was mixed with $370\mu\text{l}$ serum-free medium in a separate tube and $15\mu\text{l}$ of this solution was pipetted into each DNA-treated and K4-treated well. This was repeated for all 3 plates, which were then incubated at 37°C for 4 hours.

2.1.4. Cell Lysis

Cell lysis solution was prepared by mixing lysis buffer 100:1 with both protease inhibitor P8340 and phosphatase inhibitor P5726 by Sigma. Media was removed from control and treated wells, and 200µl of cell lysis solution was added. The adherent HIEC cells were dislodged from the well surface into the solution, transferred to an Eppendorf tube and stored on ice overnight.

2.2. Western Blot

Laemmli sample buffer (4x; Bio-Rad #1610747) was mixed with β -mercaptoethanol in a 9:1 ratio, and added to samples in a 3:1 (sample:buffer) ratio. Samples were boiled at 95°C for 5 minutes to denature the proteins and then loaded onto a prepared Mini-PROTEAN TGX gel (Bio-Rad #4569036). Sodium dodecyl sulphate–polyacrylamide gel electrophoresis (SDS PAGE, 200V) was used to separate the proteins according to molecular weight. Proteins were transferred onto nitrocellulose membranes using the Trans-Blot Turbo Transfer system (Bio-Rad #17001918). Membranes were incubated in blocking buffer (5% BSA in TBST) for 1 hour at room temperature to prevent non-specific binding and then overnight at 4°C in primary antibody solution (Table 2.1). Membranes were washed 3 times in TBST (1% Tween) for 10 minutes and then incubated for 1 hour at room temperature in secondary antibody solution (Table 2.1). Primary and secondary antibodies were diluted in blocking buffer and TBST respectively, in accordance with supplier instructions. Membranes were washed twice for 10 minutes in TBST, then once for 10 minutes in TBS. ECL substrate (Bio-Rad #1705060) was applied for 5 minutes. Membranes were imaged using the ChemiDoc System by Bio-Rad and analysed using Image Lab software. Densitometry analysis was used to quantify and standardise the expression of all proteins relative to constitutively expressed β -actin.

Antibody	Supplier	Product number
pSTAT3	Santa Cruz Biotechnology	Sc-0859
STAT3	Cell Signalling	#9139
STING	Cell Signalling	#13647
SOCS3	Cell Signalling	#2932
β -actin	Cell Signalling	#3700
LC3B	Cell Signalling	#3868
Beclin-1	Cell Signalling	#3495
Anti-mouse	Cell Signalling	#7076
Anti-rabbit	Cell Signalling	#7074

Table 2.1. Antibodies used in western blot and their product numbers.

2.3. qPCR Analysis

2.3.1. mRNA Extraction

For cell analysis, media was removed from wells and 200 μ l TRI reagent (Sigma T9424) was added. Adherent cells were dislodged into TRI, transferred to Eppendorf tubes, and stored on ice overnight. For tissue analysis, homogenised tissue samples stored in TRI reagent (Sigma T9424) at a concentration of approximately 50mg/ml were thawed at room temperature.

Chloroform (Sigma 319988) was added (200 μ l per 1ml of TRI) and samples were shaken vigorously, incubated at room temperature for 10 minutes and centrifuged at 12,000g for 15 minutes at 4 $^{\circ}$ c. Upper aqueous phases were transferred to sterile Eppendorf tubes and the lower phases were discarded. 2-propanol (Sigma I9516) was then added (500 μ l per 1ml of TRI reagent) and samples were incubated at room temperature for 10 minutes, then centrifuged at 12,000g for 10 minutes at 4 $^{\circ}$ c. Supernatant was discarded, then RNA pellets were washed with a minimum of 1ml 75% ethanol per 1ml of TRI reagent. Samples were vortexed and then centrifuged for 5 minutes at 7,500g. Excess ethanol was removed, and samples were air dried at room temperature for 10 minutes. Pellets were dissolved in nuclease free water (30 μ l for cell analysis, 100 μ l for tissue analysis) by pipetting. The concentration and purity of mRNA was determined using the Thermo Scientific NanoDrop 2000 spectrophotometer.

2.3.2. Reverse Transcription

cDNA was generated from 1 μ g of mRNA. mRNA (1 μ g) in solution was transferred to a sterile Eppendorf tube and volume was made up to 12 μ l using nuclease-free water. 0.5 μ l of oligo(dT) primer was added and the tubes were incubated at 65 $^{\circ}$ c for 5 minutes, centrifuged briefly and stored on ice. Each tube received 4 μ l 5x reaction buffer (Thermo), 1 μ l 10mM dNTP (Fermentas) and 1 μ l of Revertaid reverse transcriptase (Thermo #EP0441). Reactions were

incubated at 42°C for 60 minutes, then at 70°C for 10 minutes. Resulting cDNA was stored on ice until further use.

2.3.3. qPCR

Relative SOCS3 expression was measured using qPCR and normalized through comparison with expression of the housekeeping gene ribosomal protein lateral stalk subunit P0 (RPLP0). Cycle threshold (Ct) values for both genes in each cell line were used to calculate the ΔC_t , which normalises SOCS3 expression against the control. SOCS3 expression was then calculated as fold change relative to empty vector controls. hSOCS3 and RPLP0 forward and reverse primers (100 μ M) were diluted 10-fold with nuclease-free water. Master Mix was prepared using either hSOCS3 or RPLP0 primers, and sufficient volumes were prepared to run all samples in duplicate, according to manufacturer instructions. Real-Time PCR was performed using SYBR Green JumpStart Taq ReadyMix, 10 μ M forward primer, 10mM reverse primer and nuclease-free water by Sigma. Master mix (19 μ l) was aliquoted into all plate wells. cDNA and nuclease-free water (1 μ l each) were added to test wells and no template control wells, respectively. Cycling conditions were 94°C for 2 min, 40 \times 94°C for 15 s, and 60°C for 1 min. Primer sequences used to amplify hSOCS3 were as follows. Forward: 5'-GGCCACTCTTCAGCATCTC and Reverse: 5'-ATCGTACTGGTCCAGGAACTC. Primer sequences used to amplify RPLP0 were Forward: 5'-GCAATGTTGCCAGTGTCTG and Reverse: 5'-GCCTTGACCTTTTCAGCAA

2.4. Intestinal Tissue Homogenisation

From each of 13 patients undergoing loop ileostomy surgery reversal, one functioning and one defunctioned ileal resection specimen was obtained and stored at -80°C . Cell lysis solution was prepared using lysis buffer, protease inhibitor and phosphatase inhibitor in a 1000:1:1 ratio. Samples were weighed and the volume of lysis buffer required to achieve total protein concentrations of approximately 10mg/ml of homogenized tissue were calculated. Tissue samples were bisected accordingly and homogenized in lysis solution to extract the protein content. Samples were homogenized using the LabGEN 125 tissue homogenizer by Cole-Palmer and stored at -80°C .

2.5. Bradford Assay

Protein concentration was determined using the Bradford assay. Bradford reagent was brought to room temperature. Protein standards ranging from 5mg/ml to 0.156mg/ml were prepared by conducting a 2-fold serial dilution of BSA in 1 x PBS. Homogenised tissue samples in lysis buffer were thawed on ice. The range of protein concentrations detectable by the Bradford assay is 0.1–1.4 mg/ml. Samples were homogenised at approximately 10mg/ml and therefore were diluted 10-fold to fall within this range. 5 μl of BSA standards were pipetted into 6 of the 96 wells, and 6 μl of 1 X PBS only was pipetted into the seventh. 5 μl of protein samples (concentrations unknown) were pipetted into subsequent wells in duplicate. 250 μl of Bradford reagent was added to all control and test wells and mixed gently. Absorbance at 595nm was measured using the Tecan spectrophotometer. Net absorbance by BSA protein standards at 595nm was calculated and used to create a standard curve from which the concentrations of test samples could be deduced.

2.6. Measurement of Villous Height

Tissue biopsies from functioning and defunctioned intestine were examined using a Motic BA210E microscope at 200x magnification. Sections were fixed for 24 hours in 4% paraformaldehyde solution and haematoxylin and eosin (H&E) stained, as described in Beamish et al (Beamish et al., 2017). Scale was calculated using the line drawing function to mark the known distance between two hash marks on a graticule. Per patient, all villi which had not been structurally altered or impaired during preparation were identified and measured using the line drawing function (Figure 2.1). The biopsies examined were those prepared in Beamish et al (2017), which had not yet been examined

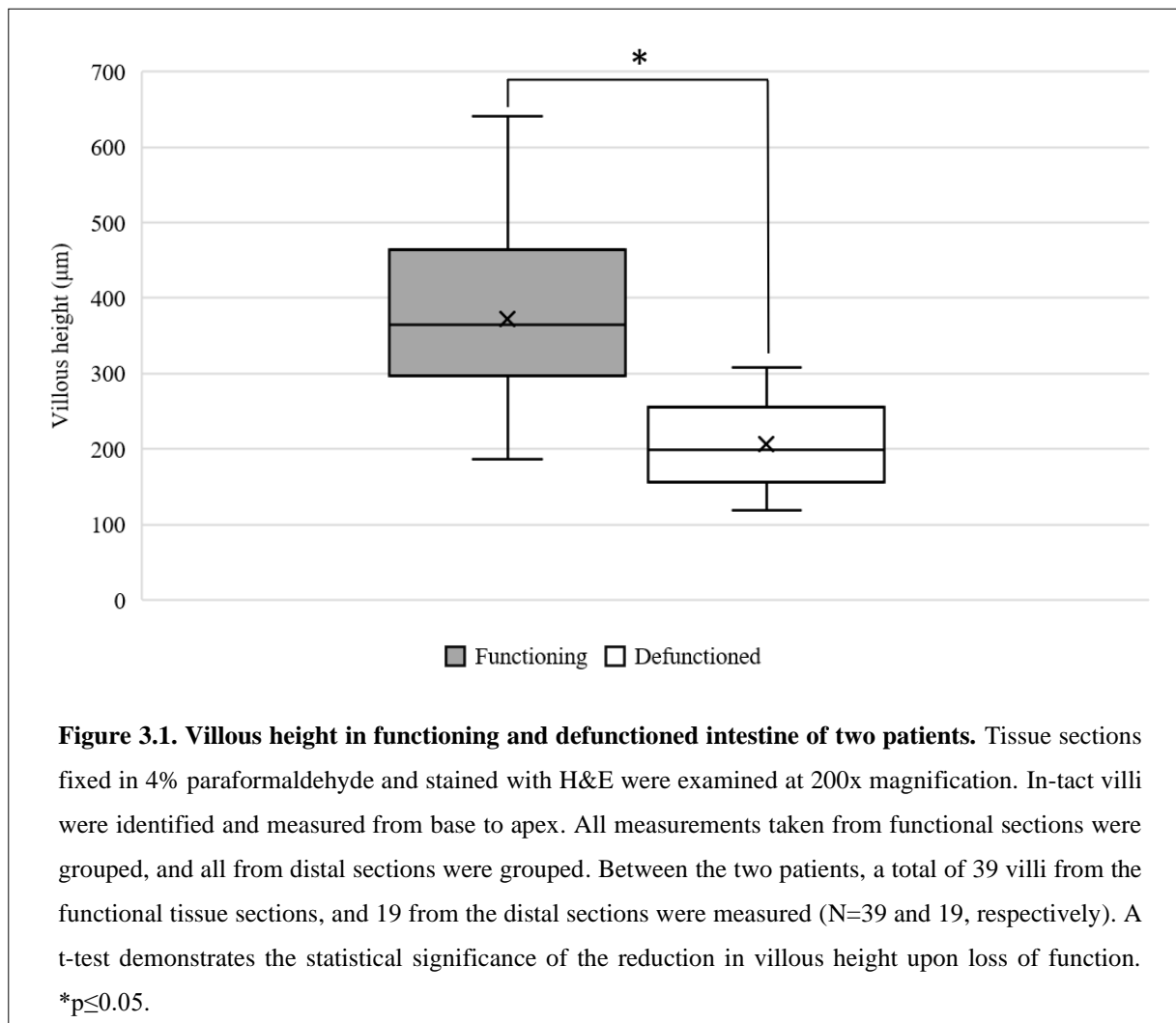


Figure 2.1. Measurement of villous height. Scale was calculated using magnification and actual distance between 2 hash markings on a graticule. The line drawing function was then used to mark the distance between the base and apex of intact crypts seen in tissue sections fixed with 4% paraformaldehyde and stained with H&E stain.

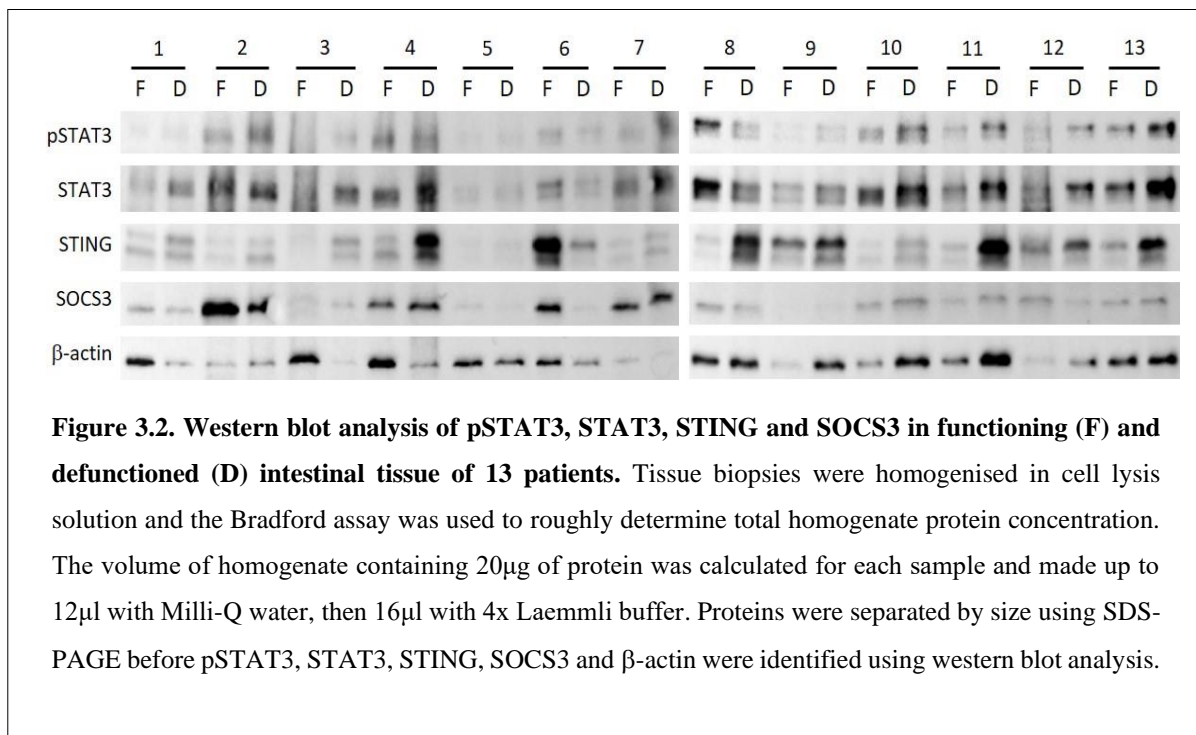
3. The Impact of Microbiome Manipulation on Signalling in the Human Intestine

3.1. Results

Villi were measured in both the functioning and defunctioned intestine of each patient, and all measurements were grouped to form one set of data for functional tissue, and one for defunctioned. The biopsies examined were those prepared in Beamish et al (2017), which had not yet been analysed, therefore two individuals were used. Histological examination of the tissue revealed that loss of function caused atrophy, characterised by significant reductions in villous height, ranging from 27.7% - 75.5% (Figure 3.1).



The expression of inflammation signalling proteins STAT3, STING and SOCS3 was compared between tissue biopsies taken from functioning (F) and defunctioned (D) human intestine (Figure 3.2). Expression in defunctioned tissue was calculated as a percentage change from the expression in normal tissue. Outliers greater than two standard deviations from the mean were excluded. Patients 2 and 12 were consistently identified as outliers and excluded from the dataset. We find that bowel defunction did not significantly impact the expression of these inflammatory signalling proteins (Figure 3.3). This suggests that the observed reduction in villous height was not a consequence of the inflammatory signalling pathways studied, and substantiates the conclusion that chronic inflammation was not present at the time of reversal drawn by Beamish et al.



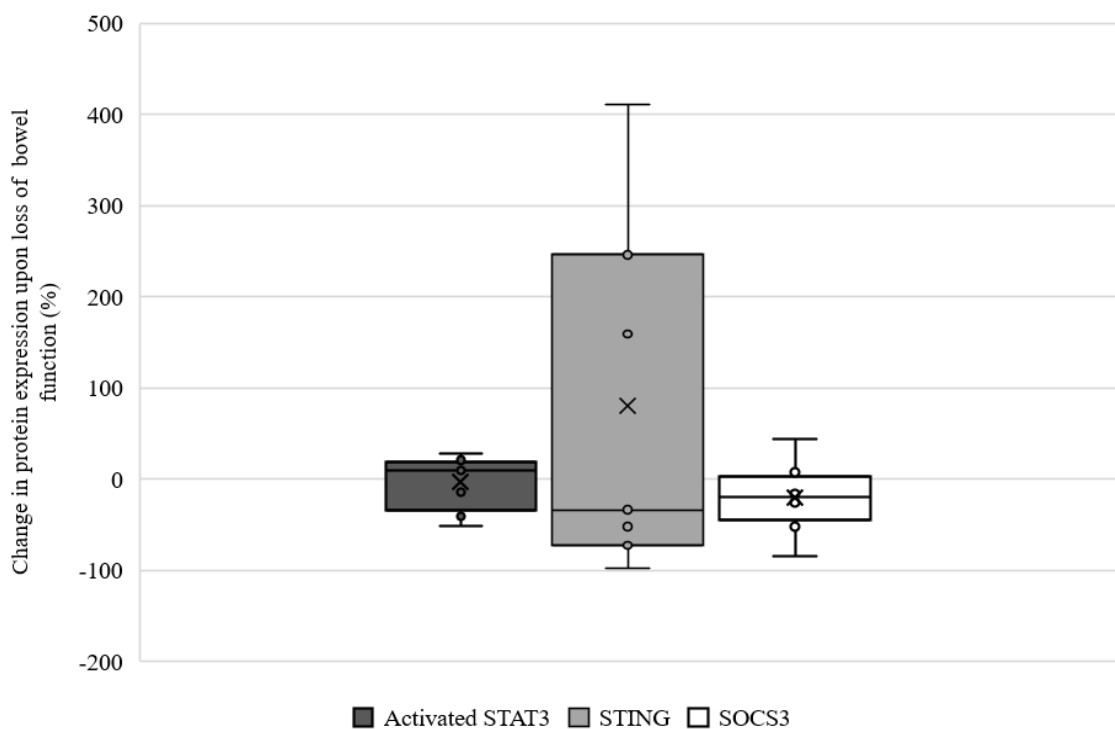


Figure 3.3. Percentage change in activated STAT3, STING and SOCS3 in defunctioned bowel, relative to functioning tissue. Densitometry analysis was used to calculate normalised expression of activated STAT3, STING and SOCS3. The abundance of protein was determined relative to β -actin in each sample. Normalised protein expression in the defunctioned bowel was then expressed as percent change from that in the functional tissue of each individual patient. STAT3 activation by phosphorylation at Tyr 705 was determined by calculating pSTAT3 as a proportion of total STAT3. Instances in which either the protein of interest or beta actin produced insufficient signal to obtain an accurate result were excluded therefore N=8, 7 and 8, respectively.

The role of autophagy in the reported villous atrophy was then examined using western blot to compare the expression of the marker of autophagy beclin-1 in the functioning and defunctioned tissue (Figure 3.4). Again, patients 2 and 12 were excluded from the dataset and the remaining samples were analysed. Expression in defunctioned tissue was calculated as a percentage change from the expression in normal tissue (Figure 3.5). There was a significant increase in beclin-1 expression upon loss of ileal function ($p < 0.05$) which implicates autophagy in the atrophy of defunctioned tissue.

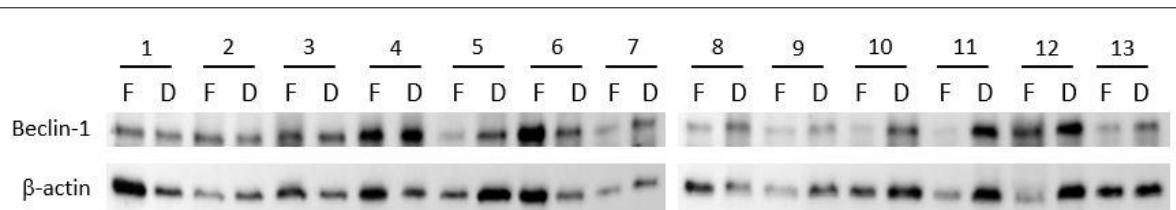


Figure 3.4. Western blot analysis of the autophagy marker beclin-1 in functioning and defunctioned intestinal tissue of 13 patients. Tissue biopsies were homogenised in cell lysis solution and the Bradford assay was used to roughly determine total homogenate protein concentration. The volume of homogenate containing 20µg of protein was calculated for each sample and made up to 12µl with Milli-Q water, then 16µl with 4x Laemmli buffer. Proteins were separated by size using SDS-PAGE before beclin-1 and β-actin were identified using western blot analysis.

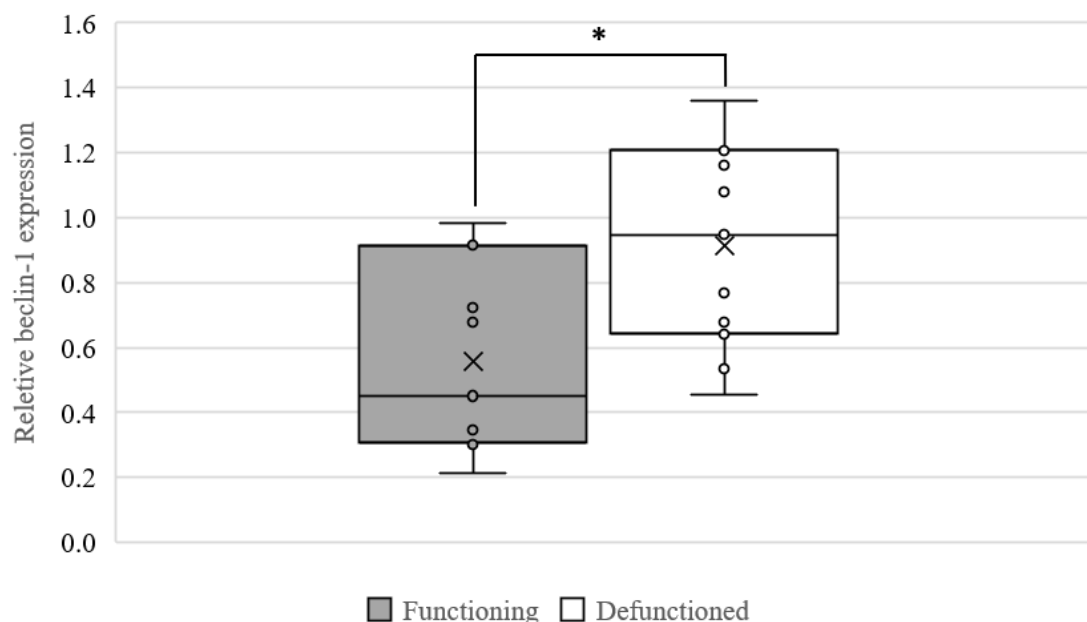
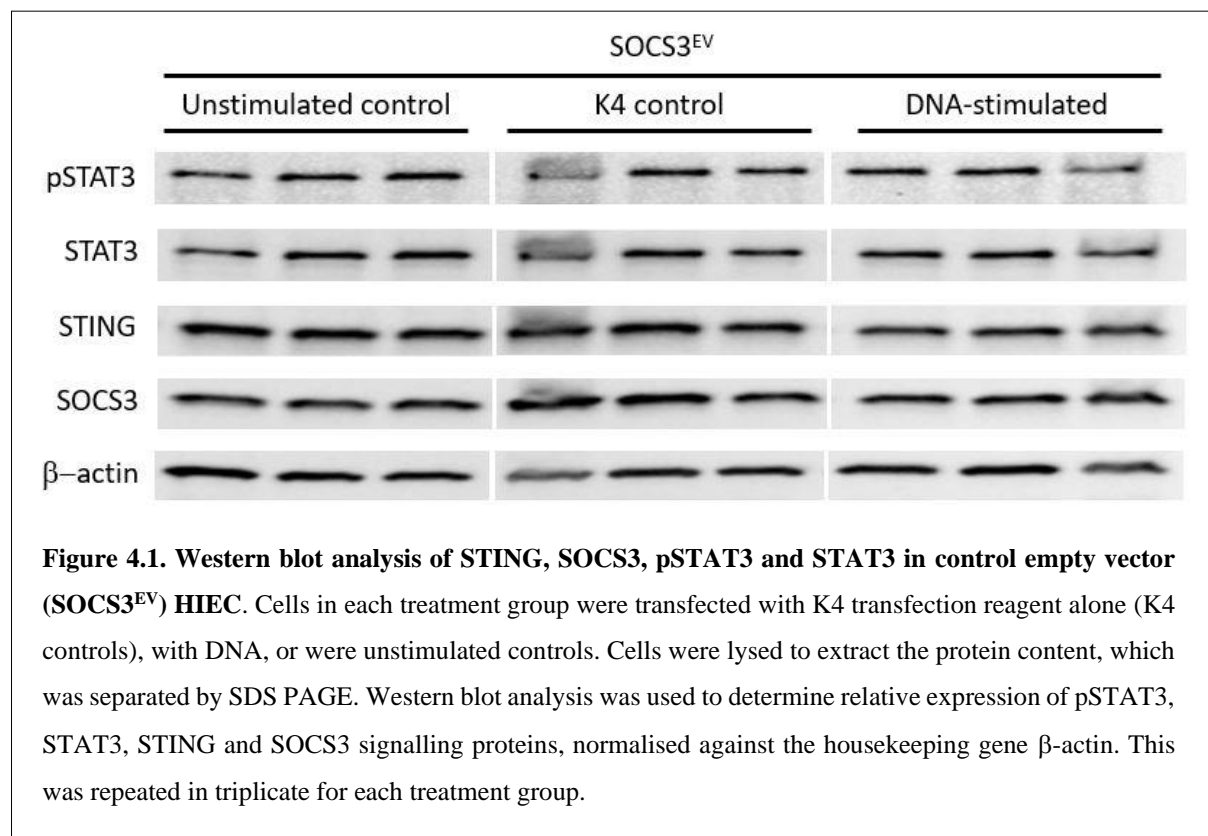


Figure 3.5. Beclin-1 expression in functioning and defunctioned bowel. Densitometry analysis was used to determine the abundance of beclin-1 relative to β-actin in each sample. Normalised beclin-1 expression in the defunctioned bowel was expressed as percent change from that in the functional tissue of each individual. N=11. * $p \leq 0.05$.

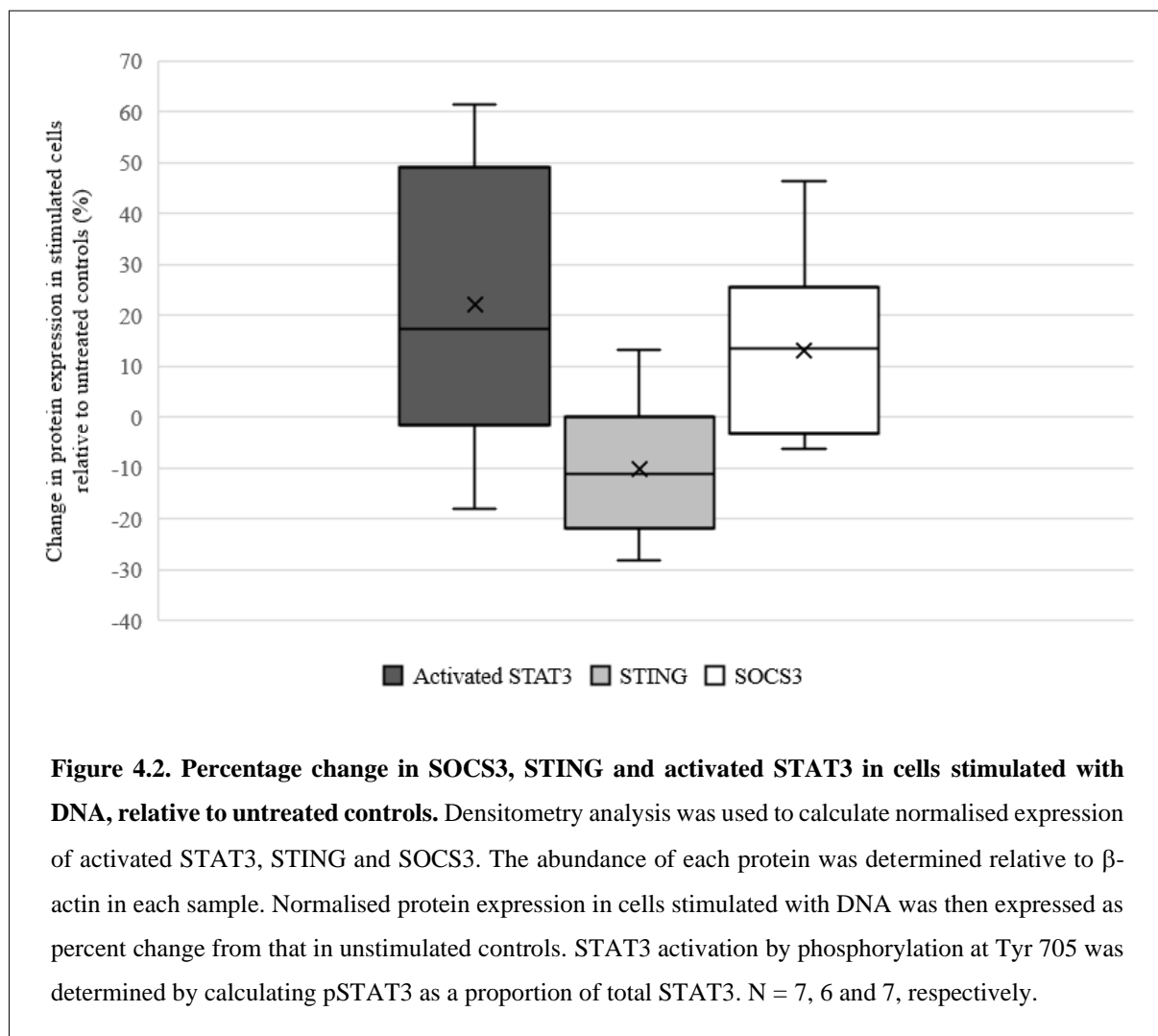
4. The Impact of SOCS3 on Microbiome Signalling in Human Intestinal Epithelial Cells (HIEC)

4.1. Results

Microbiome modulation was modelled using DNA transfection in control SOCS3^{EV} HIEC and the expression of inflammatory signalling proteins STAT3, STING and SOCS3 in both transfected and untreated control cells was assessed (Figure 4.1).

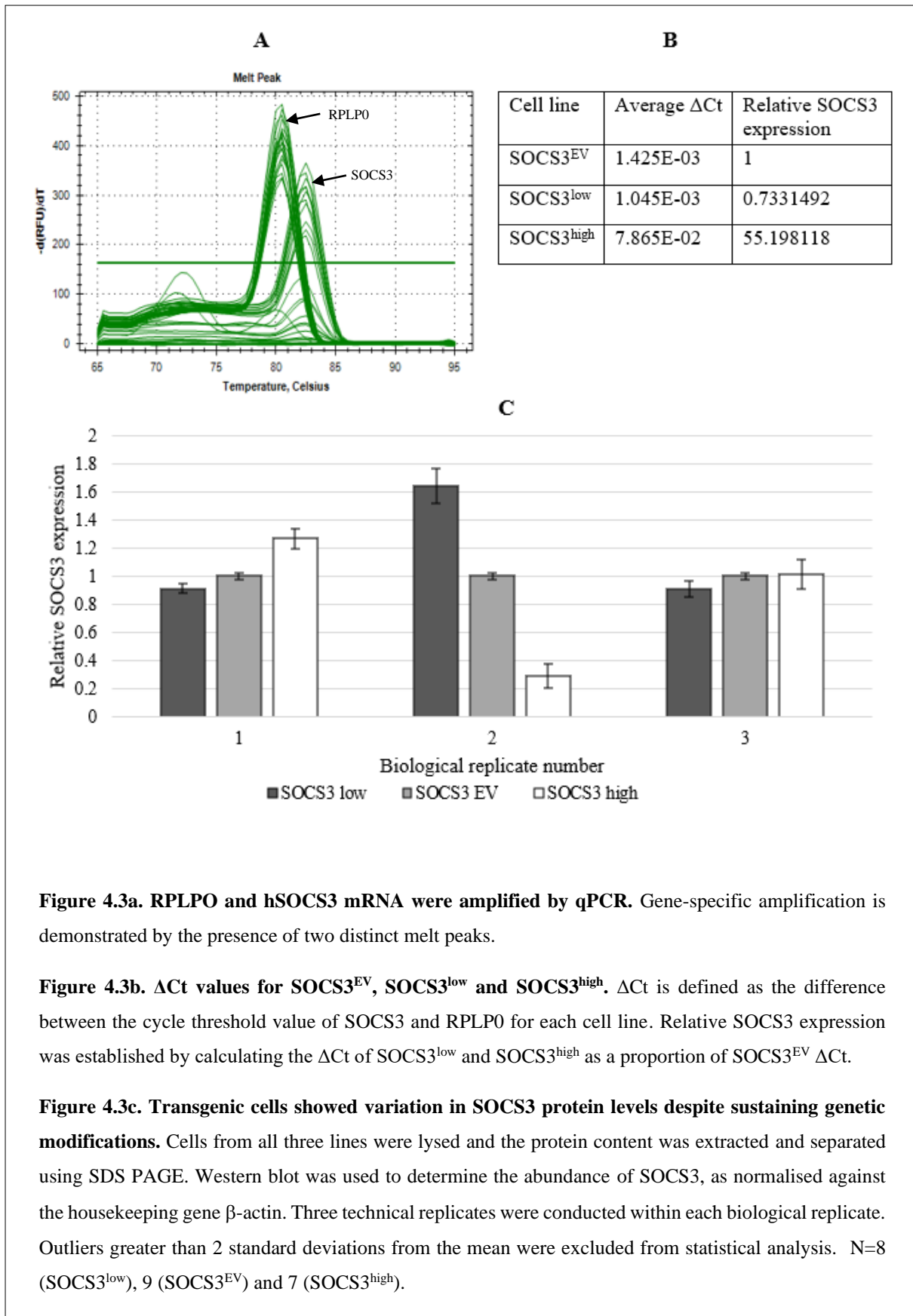


The expression of each protein within DNA-stimulated cells was determined relative to that in untreated controls, and the percentage change was calculated. Outliers greater than two standard deviations from the mean were excluded from the dataset. Although the results imply a tendency for increased SOCS3 and STAT3 activation, STING activation tends to decrease (Figure 4.2). The calculated p values were however non-significant and so modelling microbiome manipulation using DNA transfection did not affect the expression of inflammatory signalling proteins SOCS3, STAT3 or STING signalling in control HIEC.

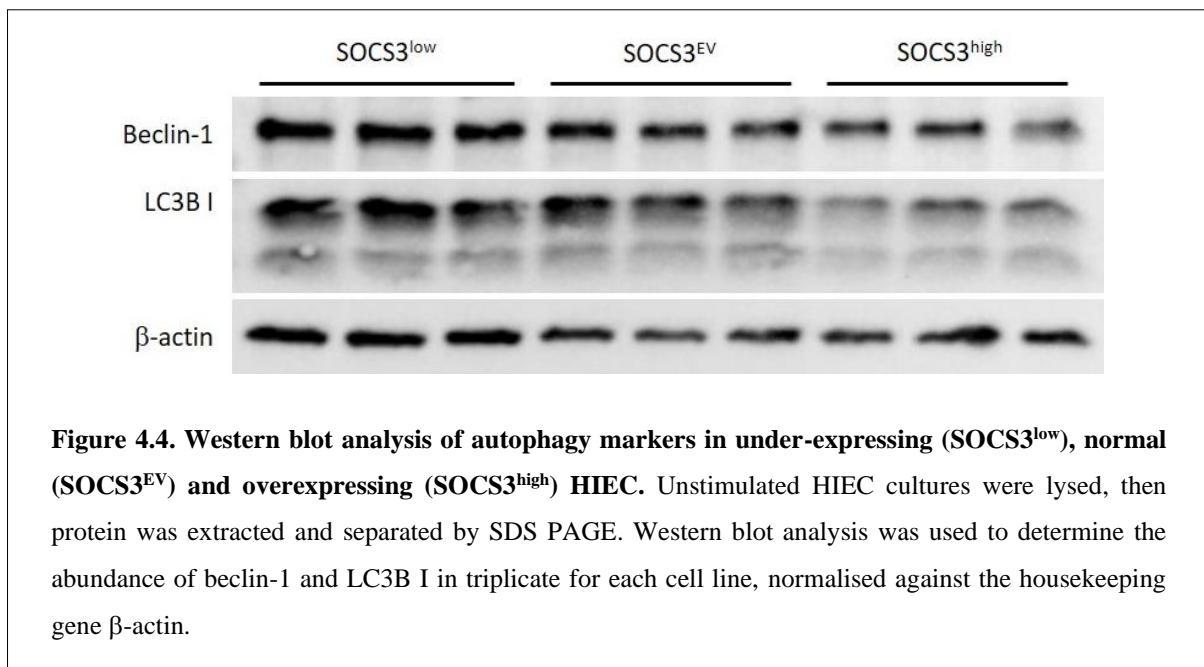


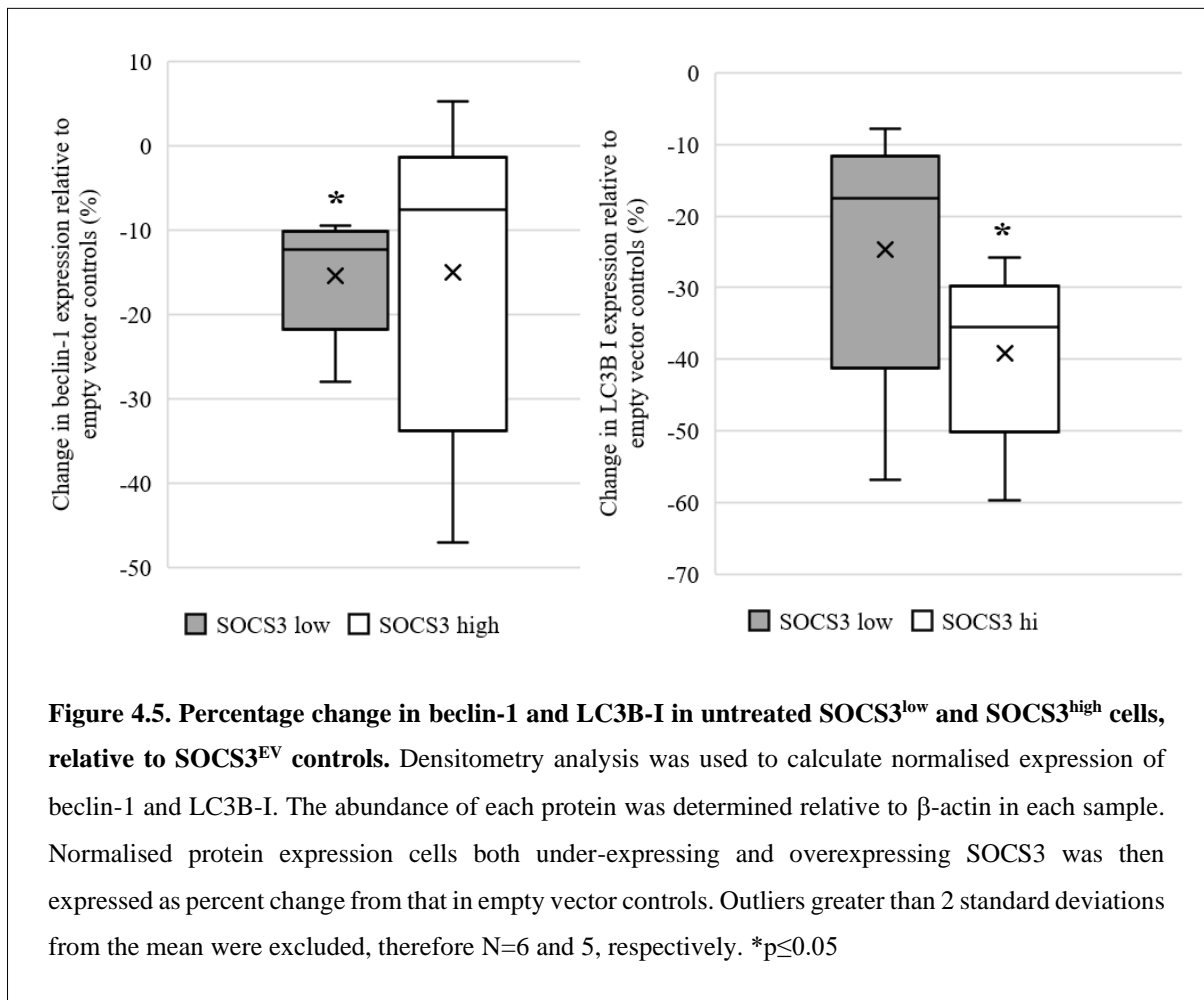
We then sought to determine the effect of SOCS3 expression on the response of HIEC to DNA transfection. Firstly, qPCR verified that transgenic cells were expressing SOCS3 as intended. SOCS3 mRNA was normalized against the housekeeping gene RPLP0 (Figure 4.3a) and compared between the three cell lines. Ct values confirmed that relative to empty vector controls, SOCS3 mRNA transcription was 30% lower and 55-fold greater in SOCS3^{low} and SOCS3^{high} cells, respectively (Figure 4.3b). The expression of SOCS3 by SOCS3^{low}, SOCS3^{EV} and SOCS3^{high} cells under normal conditions was normalised against β -actin. Within the first biological replicate, SOCS3 protein was present as expected in all three cell lines. However, within the second replicate, the protein levels in both transgenic cell lines appeared completely inverted; SOCS3^{low} cells seemingly upregulated the protein relative to empty vector controls, and SOCS3^{high} the contrary. Within the third replicate, SOCS3 protein levels were similar across all three cell lines (Figure 4.3c).

Overall, based on average protein levels alone, SOCS3 expression showed little variation between the three cell lines. However, Ct values generated by qPCR demonstrated that modifications were sustained at the genetic level. Furthermore, all three cell lines maintained their expected phenotype throughout. SOCS3^{low} cells proliferated rapidly, meanwhile SOCS3^{high} cells displayed a much slower turnover rate.



To investigate the potential link between SOCS3 and autophagy, beclin-1 and LC3B-I expression was assessed (Figure 4.4). Relative to empty vector controls, beclin-1 and LC3B-I were downregulated in both SOCS3^{low} and SOCS3^{high} cells (Figure 4.5). There was a mean decrease of 15.4% in beclin-1 expression by SOCS3^{low} cells and a mean decrease of 39.1% in LC3B-I by SOCS3^{high} cells. From these results, we can deduce that, relative to SOCS3^{EV} controls, autophagy is downregulated in SOCS3^{low} cells and upregulated in SOCS3^{high} cells.





Finally, to investigate the effect of SOCS3 expression on the response of HIEC to cytosolic DNA, SOCS3^{low}, SOCS3^{EV} and SOCS3^{high} HIEC were transfected with DNA as described in section 2.1.3. Activation of STAT3 and expression of STING was assessed using western blot analysis, as described in section 2.2. (Figure 4.6). The expression in SOCS3^{low} and SOCS3^{high} cells was calculated as percentage change from that in SOCS3^{EV} controls (Figure 4.7). Although the data may illustrate modest increases in STAT3 and STING activation in cells both under-expressing and overexpressing SOCS3, the p values are non-significant. Therefore, SOCS3 expression did not affect the response of HIEC to the presence of cytosolic DNA.

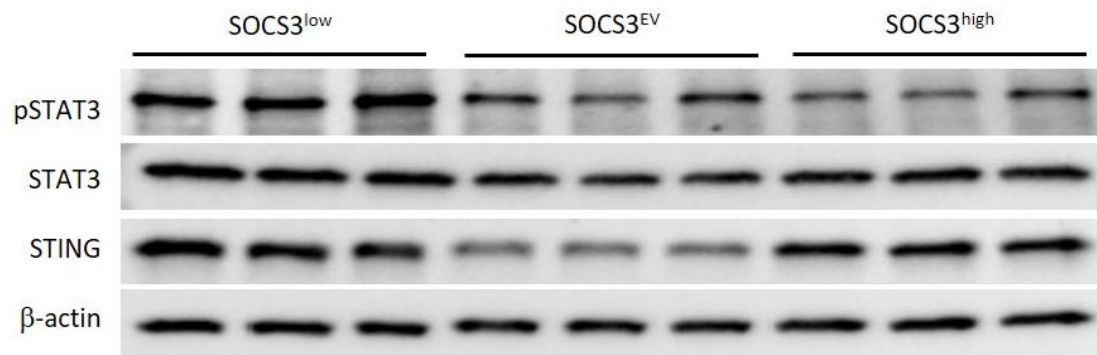


Figure 4.6. Western blot analysis of pSTAT3, STAT3 and STING in under-expressing (SOCS3^{low}), normally expressing (SOCS3^{EV}) and over-expressing (SOCS3^{high}) HIEC transfected with DNA. HIEC cultures which normally expressed, under-expressed and overexpressed SOCS3 were transfected with herring sperm DNA and lysed. Protein from the cell lysate was separated by SDS PAGE and used for western blot analysis of pSTAT3, STAT3 and STING signalling protein expression, normalised against the housekeeping gene β -actin. This was repeated in triplicate for each cell line.

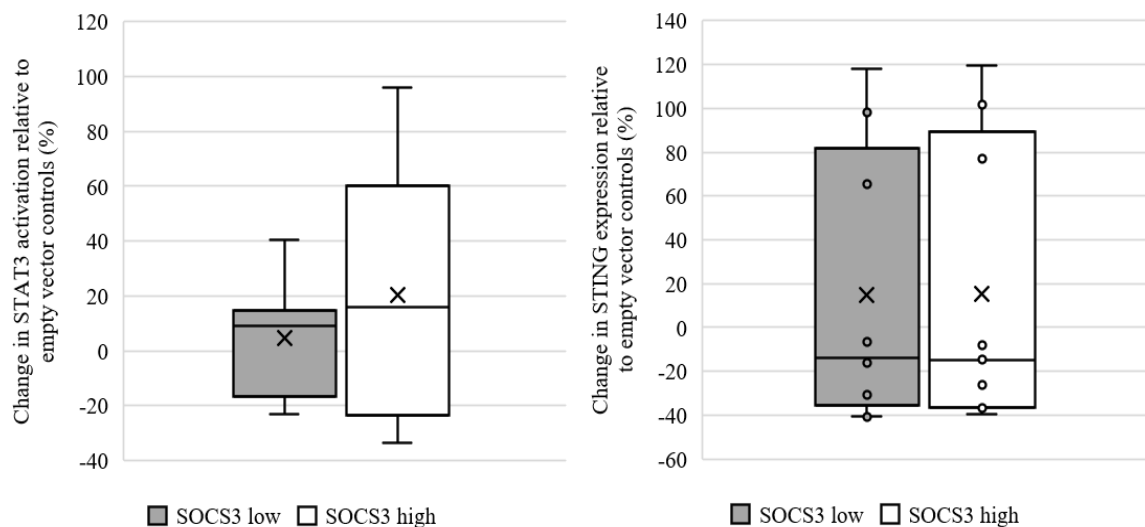


Figure 4.7. Percentage change in the expression of activated STAT3 and STING in under-expressing (SOCS3^{low}) and overexpressing (SOCS3^{high}) cells, relative to empty vector controls (SOCS3^{EV}) following transfection with DNA. Densitometry analysis was used to calculate normalised activation of STAT3 and expression of STING. The abundance of each protein was determined relative to β -actin in each sample. Normalised protein expression cells both under-expressing and overexpressing SOCS3 was then expressed as percent change from that in empty vector controls. STAT3 activation by phosphorylation at Tyr 705 was determined by calculating pSTAT3 as a proportion of total STAT3. N=9.

5. Discussion

5.1. Summary of Findings

This thesis sought to investigate the effects of microbiome manipulation and SOCS3 expression on cell signalling and autophagy in human intestinal epithelial cells and in functioning and defunctioned human intestine.

In HIECs, DNA transfection was used as a model for viral infection and instigation of microbiome modulation, meanwhile SOCS3 expression was modulated using cell lines transfected with empty vector plasmids, SOCS3 expression plasmids and non-silencing shRNA lentiviral constructs. In human intestine, biopsies were taken from tissue adjacent to the site of loop ileostomy surgery which rendered it functional or defunctioned and thus harbouring a normal or depleted microbiota, respectively (Beamish et al., 2017). SDS PAGE, western blot and densitometry analysis were then used to quantify protein expression.

Whilst microbiome depletion affected autophagy in the human intestine, it did not impact SOCS3, STAT3 or STING signalling in human intestine or in HIECs. Furthermore, manipulation of SOCS3 was not found to impact STAT3 or STING signalling in HIECs but was again closely linked with autophagy.

5.2. Clinical Relevance

Loop ileostomy is a procedure used to protect intestinal anastomoses formed upon removal of a tumour from the colon and is usually reversed upon anastomotic healing, although some stoma formations are non-reversible due to complications and various patient morbidities

(Gessler et al., 2012, Chow et al., 2009). It is well known that the initial procedure renders the distal ileum defunctioned and atrophied (Winslet et al., 1991, Williams et al., 2007) however more recent research has suggested that despite this, there is no chronic inflammation in the defunctioned tissue based upon histological examination (Beamish et al., 2017). Furthermore, loss of function leads to decreased IEC proliferation and induces dysbiosis, with reductions in both bacterial load and diversity owed to nutrient deprivation (Beamish et al., 2017).

5.3. Defunctioned Bowel Shows no Biochemical Signs of Inflammation

Throughout the elucidation of the composition and function of the gut microbiome, our understanding of the virome – its viral component – remained poor. In fact, our acceptance of viruses as a component of a healthy microbiota is due to technological advances which have only recently made it possible to sequence these residents of the gut (Angly et al., 2005, Reyes et al., 2012). The virome is predominantly, but not exclusively, composed of bacteriophages which infect the bacteria of the microbiome and hence are heavily influential in the composition of the microbiota. In addition, viruses which infect both human cells and resident archaea are present.

We have now obtained further evidence that the atrophied intestine is not chronically inflamed despite the occurrence of dysbiosis. Firstly, biochemical analysis of functioning and defunctioned tissue revealed that SOCS3, STAT3 and STING signalling pathways were not significantly impacted by DNA transfection by way of bowel defunction. Further non-significant changes were observed during *in vitro* studies, in which microbiome modulation was modelled by DNA transfection of HIECs with exogenous DNA.

5.4. Autophagy is Implicated in Atrophy of the Defunctioned Bowel

The histological analysis of functioning and defunctioned tissues conducted in this study supplemented the data collected by Beamish and colleagues (Beamish et al., 2017). Collaboratively, we observe villous atrophy in the defunctioned tissue, with a mean height reduction of $47\% \pm 13.7$.

Loss of ileal function led to significant upregulation of autophagy, as indicated by beclin-1 expression. The nutrient-deprived ileum is subject to villous atrophy as well as loss of contractility and smooth muscle strength, which ultimately contribute to the complications experienced by many patients (Williams et al., 2007, Beamish et al., 2017).

Upon diversion of the faecal stream, the distal ileal limb was deprived of enteral nutrition. Autophagy is a crucial process in sustaining cells placed under a range of stressors (Mizushima and Klionsky, 2007). It is likely that nutrient deprivation activated autophagy in the affected cells and recycled amino acids derived from the degraded proteins and organelles to obtain energy. In the short term, this mechanism allows cells to remain viable. However, to maintain tissue mass the rate of breakdown must equal the rate of synthesis. The tissues examined here were deprived of nutrition for prolonged periods and as such protein synthesis could not match its lysosomal degradation.

In intestinal epithelial cells, such as those lining the crypts and villi, the most immediate response to nutrient deprivation is repression of cell growth and proliferation, as observed by Beamish et al. (Beamish et al., 2017). These processes require an energy surplus to proceed, but during prolonged periods of stress their termination is likely insufficient to retain cell viability and so lysosomal degradation of long-lived proteins and organelles may be upregulated. Reduced IEC proliferation to preserve energy, coupled with upregulated

autophagy to obtain it, creates an imbalance which favours atrophy of the intestinal epithelium, as seen by Williams and colleagues (Williams et al., 2007).

Muscle tissue is the most abundant source of protein in the body. As well as numerous regulatory proteins found ubiquitously throughout eukaryotic cells, muscle cells harbour contractile proteins which generate the forces required to elicit contractions (Eddinger, 2014). In the case of smooth muscle within the intestine, these contractile forces are necessary to move the bolus through the gastrointestinal tract. Prolonged lysosomal degradation of protein comprising smooth muscle within the intestine will almost certainly have detrimental impacts to the function of the muscle, accounting for the well-documented loss of contractility and strength (Williams et al., 2007), as well as the marked increase in beclin-1 in defunctioned tissue observed in this study.

5.5. The Link Between STING and SOCS3 Expression

Whilst the results suggest a tendency for reduced STING activation in both transgenic cell lines in response to microbiome manipulation, the p value indicates that this is non-significant. Upon closer investigation of the results, it is apparent that such a reduction is only observed in cells where SOCS3 protein levels have begun to fluctuate. Meanwhile in cells where SOCS3 protein is expressed as expected, there is a statistically significant upregulation of STING in cells both under- and overexpressing SOCS3, relative to empty vector controls.

Overall, these data indicate that SOCS3 expression does not impact the cGAS-STING mediated response to cytosolic DNA. Within the first biological replicate, the relative increase in STING expression in both SOCS3^{high} and SOCS3^{low} cell lines was comparable in mean and range. Similarly, within the second and third biological replicates the relative decrease was near-identical in both measures. Whilst this indicates that SOCS3 under- and overexpression

does not impact STING signalling, it is worth noting that the apparent compensatory modulation of SOCS3 by the cells themselves coincides with the change from upregulation to downregulation of STING in both transgenic lines. It should therefore perhaps be considered that the mechanisms negating the changes to SOCS3 expression are also impeding the ability of these cells to activate STING in response to cytosolic DNA sensing. Meanwhile, in SOCS3^{EV} cells, where no changes to SOCS3 expression were introduced, STING expression remained consistent.

Whilst transgenic cells within the third biological replicate continued to underexpress STING relative to normal controls, beclin-1 expression became upregulated at this point. Upregulation of beclin-1 is an indicator of autophagy and has been linked with STING degradation (Liang et al., 2014). STING activation is required for the degradation of cytosolic DNA, however sustained activation would cause prolonged inflammation and have catastrophic effects on the host, meaning its termination is as important as its activation (Li et al., 2017). Both the activation and the subsequent repression of STING are dependent on the production of cyclic dinucleotides by cGAS. Initially, cGAS catalyses a reaction between GTP and ATP to form the cyclic dinucleotide cGAMP, which binds and activates STING (Wu et al., 2013). However, once a sufficient response is elicited, cyclic dinucleotides also activate the Unc-51 like autophagy activating kinase 1 (ULK1), which represses STING via IRF3 (Konno et al., 2013). Additionally, beclin-1 interacts with cGAS to inhibit cGAMP production and STING activation. This interaction also releases the beclin-1 inhibitor Rubicon from its complex and induces beclin-1-mediated autophagy (Matsunaga et al., 2009, Liang et al., 2014). Collectively, these mechanisms culminate in inverse activation of beclin-1 and STING.

5.6. Limitations

5.6.1. The Reliability of LC3B as a Measure of Autophagic Flux

Under standard conditions, the LC3B protein, encoded by the *MAP1LC3B* gene is expressed and cleaved to form LC3B-I (He et al., 2003). During nutrient deprivation cytosolic LC3B-I is converted to the autophagosome membrane component LC3B-II (Tanida et al., 2008). Although both forms are detectable by western blot, the use of LC3B as a measure of autophagic flux is controversial. On one hand, formation of LC3B-II is an unequivocal indication of autophagy induction as it directly corresponds with autophagosome formation. On the other hand, LC3B-II itself is degraded by autophagy, making its quantification an inaccurate reflection of autophagic flux (Mizushima and Yoshimori, 2007). With this limitation in mind, the optimal technique would be to measure LC3B-II levels in the presence and absence of lysosomal inhibitor, considering the difference to represent the protein utilised in autophagosome formation (Chittaranjan et al., 2015). Furthermore, LC3B-I and LC3B-II are often unequal in their affinity for the anti-LC3B antibody (Barth et al., 2010).

It was apparent from the western blots (Figure 4.4.) that LC3B-I has a higher affinity for the antibody used in this instance, and so its abundance must be considered our most reliable indication of autophagic flux. Lacking a means of inhibiting lysosome formation, LC3B analysis is used simply to support or dispute the conclusions drawn upon analysis of beclin-1 data. In HIEC, we associate high LC3B-I band density with lower rates of conversion to LC3B-II, given the consistency in LC3B-II. We therefore negatively correlate LC3B-I and autophagy.

Unfortunately, a similar approach could not be applied to the human intestine. The Bradford assay was used to calculate the crude total protein concentration in each tissue specimen, however this technique is prone to inter- and intra-assay variability (Rossi et al.,

2015b). Furthermore, serial dilution of BSA was conducted to calibrate the assay and this is often associated with error propagation, resulting in inaccurate interpretation (Higgins et al., 1998). In accordance with the concentrations calculated, 20µg of protein was used for SDS PAGE but western blot still revealed discrepancies in the protein concentration of different samples. As a result – and given its relatively low affinity for the antibody used – LC3B-II in human intestinal tissue was often undetectable and LC3B-I band density could not be used as a surrogate for conversion.

5.6.2. The Impact of SOCS3 Regulation by Autophagy

Western blot analysis revealed that within the first biological replicate, cells expressed the SOCS3 protein as expected. However, this appeared to be completely reversed in cells within the second biological replicate. By the time cells within the third biological replicate were harvested, SOCS3 protein levels were similar across all cells. However, all cell lines maintained the expected phenotypes throughout; SOCS3^{low} cells rapidly proliferated, meanwhile the larger SOCS3^{high} cells divided slowly. This phenotypic stability suggested that there had been no disruption to the changes made at the genetic level. Furthermore, the phenomenon of genetic compensation has been frequently reported in knockout cells but not in knockdowns, so it is unlikely that the transgenic cells produced would be capable of reversing the genetic modifications incurred (Tondeleir et al., 2012, Rossi et al., 2015b, Rossi et al., 2015a, Buglo et al., 2020). qPCR demonstrated that relative to empty vector controls, SOCS3 mRNA transcription was 30% lower and 55-fold greater in SOCS3^{low} and SOCS3^{high} cells, respectively. This confirmed that genetic compensation was not responsible for the changes observed and justified categorization of SOCS3 expression as ‘high’, ‘normal’ or ‘low’ based on functional characteristics, as opposed to protein levels. Afterall, SOCS3 is an

oscillatory protein and its expression is regulated in a number of ways (Yoshiura et al., 2007). In the intestinal epithelium, SOCS3 overexpression inhibits JAK/STAT signalling and is associated with IBD pathogenesis and relapse (Li et al., 2013). Meanwhile, under-expression facilitates hyperproliferation within intestinal crypts, causing inflammation and potentially tumour formation (Rigby et al., 2007). Furthermore, complete SOCS3 knockout causes embryonic lethality, reinstating the critical nature of its tight regulation (Roberts et al., 2001). With this in mind, it is unsurprising that transgenic cells should so stringently modulate the expression of this protein, despite changes at the genetic level.

Given that the SOCS3 gene was transcribed as expected in all cell lines, it was logical to propose that degradation was occurring at the SOCS3 protein level. To investigate this possibility, the markers of autophagy beclin-1 and LC3B-I were analysed using western blot. In cells within the second and third biological replicates, there was a significant reduction in beclin-1 expression between SOCS3^{EV} controls and SOCS3^{low} cells, but no significant difference was observed between SOCS3^{EV} and SOCS3^{high}. Conversely, LC3B-I was significantly decreased in SOCS3^{high} cells relative to SOCS3^{EV} controls, but no significant difference was observed in SOCS3^{low} cells. Relative to cells expressing SOCS3 normally, we observe decreased autophagy in under-expressing cells, and increased autophagy in over-expressing cells. These findings are consistent with those of Koay and colleagues, who implicated autophagy in SOCS3 regulation (Koay et al., 2014).

Although qPCR confirmed that transgenic cells maintained the correct genotype throughout, autophagy was regulating the abundance of the protein post-transcription. It should be considered that interactions involving the SOCS3 protein itself may be responsible for changes in the signalling pathways investigated in transgenic cells.

5.7. Future Direction

Although the results indicate that activation of the cGAS-STING pathway is not impacted by SOCS3, the results are inconsistent. In the first biological replicate, STING activation was significantly elevated in both transgenic cell lines, relative to empty vector controls. Meanwhile, in the second and third replicates, significant reductions in STING activation were observed in all transgenic cells. The significance of these results implies that SOCS3 expression does impact activation of cGAS-STING upon detection of cytosolic DNA, but this impact remains undefined. The conflicting results should be addressed by conducting additional repeat experiments. Furthermore, additional read-outs including phosphorylation of STING or activation of downstream transcription factors should be tested using western Blot to quantify phospho-STING and IRF3, respectively.

Our measurement of autophagic flux was limited by our inability to quantify the LC3B-II used in autophagosome membrane synthesis. Further investigation, in which lysosomal degradation is inhibited, should be considered. However, given the statistical significance of the results obtained using beclin-1 as a measure of autophagic flux, this is not essential.

Autophagy was found to regulate SOCS3 protein levels in transgenic cells. Therefore, potential interactions involving the protein itself, which cannot yet be considered, may be associated with modulating the response of transgenic cells to cytosolic DNA and should be further investigated.

5.8. Conclusion

Based on both histological and biochemical analysis, we have demonstrated that in our model, chronic inflammation is not always a consequence of dysbiosis. Rather, villous atrophy occurs and appears to be mediated by autophagy, which is likely important maintaining the dysbiotic environment.

Autophagy was downregulated in SOCS3^{low} HIEC. Meanwhile, crude measurement of LC3B-I to LC3B-II conversion infers that the opposite is true when SOCS3 expression is increased, suggesting that SOCS3 may impact autophagy in the intestinal epithelium. Although this is true for our HIEC model of dysbiosis, it may not extend to the other cell types in the intestinal mucosa, as SOCS3 expression was unchanged in resection tissue.

SOCS3 is often silenced in tumours and upregulated in IBD (Lund and Rigby, 2006, Li et al., 2010). Overall, our results may suggest that SOCS3^{low} cells, which may be considered a model for tumour cells, are less responsive to exogenous microbial stimuli and that SOCS3^{high} cells, which may be considered a model for cells of the inflamed intestine are more responsive to microbial challenge.

6. Appendix

6.1. Supplementary Material for Chapter 3.....	65
6.2. Supplementary Material for Chapter 4.....	67

6.1. Supplementary Material for Chapter 3

Tissue	pSTAT3 band density												
Functioning	0.0110	1.9047	0.2051	0.4411	0.1709	0.3326	1.5101	0.9729	1.9349	1.3057	0.5330	2.9578	0.6630
Defunctioned	0.2600	1.4784	6.5157	1.0996	0.2577	0.5418	5.2513	0.2865	0.1993	0.6228	0.5589	1.1754	0.9363

Tissue	STAT3 band density												
Functioning	0.0945	1.4369	0.4358	0.5791	0.0971	0.6665	0.5378	1.2278	6.4265	2.4836	0.9150	5.4016	1.0109
Defunctioned	0.7504	0.7966	1.6332	1.3152	0.1707	0.3862	3.9112	0.6101	0.5199	0.9829	0.8792	2.0232	1.2936

Tissue	STING band density												
Functioning	0.0090	0.0734	0.0696	0.2482	0.0010	0.9755	0.2544	0.0446	2.5668	0.0520	0.4273	1.3673	0.3315
Defunctioned	0.1702	0.5432	1.4631	0.0040	0.3770	0.2629	0.1679	2.1771	1.2236	0.2654	1.1061	0.6604	1.1467

Tissue	SOCS3 band density												
Functioning	0.1024	7.2187	0.0341	0.6445	0.0772	1.0716	4.4775	0.1705	0.0734	0.6809	0.2835	2.7744	0.3192
Defunctioned	0.1471	2.7726	2.3426	2.1897	0.0648	0.1638	9.2794	0.1267	0.0567	0.3266	0.2567	0.4260	0.3428

Tissue	Beclin-1 band density												
Functioning	0.4509	1.6696	0.9165	0.9815	0.3009	0.9157	0.7224	0.3083	0.6767	0.2115	0.3481	2.4082	0.3132
Defunctioned	0.5348	0.6543	1.1613	1.3589	0.6787	1.2291	0.9473	1.2077	0.4548	0.7698	1.0808	1.0499	0.6431

Band densities for pSTAT3, STAT3, STING and SOCS3 and beclin-1 tissue from defunctioned and functioning human intestine, normalised against β actin. N=13 per environment.

6.2. Supplementary Material for Chapter 4

Treatment	pSTAT3 band density								
Control	1.0881	1.0842	0.8529	1.1538	0.7828	0.7584	0.7113	0.7412	1.0129
K4 transfection	0.9559	0.8995	0.8617	0.8955	0.9437	0.9619	0.8375	0.9880	0.8889
DNA stimulation	1.2683	1.1654	1.6075	0.7534	0.9890	0.7001	1.0074	0.6376	0.7855

Treatment	STAT3 band density								
Control	1.2705	1.0366	1.1656	0.2687	1.4458	0.9849	0.6072	0.8572	1.1629
K4 transfection	1.1020	1.0134	0.9238	0.9843	0.8992	1.0372	1.0981	1.0774	0.8721
DNA stimulation	0.9936	0.9491	1.3606	1.1027	0.6196	0.6392	0.8738	0.7110	1.0982

Treatment	STING band density								
Control	0.3328	0.2328	0.2529	1.1659	1.7792	1.0656	0.9892	0.9970	1.0620
K4 transfection	0.3966	0.4122	0.6113	0.6514	1.2513	1.1329	1.4548	1.0000	1.0226
DNA stimulation	0.2948	0.3257	0.3982	1.1159	0.6611	0.8543	0.8801	0.7173	1.2035

Treatment	SOCS3 band density								
Control	0.8481	0.7184	0.7468	0.9444	1.5110	0.9114	0.7214	0.7330	0.9141
K4 transfection	0.9348	0.9447	1.0294	1.1026	1.0448	1.1579	1.4118	1.1230	0.9223
DNA stimulation	0.5918	0.7202	0.9372	1.0712	0.6607	0.8823	0.8327	0.6867	1.3383

Band densities for pSTAT3, STAT3, STING and SOCS3 in untreated controls, cells transfected with K4 transfection reagent and DNA-stimulated cells, normalised against β actin. N=9 per treatment.

Cell line	SOCS3 band density								
SOCS3 ^{low}	0.5879	0.5471	0.3963	1.7025	0.9198	0.7457	0.3453	0.5948	0.5314
SOCS3 ^{EV}	0.6389	0.6028	0.7497	0.4890	0.4395	0.5230	1.3067	1.3715	1.4336
SOCS3 ^{high}	1.0380	0.7389	0.8348	0.2064	0.4761	0.0862	5.0299	1.5521	9.6859

Band densities for SOCS3 in untreated SOCS3^{low}, SOCS3^{EV} and SOCS3^{high} cells, normalised against β actin. N=9 per cell line.

Cell line	Beclin-1 band density					
SOCS3 ^{low}	0.8041	0.9511	0.8115	0.6064	0.5881	0.7604
SOCS3 ^{EV}	0.9140	1.0609	1.0116	0.6929	0.8169	0.8398
SOCS3 ^{high}	0.8811	1.1177	0.7150	0.6220	0.7763	0.4445

Cell line	LC3B-I band density					
SOCS3 ^{low}	0.8241	1.0019	0.9038	0.3621	0.4846	0.7827
SOCS3 ^{EV}	0.9995	1.1837	0.9810	1.0550	1.1224	1.0505
SOCS3 ^{high}	0.5919	0.8789	0.6326	0.6976	0.4529	0.3191

Band densities for beclin-1 and LC3B-I in untreated SOCS3^{low}, SOCS3^{EV} and SOCS3^{high} cells, normalised against β actin. N=9 per cell line.

ANOVA					
	Sum of Squares	Degree of Freedom	Mean Square	F	Significance
Between cell lines	0.071	2	0.035	1.181	0.334
Within cell lines	0.449	15	0.030		
Total	0.519	17			

Bonferroni						
Beclin1		Mean Difference	Standard Error	Significance	95% Confidence Interval	
					Lower Bound	Upper Bound
SOCS3 low	SOCS3 EV	-0.1357667	0.0998660	0.582	-0.404780	0.133246
	SOCS3 high	-0.0058359	0.0998660	1.000	-0.274849	0.263177
SOCS3 EV	SOCS3 low	0.1357667	0.0998660	0.582	-0.133246	0.404780
	SOCS3 high	0.1299308	0.0998660	0.639	-0.139082	0.398944
SOCS3 high	SOCS3 low	0.0058359	0.0998660	1.000	-0.263177	0.274849
	SOCS3 EV	-0.1299308	0.0998660	0.639	-0.398944	0.139082

Analysis of variance (ANOVA) and Bonferroni tests to compare the mean beclin-1 expression between and within untreated SOCS3^{low}, SOCS3^{EV} and SOCS3^{high} cell lines.

ANOVA					
	Sum of Squares	Degree of Freedom	Mean Square	F	Significance
Between cell lines	0.705	2	0.353	9.999	0.002
Within cell lines	0.529	15	0.035		
Total	1.235	17			

Bonferroni						
LC3B		Mean Difference	Standard Error	Significance	95% Confidence Interval	
					Lower Bound	Upper Bound
SOCS3 low	SOCS3 EV	-.3388341*	0.1084407	0.021	-0.630945	-0.046723
	SOCS3 high	0.1310235	0.1084407	0.737	-0.161088	0.423135
SOCS3 EV	SOCS3 low	.3388341*	0.1084407	0.021	0.046723	0.630945
	SOCS3 high	.4698576*	0.1084407	0.002	0.177746	0.761969
SOCS3 high	SOCS3 low	-0.1310235	0.1084407	0.737	-0.423135	0.161088
	SOCS3 EV	-.4698576*	0.1084407	0.002	-0.761969	-0.177746

*. The mean difference is significant at the 0.05 level.

Analysis of variance (ANOVA) and Bonferroni tests to compare the mean LC3B-I expression between and within untreated SOCS3^{low},

SOCS3^{EV} and SOCS3^{high} cell lines.

Cell line	PSTAT3 band density								
SOCS3 ^{low}	1.0634	0.9891	1.1542	0.2972	0.3416	0.3978	0.8958	0.8301	0.9813
SOCS3 ^{EV}	1.0240	0.6818	0.7997	0.2431	0.2416	0.2456	0.9788	0.8817	0.9996
SOCS3 ^{high}	0.6293	0.5769	0.6440	0.1471	0.1822	0.0856	0.8990	0.8407	0.9846

Cell line	STAT3 band density								
SOCS3 ^{low}	1.2377	1.0365	1.1244	0.3860	0.2651	0.4593	1.0373	1.0072	1.1269
SOCS3 ^{EV}	0.9159	1.0040	0.8667	0.3474	0.3135	0.3064	0.9089	0.9961	1.3317
SOCS3 ^{high}	0.7986	0.8996	1.0476	0.1072	0.1053	0.0791	0.8602	0.5638	0.9644

Cell line	STING band density								
SOCS3 ^{low}	0.9397	1.0250	0.8575	0.5958	0.5942	0.9666	0.8671	0.7277	0.9571
SOCS3 ^{EV}	0.4740	0.4707	0.5177	1.0044	1.0010	1.0327	1.0344	1.0509	1.1134
SOCS3 ^{high}	1.0402	0.9495	0.9166	0.6057	0.6309	0.6636	0.7609	0.8968	1.0210

Band densities for pSTAT3, STAT3 and STING in SOCS3^{low}, SOCS3^{EV} and SOCS3^{high} cells stimulated with DNA, normalised against β actin.

N=9 per treatment.

ANOVA					
	Sum of Squares	Degree of Freedom	Mean Square	F	Significance
Between cell lines	0.254	2	0.127	1.944	0.165
Within cell lines	1.568	24	0.065		
Total	1.822	26			

Bonferroni						
Activated STAT3		Mean Difference	Standard Error	Significance	95% Confidence Interval	
					Lower Bound	Upper Bound
SOCS3 low	SOCS3 EV	0.0687306	0.1204799	1.000	-0.241342	0.378803
	SOCS3 high	-0.1625631	0.1204799	0.570	-0.472635	0.147509
SOCS3 EV	SOCS3 low	-0.0687306	0.1204799	1.000	-0.378803	0.241342
	SOCS3 high	-0.2312937	0.1204799	0.201	-0.541366	0.078778
SOCS3 high	SOCS3 low	0.1625631	0.1204799	0.570	-0.147509	0.472635
	SOCS3 EV	0.2312937	0.1204799	0.201	-0.078778	0.541366

Analysis of variance (ANOVA) and Bonferroni tests to compare the mean STAT3 activation between and within DNA-stimulated SOCS3^{low}, SOCS3^{EV} and SOCS3^{high} cell lines.

ANOVA					
	Sum of Squares	Degree of Freedom	Mean Square	F	Significance
Between cell lines	0.003	2	0.001	0.032	0.968
Within cell lines	1.056	24	0.044		
Total	1.059	26			

Bonferroni						
STING		Mean Difference	Standard Error	Significance	95% Confidence Interval	
					Lower Bound	Upper Bound
SOCS3 low	SOCS3 EV	-0.0187165	0.0988830	1.000	-0.273206	0.235773
	SOCS3 high	0.0050522	0.0988830	1.000	-0.249437	0.259542
SOCS3 EV	SOCS3 low	0.0187165	0.0988830	1.000	-0.235773	0.273206
	SOCS3 high	0.0237687	0.0988830	1.000	-0.230721	0.278258
SOCS3 high	SOCS3 low	-0.0050522	0.0988830	1.000	-0.259542	0.249437
	SOCS3 EV	-0.0237687	0.0988830	1.000	-0.278258	0.230721

Analysis of variance (ANOVA) and Bonferroni tests to compare the mean STING expression between and within DNA-stimulated SOCS3^{low}, SOCS3^{EV} and SOCS3^{high} cell lines.

7. References

1. ABE, T. & BARBER, G. N. 2014. Cytosolic-DNA-mediated, STING-dependent proinflammatory gene induction necessitates canonical NF- κ B activation through TBK1. *J Virol*, 88, 5328-41.
2. ABLASSER, A., GOLDECK, M., CAVLAR, T., DEIMLING, T., WITTE, G., RÖHL, I., HOPFNER, K. P., LUDWIG, J. & HORNUNG, V. 2013. cGAS produces a 2'-5'-linked cyclic dinucleotide second messenger that activates STING. *Nature*, 498, 380-4.
3. AITA, V. M., LIANG, X. H., MURTY, V. V., PINCUS, D. L., YU, W., CAYANIS, E., KALACHIKOV, S., GILLIAM, T. C. & LEVINE, B. 1999. Cloning and genomic organization of beclin 1, a candidate tumor suppressor gene on chromosome 17q21. *Genomics*, 59, 59-65.
4. AKIRA, S. 2000. Roles of STAT3 defined by tissue-specific gene targeting. *Oncogene*, 19, 2607-11.
5. ALEXOPOULOU, L., HOLT, A. C., MEDZHITOV, R. & FLAVELL, R. A. 2001. Recognition of double-stranded RNA and activation of NF-kappaB by Toll-like receptor 3. *Nature*, 413, 732-8.
6. ALLISON, J. E., TEKAWA, I. S., RANSOM, L. J. & ADRAIN, A. L. 1996. A comparison of fecal occult-blood tests for colorectal-cancer screening. *N Engl J Med*, 334, 155-9.
7. ANGLY, F., RODRIGUEZ-BRITO, B., BANGOR, D., MCNAIRNIE, P., BREITBART, M., SALAMON, P., FELTS, B., NULTON, J., MAHAFFY, J. & ROHWER, F. 2005. PHACCS, an online tool for estimating the structure and diversity of uncultured viral communities using metagenomic information. *BMC Bioinformatics*, 6, 41.
8. ANTONSSON, B., MONTESSUIT, S., SANCHEZ, B. & MARTINOU, J. C. 2001. Bax is present as a high molecular weight oligomer/complex in the mitochondrial membrane of apoptotic cells. *J Biol Chem*, 276, 11615-23.
9. ASSELAH, T. 2010. Genetic polymorphism and response to treatment in chronic hepatitis C: the future of personalized medicine. *J Hepatol*, 52, 452-4.
10. AU, W. C., MOORE, P. A., LOWTHER, W., JUANG, Y. T. & PITHA, P. M. 1995. Identification of a member of the interferon regulatory factor family that binds to the

interferon-stimulated response element and activates expression of interferon-induced genes. *Proc Natl Acad Sci U S A*, 92, 11657-61.

11. BABON, J. J., MCMANUS, E. J., YAO, S., DESOUZA, D. P., MIELKE, L. A., SPRIGG, N. S., WILLSON, T. A., HILTON, D. J., NICOLA, N. A., BACA, M., NICHOLSON, S. E. & NORTON, R. S. 2006. The structure of SOCS3 reveals the basis of the extended SH2 domain function and identifies an unstructured insertion that regulates stability. *Mol Cell*, 22, 205-16.
12. BAKHOUM, S. F., NGO, B., LAUGHNEY, A. M., CAVALLO, J. A., MURPHY, C. J., LY, P., SHAH, P., SRIRAM, R. K., WATKINS, T. B. K., TAUNK, N. K., DURAN, M., PAULI, C., SHAW, C., CHADALAVADA, K., RAJASEKHAR, V. K., GENOVESE, G., VENKATESAN, S., BIRKBAK, N. J., MCGRANAHAN, N., LUNDQUIST, M., LAPLANT, Q., HEALEY, J. H., ELEMENTO, O., CHUNG, C. H., LEE, N. Y., IMIELENSKI, M., NANJANGUD, G., PE'ER, D., CLEVELAND, D. W., POWELL, S. N., LAMMERDING, J., SWANTON, C. & CANTLEY, L. C. 2018. Chromosomal instability drives metastasis through a cytosolic DNA response. *Nature*, 553, 467-472.
13. BANDYOPADHYAY, U., KAUSHIK, S., VARTICOVSKI, L. & CUERVO, A. M. 2008. The chaperone-mediated autophagy receptor organizes in dynamic protein complexes at the lysosomal membrane. *Mol Cell Biol*, 28, 5747-63.
14. BARKER, N., HUCH, M., KUJALA, P., VAN DE WETERING, M., SNIPPERT, H. J., VAN ES, J. H., SATO, T., STANGE, D. E., BEGTHEL, H., VAN DEN BORN, M., DANENBERG, E., VAN DEN BRINK, S., KORVING, J., ABO, A., PETERS, P. J., WRIGHT, N., POULSOM, R. & CLEVERS, H. 2010. Lgr5(+ve) stem cells drive self-renewal in the stomach and build long-lived gastric units in vitro. *Cell Stem Cell*, 6, 25-36.
15. BARKER, N., ROOKMAAKER, M. B., KUJALA, P., NG, A., LEUSHACKE, M., SNIPPERT, H., VAN DE WETERING, M., TAN, S., VAN ES, J. H., HUCH, M., POULSOM, R., VERHAAR, M. C., PETERS, P. J. & CLEVERS, H. 2012. Lgr5(+ve) stem/progenitor cells contribute to nephron formation during kidney development. *Cell Rep*, 2, 540-52.
16. BARKER, N., VAN ES, J. H., KUIPERS, J., KUJALA, P., VAN DEN BORN, M., COZIJNSEN, M., HAEGEBARTH, A., KORVING, J., BEGTHEL, H., PETERS, P. J. & CLEVERS, H. 2007. Identification of stem cells in small intestine and colon by marker gene Lgr5. *Nature*, 449, 1003-7.

17. BARTH, S., GLICK, D. & MACLEOD, K. F. 2010. Autophagy: assays and artifacts. *J Pathol*, 221, 117-24.
18. BEAMISH, E. L., JOHNSON, J., SHAW, E. J., SCOTT, N. A., BHOWMICK, A. & RIGBY, R. J. 2017. Loop ileostomy-mediated fecal stream diversion is associated with microbial dysbiosis. *Gut Microbes*, 8, 467-478.
19. BELL, L. V. & ELSE, K. J. 2011. Regulation of colonic epithelial cell turnover by IDO contributes to the innate susceptibility of SCID mice to *Trichuris muris* infection. *Parasite Immunol*, 33, 244-9.
20. BISHEHSARI, F., MAHDAVINIA, M., VACCA, M., MALEKZADEH, R. & MARIANI-COSTANTINI, R. 2014. Epidemiological transition of colorectal cancer in developing countries: environmental factors, molecular pathways, and opportunities for prevention. *World J Gastroenterol*, 20, 6055-72.
21. BJERKNES, M. & CHENG, H. 1999. Clonal analysis of mouse intestinal epithelial progenitors. *Gastroenterology*, 116, 7-14.
22. BOYLE, P. & LANGMAN, J. S. 2000. ABC of colorectal cancer: Epidemiology. *BMJ*, 321, 805-8.
23. BRAND, S., BEIGEL, F., OLSZAK, T., ZITZMANN, K., EICHHORST, S. T., OTTE, J. M., DIEPOLDER, H., MARQUARDT, A., JAGLA, W., POPP, A., LECLAIR, S., HERRMANN, K., SEIDERER, J., OCHSENKÜHN, T., GÖKE, B., AUERNHAMMER, C. J. & DAMBACHER, J. 2006. IL-22 is increased in active Crohn's disease and promotes proinflammatory gene expression and intestinal epithelial cell migration. *Am J Physiol Gastrointest Liver Physiol*, 290, G827-38.
24. BREITBART, M., HEWSON, I., FELTS, B., MAHAFFY, J. M., NULTON, J., SALAMON, P. & ROHWER, F. 2003. Metagenomic analyses of an uncultured viral community from human feces. *J Bacteriol*, 185, 6220-3.
25. BRITTON, G. J., CONTIJOCH, E. J., MOGNO, I., VENNARO, O. H., LLEWELLYN, S. R., NG, R., LI, Z., MORTHA, A., MERAD, M., DAS, A., GEVERS, D., MCGOVERN, D. P. B., SINGH, N., BRAUN, J., JACOBS, J. P., CLEMENTE, J. C., GRINSPAN, A., SANDS, B. E., COLOMBEL, J. F., DUBINSKY, M. C. & FAITH, J. J. 2019. Microbiotas from Humans with Inflammatory Bowel Disease Alter the Balance of Gut Th17 and ROR γ t. *Immunity*, 50, 212-224.e4.
26. BUGLO, E., SARMIENTO, E., MARTUSCELLI, N. B., SANT, D. W., DANZI, M. C., ABRAMS, A. J., DALLMAN, J. E. & ZÜCHNER, S. 2020. Genetic compensation in a

- stable *slc25a46* mutant zebrafish: A case for using F0 CRISPR mutagenesis to study phenotypes caused by inherited disease. *PLoS One*, 15, e0230566.
27. BUTTÓ, L. F., SCHAUBECK, M. & HALLER, D. 2015. Mechanisms of Microbe-Host Interaction in Crohn's Disease: Dysbiosis vs. Pathobiont Selection. *Front Immunol*, 6, 555.
 28. BÉNARD, F., BARKUN, A. N., MARTEL, M. & VON RENTELN, D. 2018. Systematic review of colorectal cancer screening guidelines for average-risk adults: Summarizing the current global recommendations. *World J Gastroenterol*, 24, 124-138.
 29. Cancer Research UK (2019) *Cancer incidence for common cancers* [online] available at <https://www.cancerresearchuk.org/health-professional/cancer-statistics/incidence/common-cancers-compared#heading=Two> [accessed October 2019]
 30. Cancer Research UK (2020) *Small Intestine Cancer Incidence Statistics* [online] available at <https://www.cancerresearchuk.org/health-professional/cancer-statistics/statistics-by-cancer-type/small-intestine-cancer/incidence> [accessed October 2020]
 31. CAROW, B. & ROTTENBERG, M. E. 2014. SOCS3, a Major Regulator of Infection and Inflammation. *Front Immunol*, 5, 58.
 32. CERBONI, S., JEREMIAH, N., GENTILI, M., GEHRMANN, U., CONRAD, C., STOLZENBERG, M. C., PICARD, C., NEVEN, B., FISCHER, A., AMIGORENA, S., RIEUX-LAUCAT, F. & MANEL, N. 2017. Intrinsic antiproliferative activity of the innate sensor STING in T lymphocytes. *J Exp Med*, 214, 1769-1785.
 33. CHATTOPADHYAY, S., MARQUES, J. T., YAMASHITA, M., PETERS, K. L., SMITH, K., DESAI, A., WILLIAMS, B. R. & SEN, G. C. 2010. Viral apoptosis is induced by IRF-3-mediated activation of Bax. *EMBO J*, 29, 1762-73.
 34. CHENG, H. & LEBLOND, C. P. 1974. Origin, differentiation and renewal of the four main epithelial cell types in the mouse small intestine. III. Entero-endocrine cells. *Am J Anat*, 141, 503-19.
 35. CHITTARANJAN, S., BORTNIK, S. & GORSKI, S. M. 2015. Monitoring Autophagic Flux by Using Lysosomal Inhibitors and Western Blotting of Endogenous MAP1LC3B. *Cold Spring Harb Protoc*, 2015, 743-50.
 36. CHOW, A., TILNEY, H. S., PARASKEVA, P., JEYARAJAH, S., ZACHARAKIS, E. & PURKAYASTHA, S. 2009. The morbidity surrounding reversal of defunctioning ileostomies: a systematic review of 48 studies including 6,107 cases. *Int J Colorectal Dis*, 24, 711-23.

37. COLLABORATORS, G. I. B. D. 2020. The global, regional, and national burden of inflammatory bowel disease in 195 countries and territories, 1990-2017: a systematic analysis for the Global Burden of Disease Study 2017. *Lancet Gastroenterol Hepatol*, 5, 17-30.
38. CORVINUS, F. M., ORTH, C., MORIGGL, R., TSAREVA, S. A., WAGNER, S., PFITZNER, E. B., BAUS, D., KAUFMANN, R., HUBER, L. A., ZATLOUKAL, K., BEUG, H., OHLSCHLÄGER, P., SCHÜTZ, A., HALBHUBER, K. J. & FRIEDRICH, K. 2005. Persistent STAT3 activation in colon cancer is associated with enhanced cell proliferation and tumor growth. *Neoplasia*, 7, 545-55.
39. COUGHLIN, R. J. & FRIEND, W. G. 1987. Dietary restrictions and fecal occult blood testing. *Am Fam Physician*, 35, 118-20.
40. CROHN, B. B., GINZBURG, L. & OPPENHEIMER, G. D. 1952. Regional ileitis; a pathologic and clinical entity. *Am J Med*, 13, 583-90.
41. CUERVO, A. M. & DICE, J. F. 1996. A receptor for the selective uptake and degradation of proteins by lysosomes. *Science*, 273, 501-3.
42. CUERVO, A. M. & DICE, J. F. 1998. Lysosomes, a meeting point of proteins, chaperones, and proteases. *J Mol Med (Berl)*, 76, 6-12.
43. CUERVO, A. M. & WONG, E. 2014. Chaperone-mediated autophagy: roles in disease and aging. *Cell Res*, 24, 92-104.
44. CUI, S. & CHANG, P. Y. 2016. Current understanding concerning intestinal stem cells. *World J Gastroenterol*, 22, 7099-110.
45. CUI, S., EISENÄCHER, K., KIRCHHOFER, A., BRZÓZKA, K., LAMMENS, A., LAMMENS, K., FUJITA, T., CONZELMANN, K. K., KRUG, A. & HOPFNER, K. P. 2008. The C-terminal regulatory domain is the RNA 5'-triphosphate sensor of RIG-I. *Mol Cell*, 29, 169-79.
46. DALE, T. C., IMAM, A. M., KERR, I. M. & STARK, G. R. 1989. Rapid activation by interferon alpha of a latent DNA-binding protein present in the cytoplasm of untreated cells. *Proc Natl Acad Sci U S A*, 86, 1203-7.
47. DANCOURT, V., LEJEUNE, C., LEPAGE, C., GAILLIARD, M. C., MENY, B. & FAIVRE, J. 2008. Immunochemical faecal occult blood tests are superior to guaiac-based tests for the detection of colorectal neoplasms. *Eur J Cancer*, 44, 2254-8.
48. DARNELL, J. E., KERR, I. M. & STARK, G. R. 1994. Jak-STAT pathways and transcriptional activation in response to IFNs and other extracellular signaling proteins. *Science*, 264, 1415-21.

49. DATTA, R., DESCHOOLMEESTER, M. L., HEDELER, C., PATON, N. W., BRASS, A. M. & ELSE, K. J. 2005. Identification of novel genes in intestinal tissue that are regulated after infection with an intestinal nematode parasite. *Infect Immun*, 73, 4025-33.
50. DE DUVE, C. & WATTIAUX, R. 1966. Functions of lysosomes. *Annu Rev Physiol*, 28, 435-92.
51. DE QUEIROZ, N. M. G. P., XIA, T., KONNO, H. & BARBER, G. N. 2019. Ovarian Cancer Cells Commonly Exhibit Defective STING Signaling Which Affects Sensitivity to Viral Oncolysis. *Mol Cancer Res*, 17, 974-986.
52. DEB, P., DAI, J., SINGH, S., KALYOUSSEF, E. & FITZGERALD-BOCARSLY, P. 2020. Triggering of the cGAS-STING Pathway in Human Plasmacytoid Dendritic Cells Inhibits TLR9-Mediated IFN Production. *J Immunol*, 205, 223-236.
53. DHIMAN, V. K., BOLT, M. J. & WHITE, K. P. 2018. Nuclear receptors in cancer - uncovering new and evolving roles through genomic analysis. *Nat Rev Genet*, 19, 160-174.
54. DINARELLO, C. A. 2000. Proinflammatory cytokines. *Chest*, 118, 503-8.
55. DOYLE, S., VAIDYA, S., O'CONNELL, R., DADGOSTAR, H., DEMPSEY, P., WU, T., RAO, G., SUN, R., HABERLAND, M., MODLIN, R. & CHENG, G. 2002. IRF3 mediates a TLR3/TLR4-specific antiviral gene program. *Immunity*, 17, 251-63.
56. EDDINGER, T. J. 2014. Smooth muscle-protein translocation and tissue function. *Anat Rec (Hoboken)*, 297, 1734-46.
57. ELMUNZER, B. J., HAYWARD, R. A., SCHOENFELD, P. S., SAINI, S. D., DESHPANDE, A. & WALJEE, A. K. 2012. Effect of flexible sigmoidoscopy-based screening on incidence and mortality of colorectal cancer: a systematic review and meta-analysis of randomized controlled trials. *PLoS Med*, 9, e1001352.
58. FENG, Y., HE, D., YAO, Z. & KLIONSKY, D. J. 2014. The machinery of macroautophagy. *Cell Res*, 24, 24-41.
59. FLETCHER, T. C., DIGIANDOMENICO, A. & HAWIGER, J. 2010. Extended anti-inflammatory action of a degradation-resistant mutant of cell-penetrating suppressor of cytokine signaling 3. *J Biol Chem*, 285, 18727-36.
60. FRANCIS, G. A., FAYARD, E., PICARD, F. & AUWERX, J. 2003. Nuclear receptors and the control of metabolism. *Annu Rev Physiol*, 65, 261-311.
61. GADINA, M., HILTON, D., JOHNSTON, J. A., MORINOBU, A., LIGHVANI, A., ZHOU, Y. J., VISCONTI, R. & O'SHEA, J. J. 2001. Signaling by type I and II cytokine receptors: ten years after. *Curr Opin Immunol*, 13, 363-73.

62. GEHART, H. & CLEVERS, H. 2019. Tales from the crypt: new insights into intestinal stem cells. *Nat Rev Gastroenterol Hepatol*, 16, 19-34.
63. GEIGL, J. B., OBENAU, A. C., SCHWARZBRAUN, T. & SPEICHER, M. R. 2008. Defining 'chromosomal instability'. *Trends Genet*, 24, 64-9.
64. GESSLER, B., HAGLIND, E. & ANGENETE, E. 2012. Loop ileostomies in colorectal cancer patients--morbidity and risk factors for nonreversal. *J Surg Res*, 178, 708-14.
65. GIANNAKIS, M., STAPPENBECK, T. S., MILLS, J. C., LEIP, D. G., LOVETT, M., CLIFTON, S. W., IPPOLITO, J. E., GLASSCOCK, J. I., ARUMUGAM, M., BRENT, M. R. & GORDON, J. I. 2006. Molecular properties of adult mouse gastric and intestinal epithelial progenitors in their niches. *J Biol Chem*, 281, 11292-300.
66. GILL, S. R., POP, M., DEBOY, R. T., ECKBURG, P. B., TURNBAUGH, P. J., SAMUEL, B. S., GORDON, J. I., RELMAN, D. A., FRASER-LIGGETT, C. M. & NELSON, K. E. 2006. Metagenomic analysis of the human distal gut microbiome. *Science*, 312, 1355-9.
67. GLASSNER, K. L., ABRAHAM, B. P. & QUIGLEY, E. M. M. 2020. The microbiome and inflammatory bowel disease. *J Allergy Clin Immunol*, 145, 16-27.
68. GOLSHIRI, P., RASOOLI, S., EMAMI, M. & NAJIMI, A. 2016. Effects of Physical Activity on Risk of Colorectal Cancer: A Case-control Study. *Int J Prev Med*, 7, 32.
69. GREER, J. B. & O'KEEFE, S. J. 2011. Microbial induction of immunity, inflammation, and cancer. *Front Physiol*, 1, 168.
70. GREGORIEFF, A., PINTO, D., BEGTHEL, H., DESTRÉE, O., KIELMAN, M. & CLEVERS, H. 2005. Expression pattern of Wnt signaling components in the adult intestine. *Gastroenterology*, 129, 626-38.
71. GUI, X., YANG, H., LI, T., TAN, X., SHI, P., LI, M., DU, F. & CHEN, Z. J. 2019. Autophagy induction via STING trafficking is a primordial function of the cGAS pathway. *Nature*, 567, 262-266.
72. GUPTA, R. A., TAN, J., KRAUSE, W. F., GERACI, M. W., WILLSON, T. M., DEY, S. K. & DUBOIS, R. N. 2000. Prostacyclin-mediated activation of peroxisome proliferator-activated receptor delta in colorectal cancer. *Proc Natl Acad Sci U S A*, 97, 13275-80.
73. HALFVARSON, J., BRISLAWN, C. J., LAMENDELLA, R., VÁZQUEZ-BAEZA, Y., WALTERS, W. A., BRAMER, L. M., D'AMATO, M., BONFIGLIO, F., MCDONALD, D., GONZALEZ, A., MCCLURE, E. E., DUNKLEBARGER, M. F., KNIGHT, R. & JANSSON, J. K. 2017. Dynamics of the human gut microbiome in inflammatory bowel disease. *Nat Microbiol*, 2, 17004.

74. HANAHAN, D. & WEINBERG, R. A. 2011. Hallmarks of cancer: the next generation. *Cell*, 144, 646-74.
75. HARRISON, D. A. 2012. The Jak/STAT pathway. *Cold Spring Harb Perspect Biol*, 4.
76. HASSAN, C., GIORGI ROSSI, P., CAMILLONI, L., REX, D. K., JIMENEZ-CENDALES, B., FERRONI, E., BORGIA, P., ZULLO, A., GUASTICCHI, G. & GROUP, H. 2012. Meta-analysis: adherence to colorectal cancer screening and the detection rate for advanced neoplasia, according to the type of screening test. *Aliment Pharmacol Ther*, 36, 929-40.
77. HE, H., DANG, Y., DAI, F., GUO, Z., WU, J., SHE, X., PEI, Y., CHEN, Y., LING, W., WU, C., ZHAO, S., LIU, J. O. & YU, L. 2003. Post-translational modifications of three members of the human MAP1LC3 family and detection of a novel type of modification for MAP1LC3B. *J Biol Chem*, 278, 29278-87.
78. HEICHLER, C., SCHEIBE, K., SCHMIED, A., GEPPERT, C. I., SCHMID, B., WIRTZ, S., THOMA, O. M., KRAMER, V., WALDNER, M. J., BÜTTNER, C., FARIN, H. F., PEŠIĆ, M., KNIELING, F., MERKEL, S., GRÜNEBOOM, A., GUNZER, M., GRÜTZMANN, R., ROSE-JOHN, S., KORALOV, S. B., KOLLIAS, G., VIETH, M., HARTMANN, A., GRETEN, F. R., NEURATH, M. F. & NEUFERT, C. 2020. STAT3 activation through IL-6/IL-11 in cancer-associated fibroblasts promotes colorectal tumour development and correlates with poor prognosis. *Gut*, 69, 1269-1282.
79. HIGGINS, K. M., DAVIDIAN, M., CHEW, G. & BURGE, H. 1998. The effect of serial dilution error on calibration inference in immunoassay. *Biometrics*, 54, 19-32.
80. HILDEBRANDT, M. A., HOFFMANN, C., SHERRILL-MIX, S. A., KEILBAUGH, S. A., HAMADY, M., CHEN, Y. Y., KNIGHT, R., AHIMA, R. S., BUSHMAN, F. & WU, G. D. 2009. High-fat diet determines the composition of the murine gut microbiome independently of obesity. *Gastroenterology*, 137, 1716-24.e1-2.
81. HOLDSWORTH, S. R. & GAN, P. Y. 2015. Cytokines: Names and Numbers You Should Care About. *Clin J Am Soc Nephrol*, 10, 2243-54.
82. HOOPER, L. V., STAPPENBECK, T. S., HONG, C. V. & GORDON, J. I. 2003. Angiogenins: a new class of microbicidal proteins involved in innate immunity. *Nat Immunol*, 4, 269-73.
83. HOSHINO, K., TAKEUCHI, O., KAWAI, T., SANJO, H., OGAWA, T., TAKEDA, Y., TAKEDA, K. & AKIRA, S. 1999. Cutting edge: Toll-like receptor 4 (TLR4)-deficient mice are hyporesponsive to lipopolysaccharide: evidence for TLR4 as the Lps gene product. *J Immunol*, 162, 3749-52.

84. HUGOT, J. P., CHAMAILLARD, M., ZOUALI, H., LESAGE, S., CÉZARD, J. P., BELAICHE, J., ALMER, S., TYSK, C., O'MORAIN, C. A., GASSULL, M., BINDER, V., FINKEL, Y., CORTOT, A., MODIGLIANI, R., LAURENT-PUIG, P., GOWER-ROUSSEAU, C., MACRY, J., COLOMBEL, J. F., SAHBATOU, M. & THOMAS, G. 2001. Association of NOD2 leucine-rich repeat variants with susceptibility to Crohn's disease. *Nature*, 411, 599-603.
85. INAGAKI-OHARA, K., MAYUZUMI, H., KATO, S., MINOKOSHI, Y., OTSUBO, T., KAWAMURA, Y. I., DOHI, T., MATSUZAKI, G. & YOSHIMURA, A. 2014. Enhancement of leptin receptor signaling by SOCS3 deficiency induces development of gastric tumors in mice. *Oncogene*, 33, 74-84.
86. ISHIKAWA, H. & BARBER, G. N. 2008. STING is an endoplasmic reticulum adaptor that facilitates innate immune signalling. *Nature*, 455, 674-8.
87. IVASHKIV, L. B. & DONLIN, L. T. 2014. Regulation of type I interferon responses. *Nat Rev Immunol*, 14, 36-49.
88. JAKS, V., BARKER, N., KASPER, M., VAN ES, J. H., SNIPPERT, H. J., CLEVERS, H. & TOFTGÅRD, R. 2008. Lgr5 marks cycling, yet long-lived, hair follicle stem cells. *Nat Genet*, 40, 1291-9.
89. JIANG, M., ZHANG, W. W., LIU, P., YU, W., LIU, T. & YU, J. 2017. Dysregulation of SOCS-Mediated Negative Feedback of Cytokine Signaling in Carcinogenesis and Its Significance in Cancer Treatment. *Front Immunol*, 8, 70.
90. JIANG, Z., MAK, T. W., SEN, G. & LI, X. 2004. Toll-like receptor 3-mediated activation of NF-kappaB and IRF3 diverges at Toll-IL-1 receptor domain-containing adapter inducing IFN-beta. *Proc Natl Acad Sci U S A*, 101, 3533-8.
91. JOSTINS, L., RIPKE, S., WEERSMA, R. K., DUERR, R. H., MCGOVERN, D. P., HUI, K. Y., LEE, J. C., SCHUMM, L. P., SHARMA, Y., ANDERSON, C. A., ESSERS, J., MITROVIC, M., NING, K., CLEYNEN, I., THEATRE, E., SPAIN, S. L., RAYCHAUDHURI, S., GOYETTE, P., WEI, Z., ABRAHAM, C., ACHKAR, J. P., AHMAD, T., AMININEJAD, L., ANANTHAKRISHNAN, A. N., ANDERSEN, V., ANDREWS, J. M., BAIDOO, L., BALSCHUN, T., BAMPTON, P. A., BITTON, A., BOUCHER, G., BRAND, S., BÜNING, C., COHAIN, A., CICHON, S., D'AMATO, M., DE JONG, D., DEVANEY, K. L., DUBINSKY, M., EDWARDS, C., ELLINGHAUS, D., FERGUSON, L. R., FRANCHIMONT, D., FRANSEN, K., GEARRY, R., GEORGES, M., GIEGER, C., GLAS, J., HARITUNIANS, T., HART, A., HAWKEY, C., HEDL, M., HU, X., KARLSEN, T. H., KUPCINSKAS, L., KUGATHASAN, S.,

- LATIANO, A., LAUKENS, D., LAWRENCE, I. C., LEES, C. W., LOUIS, E., MAHY, G., MANSFIELD, J., MORGAN, A. R., MOWAT, C., NEWMAN, W., PALMIERI, O., PONSIOEN, C. Y., POCOCNIK, U., PRESCOTT, N. J., REGUEIRO, M., ROTTER, J. I., RUSSELL, R. K., SANDERSON, J. D., SANS, M., SATSANGI, J., SCHREIBER, S., SIMMS, L. A., SVENTORAITYTE, J., TARGAN, S. R., TAYLOR, K. D., TREMELLING, M., VERSPAGET, H. W., DE VOS, M., WIJMENGA, C., WILSON, D. C., WINKELMANN, J., XAVIER, R. J., ZEISSIG, S., ZHANG, B., ZHANG, C. K., ZHAO, H., SILVERBERG, M. S., ANNESE, V., HAKONARSON, H., BRANT, S. R., RADFORD-SMITH, G., MATHEW, C. G., RIOUX, J. D., SCHADT, E. E., et al. 2012. Host-microbe interactions have shaped the genetic architecture of inflammatory bowel disease. *Nature*, 491, 119-24.
92. JUNG, K. B., KWON, O., LEE, M. O., LEE, H., SON, Y. S., HABIB, O., OH, J. H., CHO, H. S., JUNG, C. R., KIM, J. & SON, M. Y. 2019. Blockade of STAT3 Causes Severe In Vitro and In Vivo Maturation Defects in Intestinal Organoids Derived from Human Embryonic Stem Cells. *J Clin Med*, 8.
93. KANG, H. & SHIBATA, D. 2013. Direct measurements of human colon crypt stem cell niche genetic fidelity: the role of chance in non-darwinian mutation selection. *Front Oncol*, 3, 264.
94. KARAM, S. M. 1999. Lineage commitment and maturation of epithelial cells in the gut. *Front Biosci*, 4, D286-98.
95. KAWAI, T., TAKAHASHI, K., SATO, S., COBAN, C., KUMAR, H., KATO, H., ISHII, K. J., TAKEUCHI, O. & AKIRA, S. 2005. IPS-1, an adaptor triggering RIG-I- and Mda5-mediated type I interferon induction. *Nat Immunol*, 6, 981-8.
96. KIHARA, A., KABEYA, Y., OHSUMI, Y. & YOSHIMORI, T. 2001. Beclin-phosphatidylinositol 3-kinase complex functions at the trans-Golgi network. *EMBO Rep*, 2, 330-5.
97. KOAY, L. C., RIGBY, R. J. & WRIGHT, K. L. 2014. Cannabinoid-induced autophagy regulates suppressor of cytokine signaling-3 in intestinal epithelium. *Am J Physiol Gastrointest Liver Physiol*, 307, G140-8.
98. KONERI, K., GOI, T., HIRONO, Y., KATAYAMA, K. & YAMAGUCHI, A. 2007. Beclin 1 gene inhibits tumor growth in colon cancer cell lines. *Anticancer Res*, 27, 1453-7.

99. KONNO, H., KONNO, K. & BARBER, G. N. 2013. Cyclic dinucleotides trigger ULK1 (ATG1) phosphorylation of STING to prevent sustained innate immune signaling. *Cell*, 155, 688-98.
100. KONRAD, G. 2010. Dietary interventions for fecal occult blood test screening: systematic review of the literature. *Can Fam Physician*, 56, 229-38.
101. KOTENKO, S. V., GALLAGHER, G., BAURIN, V. V., LEWIS-ANTES, A., SHEN, M., SHAH, N. K., LANGER, J. A., SHEIKH, F., DICKENSHEETS, H. & DONNELLY, R. P. 2003. IFN-lambdas mediate antiviral protection through a distinct class II cytokine receptor complex. *Nat Immunol*, 4, 69-77.
102. KOUKOURAKIS, M. I., KALAMIDA, D., GIATROMANOLAKI, A., ZOIS, C. E., SIVRIDIS, E., POULILIOU, S., MITRAKAS, A., GATTER, K. C. & HARRIS, A. L. 2015. Autophagosome Proteins LC3A, LC3B and LC3C Have Distinct Subcellular Distribution Kinetics and Expression in Cancer Cell Lines. *PLoS One*, 10, e0137675.
103. KREBS, D. L. & HILTON, D. J. 2001. SOCS proteins: negative regulators of cytokine signaling. *Stem Cells*, 19, 378-87.
104. KRONBORG, O., FENGER, C., OLSEN, J., JØRGENSEN, O. D. & SØNDERGAARD, O. 1996. Randomised study of screening for colorectal cancer with faecal-occult-blood test. *Lancet*, 348, 1467-71.
105. KUMA, A., HATANO, M., MATSUI, M., YAMAMOTO, A., NAKAYA, H., YOSHIMORI, T., OHSUMI, Y., TOKUHISA, T. & MIZUSHIMA, N. 2004. The role of autophagy during the early neonatal starvation period. *Nature*, 432, 1032-6.
106. KURT-JONES, E. A., POPOVA, L., KWINN, L., HAYNES, L. M., JONES, L. P., TRIPP, R. A., WALSH, E. E., FREEMAN, M. W., GOLENBOCK, D. T., ANDERSON, L. J. & FINBERG, R. W. 2000. Pattern recognition receptors TLR4 and CD14 mediate response to respiratory syncytial virus. *Nat Immunol*, 1, 398-401.
107. KWON, J. & BAKHOUM, S. F. 2020. The Cytosolic DNA-Sensing cGAS-STING Pathway in Cancer. *Cancer Discov*, 10, 26-39.
108. LATHROP, S. K., BLOOM, S. M., RAO, S. M., NUTSCH, K., LIO, C. W., SANTACRUZ, N., PETERSON, D. A., STAPPENBECK, T. S. & HSIEH, C. S. 2011. Peripheral education of the immune system by colonic commensal microbiota. *Nature*, 478, 250-4.
109. LAU, S. K. P., TENG, J. L. L., CHIU, T. H., CHAN, E., TSANG, A. K. L., PANAGIOTOU, G., ZHAI, S. L. & WOO, P. C. Y. 2018. Differential Microbial

- Communities of Omnivorous and Herbivorous Cattle in Southern China. *Comput Struct Biotechnol J*, 16, 54-60.
110. LEE, K. G., XU, S., KANG, Z. H., HUO, J., HUANG, M., LIU, D., TAKEUCHI, O., AKIRA, S. & LAM, K. P. 2012. Bruton's tyrosine kinase phosphorylates Toll-like receptor 3 to initiate antiviral response. *Proc Natl Acad Sci U S A*, 109, 5791-6.
111. LEVINE, B. & DERETIC, V. 2007. Unveiling the roles of autophagy in innate and adaptive immunity. *Nat Rev Immunol*, 7, 767-77.
112. LI, Y., DE HAAR, C., CHEN, M., DEURING, J., GERRITS, M. M., SMITS, R., XIA, B., KUIPERS, E. J. & VAN DER WOUDE, C. J. 2010. Disease-related expression of the IL6/STAT3/SOCS3 signalling pathway in ulcerative colitis and ulcerative colitis-related carcinogenesis. *Gut*, 59, 227-35.
113. LI, Y., NUIJ, V. J., BAARS, J. E., BIERMANN, K., KUIPERS, E. J., PEPPELENBOSCH, M. P., DE HAAR, C. & JANNEKE VAN DER WOUDE, C. 2013. Increased suppressor of cytokine signaling-3 expression predicts mucosal relapse in ulcerative colitis. *Inflamm Bowel Dis*, 19, 132-40.
114. LI, Y., WILSON, H. L. & KISS-TOTH, E. 2017. Regulating STING in health and disease. *J Inflamm (Lond)*, 14, 11.
115. LIANG, C., FENG, P., KU, B., DOTAN, I., CANAANI, D., OH, B. H. & JUNG, J. U. 2006. Autophagic and tumour suppressor activity of a novel Beclin1-binding protein UVRAG. *Nat Cell Biol*, 8, 688-99.
116. LIANG, P., JIANG, B., LI, Y., LIU, Z., ZHANG, P., ZHANG, M., HUANG, X. & XIAO, X. 2018. Autophagy promotes angiogenesis via AMPK/Akt/mTOR signaling during the recovery of heat-denatured endothelial cells. *Cell Death Dis*, 9, 1152.
117. LIANG, Q., SEO, G. J., CHOI, Y. J., KWAK, M. J., GE, J., RODGERS, M. A., SHI, M., LESLIE, B. J., HOPFNER, K. P., HA, T., OH, B. H. & JUNG, J. U. 2014. Crosstalk between the cGAS DNA sensor and Beclin-1 autophagy protein shapes innate antimicrobial immune responses. *Cell Host Microbe*, 15, 228-38.
118. LIN, R., HEYLBROECK, C., PITHA, P. M. & HISCOTT, J. 1998. Virus-dependent phosphorylation of the IRF-3 transcription factor regulates nuclear translocation, transactivation potential, and proteasome-mediated degradation. *Mol Cell Biol*, 18, 2986-96.
119. LIU, D., WU, H., WANG, C., LI, Y., TIAN, H., SIRAJ, S., SEHGAL, S. A., WANG, X., WANG, J., SHANG, Y., JIANG, Z., LIU, L. & CHEN, Q. 2019. STING directly

- activates autophagy to tune the innate immune response. *Cell Death Differ*, 26, 1735-1749.
120. LIU, S., CAI, X., WU, J., CONG, Q., CHEN, X., LI, T., DU, F., REN, J., WU, Y. T., GRISHIN, N. V. & CHEN, Z. J. 2015. Phosphorylation of innate immune adaptor proteins MAVS, STING, and TRIF induces IRF3 activation. *Science*, 347, aaa2630.
121. LOVATO, P., BRENDER, C., AGNHOLT, J., KELSEN, J., KALTOFT, K., SVEJGAARD, A., ERIKSEN, K. W., WOETMANN, A. & ØDUM, N. 2003. Constitutive STAT3 activation in intestinal T cells from patients with Crohn's disease. *J Biol Chem*, 278, 16777-81.
122. LOVELL, J. F., BILLEN, L. P., BINDNER, S., SHAMAS-DIN, A., FRADIN, C., LEBER, B. & ANDREWS, D. W. 2008. Membrane binding by tBid initiates an ordered series of events culminating in membrane permeabilization by Bax. *Cell*, 135, 1074-84.
123. LUM, J. J., BAUER, D. E., KONG, M., HARRIS, M. H., LI, C., LINDSTEN, T. & THOMPSON, C. B. 2005a. Growth factor regulation of autophagy and cell survival in the absence of apoptosis. *Cell*, 120, 237-48.
124. LUM, J. J., DEBERARDINIS, R. J. & THOMPSON, C. B. 2005b. Autophagy in metazoans: cell survival in the land of plenty. *Nat Rev Mol Cell Biol*, 6, 439-48.
125. LUND, P. K. & RIGBY, R. J. 2006. SOC-ing it to tumors: suppressors of cytokine signaling as tumor repressors. *Gastroenterology*, 131, 317-9.
126. MANDEL, J. S., BOND, J. H., CHURCH, T. R., SNOVER, D. C., BRADLEY, G. M., SCHUMAN, L. M. & EDERER, F. 1993. Reducing mortality from colorectal cancer by screening for fecal occult blood. Minnesota Colon Cancer Control Study. *N Engl J Med*, 328, 1365-71.
127. MATSUNAGA, K., SAITOH, T., TABATA, K., OMORI, H., SATOH, T., KUROTORI, N., MAEJIMA, I., SHIRAHAMA-NODA, K., ICHIMURA, T., ISOBE, T., AKIRA, S., NODA, T. & YOSHIMORI, T. 2009. Two Beclin 1-binding proteins, Atg14L and Rubicon, reciprocally regulate autophagy at different stages. *Nat Cell Biol*, 11, 385-96.
128. MATTHEWS, J. R., SANSOM, O. J. & CLARKE, A. R. 2011. Absolute requirement for STAT3 function in small-intestine crypt stem cell survival. *Cell Death Differ*, 18, 1934-43.
129. MENNI, C., JACKSON, M. A., PALLISTER, T., STEVES, C. J., SPECTOR, T. D. & VALDES, A. M. 2017. Gut microbiome diversity and high-fibre intake are related to lower long-term weight gain. *Int J Obes (Lond)*, 41, 1099-1105.

130. MERRITT, A. J., POTTEN, C. S., KEMP, C. J., HICKMAN, J. A., BALMAIN, A., LANE, D. P. & HALL, P. A. 1994. The role of p53 in spontaneous and radiation-induced apoptosis in the gastrointestinal tract of normal and p53-deficient mice. *Cancer Res*, 54, 614-7.
131. MERRITT, A. J., POTTEN, C. S., WATSON, A. J., LOH, D. Y., NAKAYAMA, K. & HICKMAN, J. A. 1995. Differential expression of bcl-2 in intestinal epithelia. Correlation with attenuation of apoptosis in colonic crypts and the incidence of colonic neoplasia. *J Cell Sci*, 108 (Pt 6), 2261-71.
132. MIYAMOTO, M., FUJITA, T., KIMURA, Y., MARUYAMA, M., HARADA, H., SUDO, Y., MIYATA, T. & TANIGUCHI, T. 1988. Regulated expression of a gene encoding a nuclear factor, IRF-1, that specifically binds to IFN-beta gene regulatory elements. *Cell*, 54, 903-13.
133. MIZUSHIMA, N. & KLIONSKY, D. J. 2007. Protein turnover via autophagy: implications for metabolism. *Annu Rev Nutr*, 27, 19-40.
134. MIZUSHIMA, N., LEVINE, B., CUERVO, A. M. & KLIONSKY, D. J. 2008. Autophagy fights disease through cellular self-digestion. *Nature*, 451, 1069-75.
135. MIZUSHIMA, N., YAMAMOTO, A., MATSUI, M., YOSHIMORI, T. & OHSUMI, Y. 2004. In vivo analysis of autophagy in response to nutrient starvation using transgenic mice expressing a fluorescent autophagosome marker. *Mol Biol Cell*, 15, 1101-11.
136. MIZUSHIMA, N. & YOSHIMORI, T. 2007. How to interpret LC3 immunoblotting. *Autophagy*, 3, 542-5.
137. MOGENSEN, T. H. 2009. Pathogen recognition and inflammatory signaling in innate immune defenses. *Clin Microbiol Rev*, 22, 240-73, Table of Contents.
138. MOGENSEN, T. H. & PALUDAN, S. R. 2005. Reading the viral signature by Toll-like receptors and other pattern recognition receptors. *J Mol Med (Berl)*, 83, 180-92.
139. MOUSAVINEZHAD, M., MAJDZADEH, R., AKBARI SARI, A., DELAVARI, A. & MOHTASHAM, F. 2016. The effectiveness of FOBT vs. FIT: A meta-analysis on colorectal cancer screening test. *Med J Islam Repub Iran*, 30, 366.
140. MUÑOZ, J., STANGE, D. E., SCHEPERS, A. G., VAN DE WETERING, M., KOO, B. K., ITZKOVITZ, S., VOLCKMANN, R., KUNG, K. S., KOSTER, J., RADULESCU, S., MYANT, K., VERSTEEG, R., SANSOM, O. J., VAN ES, J. H., BARKER, N., VAN OUDENAARDEN, A., MOHAMMED, S., HECK, A. J. & CLEVERS, H. 2012. The Lgr5 intestinal stem cell signature: robust expression of proposed quiescent '+4' cell markers. *EMBO J*, 31, 3079-91.

141. NAKATSU, G., ZHOU, H., WU, W.K.K., WONG, S.H., COKER, O.O., DAI, Z., LI, X., SZETO, C.H., SUGIMURA, N., LAM, T.Y., YU, A.C., WANG, X., CHEN, Z., WONG, M.C., NG, S.C., CHAN, M.T.V., CHAN, P.K.S., CHAN, F.K.L., SUNG, J.J. & YU, J. 2018. Alterations in Enteric Virome Are Associated With Colorectal Cancer and Survival Outcomes. *Gastroenterology*, 155 (2), 529-541.
142. NORMAN, J.M., HANDLEY, S.A., BALDRIDGE, M.T., DROIT, L., LIU, C.Y., KELLER, B.C., KAMBAL, A., MONACO, C.L., ZHAO, G., FLESHNER, P., STAPPENBECK, T.S., MCGOVERN, D.P., KESHAVARZIAN, A., MUTLU, E.A., SAUK, J., GEVERS, D., XAVIER, R.J., WANG, D., PARKES, M. & VIRGIN, H.W. 2015. Disease-specific alterations in the enteric virome in inflammatory bowel disease. *Cell*, 160 (3), 447-60.
143. OGURA, Y., BONEN, D. K., INOHARA, N., NICOLAE, D. L., CHEN, F. F., RAMOS, R., BRITTON, H., MORAN, T., KARALIUSKAS, R., DUERR, R. H., ACHKAR, J. P., BRANT, S. R., BAYLESS, T. M., KIRSCHNER, B. S., HANAUER, S. B., NUÑEZ, G. & CHO, J. H. 2001. A frameshift mutation in NOD2 associated with susceptibility to Crohn's disease. *Nature*, 411, 603-6.
144. ORABONA, C., GROHMANN, U., BELLADONNA, M. L., FALLARINO, F., VACCA, C., BIANCHI, R., BOZZA, S., VOLPI, C., SALOMON, B. L., FIORETTI, M. C., ROMANI, L. & PUC CETTI, P. 2004. CD28 induces immunostimulatory signals in dendritic cells via CD80 and CD86. *Nat Immunol*, 5, 1134-42.
145. ORHOLM, M., MUNKHOLM, P., LANGHOLZ, E., NIELSEN, O. H., SØRENSEN, T. I. & BINDER, V. 1991. Familial occurrence of inflammatory bowel disease. *N Engl J Med*, 324, 84-8.
146. OSHIMA, H., KOK, S. Y., NAKAYAMA, M., MURAKAMI, K., VOON, D. C., KIMURA, T. & OSHIMA, M. 2019. Stat3 is indispensable for damage-induced crypt regeneration but not for Wnt-driven intestinal tumorigenesis. *FASEB J*, 33, 1873-1886.
147. OSHIUMI, H., SASAI, M., SHIDA, K., FUJITA, T., MATSUMOTO, M. & SEYA, T. 2003. TIR-containing adapter molecule (TICAM)-2, a bridging adapter recruiting to toll-like receptor 4 TICAM-1 that induces interferon-beta. *J Biol Chem*, 278, 49751-62.
148. PARK, B. H., VOGELSTEIN, B. & KINZLER, K. W. 2001. Genetic disruption of PPARdelta decreases the tumorigenicity of human colon cancer cells. *Proc Natl Acad Sci U S A*, 98, 2598-603.
149. PARRA-BLANCO, A., GIMENO-GARCÍA, A. Z., QUINTERO, E., NICOLÁS, D., MORENO, S. G., JIMÉNEZ, A., HERNÁNDEZ-GUERRA, M., CARRILLO-PALAU,

- M., EISHI, Y. & LÓPEZ-BASTIDA, J. 2010. Diagnostic accuracy of immunochemical versus guaiac faecal occult blood tests for colorectal cancer screening. *J Gastroenterol*, 45, 703-12.
150. PARZYCH, K. R. & KLIONSKY, D. J. 2014. An overview of autophagy: morphology, mechanism, and regulation. *Antioxid Redox Signal*, 20, 460-73.
151. PATTINGRE, S., TASSA, A., QU, X., GARUTI, R., LIANG, X. H., MIZUSHIMA, N., PACKER, M., SCHNEIDER, M. D. & LEVINE, B. 2005. Bcl-2 antiapoptotic proteins inhibit Beclin 1-dependent autophagy. *Cell*, 122, 927-39.
152. PICKERT, G., NEUFERT, C., LEPPKES, M., ZHENG, Y., WITTKOPF, N., WARNTJEN, M., LEHR, H. A., HIRTH, S., WEIGMANN, B., WIRTZ, S., OUYANG, W., NEURATH, M. F. & BECKER, C. 2009. STAT3 links IL-22 signaling in intestinal epithelial cells to mucosal wound healing. *J Exp Med*, 206, 1465-72.
153. PIGNONE, M., CAMPBELL, M. K., CARR, C. & PHILLIPS, C. 2001. Meta-analysis of dietary restriction during fecal occult blood testing. *Eff Clin Pract*, 4, 150-6.
154. POTTEN, C. S. 1998. Stem cells in gastrointestinal epithelium: numbers, characteristics and death. *Philos Trans R Soc Lond B Biol Sci*, 353, 821-30.
155. POWRIE, F., LEACH, M. W., MAUZE, S., MENON, S., CADDLE, L. B. & COFFMAN, R. L. 1994. Inhibition of Th1 responses prevents inflammatory bowel disease in scid mice reconstituted with CD45RBhi CD4+ T cells. *Immunity*, 1, 553-62.
156. RAKOFF-NAHOUM, S., PAGLINO, J., ESLAMI-VARZANEH, F., EDBERG, S. & MEDZHITOV, R. 2004. Recognition of commensal microflora by toll-like receptors is required for intestinal homeostasis. *Cell*, 118, 229-41.
157. RAO, S., TORTOLA, L., PERLOT, T., WIRNSBERGER, G., NOVATCHKOVA, M., NITSCH, R., SYKACEK, P., FRANK, L., SCHRAMEK, D., KOMNENOVIC, V., SIGL, V., AUMAYR, K., SCHMAUSS, G., FELLNER, N., HANDSCHUH, S., GLÖSMANN, M., PASIERBEK, P., SCHLEDERER, M., RESCH, G. P., MA, Y., YANG, H., POPPER, H., KENNER, L., KROEMER, G. & PENNINGER, J. M. 2014. A dual role for autophagy in a murine model of lung cancer. *Nat Commun*, 5, 3056.
158. REICH, N., EVANS, B., LEVY, D., FAHEY, D., KNIGHT, E. & DARNELL, J. E. 1987. Interferon-induced transcription of a gene encoding a 15-kDa protein depends on an upstream enhancer element. *Proc Natl Acad Sci U S A*, 84, 6394-8.
159. REINECKER, H. C., STEFFEN, M., WITTHOEFT, T., PFLUEGER, I., SCHREIBER, S., MACDERMOTT, R. P. & RAEDLER, A. 1993. Enhanced secretion of tumour necrosis factor-alpha, IL-6, and IL-1 beta by isolated lamina propria mononuclear

- cells from patients with ulcerative colitis and Crohn's disease. *Clin Exp Immunol*, 94, 174-81.
160. REYES, A., SEMENKOVICH, N. P., WHITESON, K., ROHWER, F. & GORDON, J. I. 2012. Going viral: next-generation sequencing applied to phage populations in the human gut. *Nat Rev Microbiol*, 10, 607-17.
161. RIGBY, R. J., SIMMONS, J. G., GREENHALGH, C. J., ALEXANDER, W. S. & LUND, P. K. 2007. Suppressor of cytokine signaling 3 (SOCS3) limits damage-induced crypt hyper-proliferation and inflammation-associated tumorigenesis in the colon. *Oncogene*, 26, 4833-41.
162. ROBERTS, A. W., ROBB, L., RAKAR, S., HARTLEY, L., CLUSE, L., NICOLA, N. A., METCALF, D., HILTON, D. J. & ALEXANDER, W. S. 2001. Placental defects and embryonic lethality in mice lacking suppressor of cytokine signaling 3. *Proc Natl Acad Sci U S A*, 98, 9324-9.
163. ROSSI, A., KONTARAKIS, Z., GERRI, C., NOLTE, H., HÖLPER, S., KRÜGER, M. & STAINIER, D. Y. 2015a. Genetic compensation induced by deleterious mutations but not gene knockdowns. *Nature*, 524, 230-3.
164. ROSSI, O., MAGGIORE, L., NECCHI, F., KOEBERLING, O., MACLENNAN, C. A., SAUL, A. & GERKE, C. 2015b. Comparison of colorimetric assays with quantitative amino acid analysis for protein quantification of Generalized Modules for Membrane Antigens (GMMA). *Mol Biotechnol*, 57, 84-93.
165. ROUT, A. K., STRUB, M. P., PISZCZEK, G. & TJANDRA, N. 2014. Structure of transmembrane domain of lysosome-associated membrane protein type 2a (LAMP-2A) reveals key features for substrate specificity in chaperone-mediated autophagy. *J Biol Chem*, 289, 35111-23.
166. SAITO, T., HIRAI, R., LOO, Y. M., OWEN, D., JOHNSON, C. L., SINHA, S. C., AKIRA, S., FUJITA, T. & GALE, M. 2007. Regulation of innate antiviral defenses through a shared repressor domain in RIG-I and LGP2. *Proc Natl Acad Sci U S A*, 104, 582-7.
167. SANGIORGI, E. & CAPECCHI, M. R. 2008. Bmi1 is expressed in vivo in intestinal stem cells. *Nat Genet*, 40, 915-20.
168. SCHINDLER, C., SHUAI, K., PREZIOSO, V. R. & DARNELL, J. E. 1992. Interferon-dependent tyrosine phosphorylation of a latent cytoplasmic transcription factor. *Science*, 257, 809-13.

169. SCHNEIDER, W. M., CHEVILLOTTE, M. D. & RICE, C. M. 2014. Interferon-stimulated genes: a complex web of host defenses. *Annu Rev Immunol*, 32, 513-45.
170. SCHREUDERS, E. H., GROBBEE, E. J., SPAANDER, M. C. & KUIPERS, E. J. 2016. Advances in Fecal Tests for Colorectal Cancer Screening. *Curr Treat Options Gastroenterol*, 14, 152-62.
171. SEIF, F., KHOSHMIRSAFA, M., AAZAMI, H., MOHSENZADEGAN, M., SEDIGHI, G. & BAHAR, M. 2017. The role of JAK-STAT signaling pathway and its regulators in the fate of T helper cells. *Cell Commun Signal*, 15, 23.
172. SETH, R. B., SUN, L., EA, C. K. & CHEN, Z. J. 2005. Identification and characterization of MAVS, a mitochondrial antiviral signaling protein that activates NF-kappaB and IRF 3. *Cell*, 122, 669-82.
173. SHAW, E. J., SMITH, E. E., WHITTINGHAM-DOWD, J., HODGES, M. D., ELSE, K. J. & RIGBY, R. J. 2017. Intestinal epithelial suppressor of cytokine signaling 3 (SOCS3) impacts on mucosal homeostasis in a model of chronic inflammation. *Immun Inflamm Dis*, 5, 336-345.
174. SRINIVASAN, T., THAN, E. B., BU, P., TUNG, K. L., CHEN, K. Y., AUGENLICHT, L., LIPKIN, S. M. & SHEN, X. 2016. Notch signalling regulates asymmetric division and inter-conversion between *lgr5* and *bmi1* expressing intestinal stem cells. *Sci Rep*, 6, 26069.
175. STAMP, C., ZUPANIC, A., SACHDEVA, A., STOLL, E. A., SHANLEY, D. P., MATHERS, J. C., KIRKWOOD, T. B. L., HEER, R., SIMONS, B. D., TURNBULL, D. M. & GREAVES, L. C. 2018. Predominant Asymmetrical Stem Cell Fate Outcome Limits the Rate of Niche Succession in Human Colonic Crypts. *EBioMedicine*, 31, 166-173.
176. STROBER, W., FUSS, I. & MANNON, P. 2007. The fundamental basis of inflammatory bowel disease. *J Clin Invest*, 117, 514-21.
177. SUGIMOTO, K. 2008. Role of STAT3 in inflammatory bowel disease. *World J Gastroenterol*, 14, 5110-4.
178. SUN, L., WU, J., DU, F., CHEN, X. & CHEN, Z. J. 2013. Cyclic GMP-AMP synthase is a cytosolic DNA sensor that activates the type I interferon pathway. *Science*, 339, 786-91.
179. TAKAYAMA, O., YAMAMOTO, H., DAMDINSUREN, B., SUGITA, Y., NGAN, C. Y., XU, X., TSUJINO, T., TAKEMASA, I., IKEDA, M., SEKIMOTO, M., MATSUURA, N. & MONDEN, M. 2006. Expression of PPARdelta in multistage

- carcinogenesis of the colorectum: implications of malignant cancer morphology. *Br J Cancer*, 95, 889-95.
180. TAKEDA, K., KAISHO, T., YOSHIDA, N., TAKEDA, J., KISHIMOTO, T. & AKIRA, S. 1998. Stat3 activation is responsible for IL-6-dependent T cell proliferation through preventing apoptosis: generation and characterization of T cell-specific Stat3-deficient mice. *J Immunol*, 161, 4652-60.
 181. TAKEUCHI, O. & AKIRA, S. 2010. Pattern recognition receptors and inflammation. *Cell*, 140, 805-20.
 182. TANCRÈDE, C. 1992. Role of human microflora in health and disease. *Eur J Clin Microbiol Infect Dis*, 11, 1012-5.
 183. TANG, C. H., ZUNDELL, J. A., RANATUNGA, S., LIN, C., NEFEDOVA, Y., DEL VALLE, J. R. & HU, C. C. 2016. Agonist-Mediated Activation of STING Induces Apoptosis in Malignant B Cells. *Cancer Res*, 76, 2137-52.
 184. TANG, D., KANG, R., COYNE, C. B., ZEH, H. J. & LOTZE, M. T. 2012. PAMPs and DAMPs: signal 0s that spur autophagy and immunity. *Immunol Rev*, 249, 158-75.
 185. TANG, E. D. & WANG, C. Y. 2009. MAVS self-association mediates antiviral innate immune signaling. *J Virol*, 83, 3420-8.
 186. TANIDA, I., UENO, T. & KOMINAMI, E. 2008. LC3 and Autophagy. *Methods Mol Biol*, 445, 77-88.
 187. TEISSIER, T. & BOULANGER, É. 2019. The receptor for advanced glycation end-products (RAGE) is an important pattern recognition receptor (PRR) for inflammaging. *Biogerontology*, 20, 279-301.
 188. TERLECKY, S. R. & DICE, J. F. 1993. Polypeptide import and degradation by isolated lysosomes. *J Biol Chem*, 268, 23490-5.
 189. TONDELEIR, D., LAMBRECHTS, A., MÜLLER, M., JONCKHEERE, V., DOLL, T., VANDAMME, D., BAKKALI, K., WATERSCHOOT, D., LEMAISTRE, M., DEBEIR, O., DECAESTECKER, C., HINZ, B., STAES, A., TIMMERMAN, E., COLAERT, N., GEVAERT, K., VANDEKERCKHOVE, J. & AMPE, C. 2012. Cells lacking β -actin are genetically reprogrammed and maintain conditional migratory capacity. *Mol Cell Proteomics*, 11, 255-71.
 190. TSUKADA, M. & OHSUMI, Y. 1993. Isolation and characterization of autophagy-defective mutants of *Saccharomyces cerevisiae*. *FEBS Lett*, 333, 169-74.
 191. UT Southwestern Medical Center (2019) Mutagenix; a database of mutations and phenotypes induced by ENU [online] available at

https://mutagenetix.utsouthwestern.edu/phenotypic/phenotypic_rec.cfm?pk=234

[accessed October 2019]

192. UZÉ, G., LUTFALLA, G. & GRESSER, I. 1990. Genetic transfer of a functional human interferon alpha receptor into mouse cells: cloning and expression of its cDNA. *Cell*, 60, 225-34.
193. VELTKAMP, C., TONKONOGY, S. L., DE JONG, Y. P., ALBRIGHT, C., GRENTHER, W. B., BALISH, E., TERHORST, C. & SARTOR, R. B. 2001. Continuous stimulation by normal luminal bacteria is essential for the development and perpetuation of colitis in Tg(epsilon26) mice. *Gastroenterology*, 120, 900-13.
194. Wilks S. Morbid appearances in the intestines of Miss Bankes. *London Medical Gazette* 1859; 2:264-5.
195. WILLETT, W. C., STAMPFER, M. J., COLDITZ, G. A., ROSNER, B. A. & SPEIZER, F. E. 1990. Relation of meat, fat, and fiber intake to the risk of colon cancer in a prospective study among women. *N Engl J Med*, 323, 1664-72.
196. WILLIAMS, L., ARMSTRONG, M. J., ARMSTRONG, M., FINAN, P., SAGAR, P. & BURKE, D. 2007. The effect of faecal diversion on human ileum. *Gut*, 56, 796-801.
197. WINSLET, M. C., DROLC, Z., ALLAN, A. & KEIGHLEY, M. R. 1991. Assessment of the defunctioning efficiency of the loop ileostomy. *Dis Colon Rectum*, 34, 699-703.
198. World Cancer Research Fund and American Institute for Cancer Research (2017); *Diet, Nutrition, Physical Activity, and Colorectal Cancer*. American Institute for Cancer Research Continuous Update Project, pp.5.
199. World Health Organization (2018) *Cancer Today* [online] available at http://gco.iarc.fr/today/online-analysis-table?v=2018&mode=cancer&mode_population=continents&population=900&populations=900&key=asr&sex=0&cancer=39&type=0&statistic=5&prevalence=0&population_group=0&ages_group%5B%5D=0&ages_group%5B%5D=17&nb_items=5&group_cancer=1&include_nmsc=1&include_nmsc_other=1 [accessed October 2019]
200. World Health Organization (2018) *Cancer* [online] available at <https://www.who.int/news-room/fact-sheets/detail/cancer> [accessed May 2020]
201. WU, J., SUN, L., CHEN, X., DU, F., SHI, H., CHEN, C. & CHEN, Z. J. 2013. Cyclic GMP-AMP is an endogenous second messenger in innate immune signaling by cytosolic DNA. *Science*, 339, 826-30.
202. XAVIER, R. J. & PODOLSKY, D. K. 2007. Unravelling the pathogenesis of inflammatory bowel disease. *Nature*, 448, 427-34.

203. YAMASHITA, M., CHATTOPADHYAY, S., FENSTERL, V., SAIKIA, P., WETZEL, J. L. & SEN, G. C. 2012. Epidermal growth factor receptor is essential for Toll-like receptor 3 signaling. *Sci Signal*, 5, ra50.
204. YAN, K. S., CHIA, L. A., LI, X., OOTANI, A., SU, J., LEE, J. Y., SU, N., LUO, Y., HEILSHORN, S. C., AMIEVA, M. R., SANGIORGI, E., CAPECCHI, M. R. & KUO, C. J. 2012. The intestinal stem cell markers Bmi1 and Lgr5 identify two functionally distinct populations. *Proc Natl Acad Sci U S A*, 109, 466-71.
205. YANG, H. E., LI, Y., NISHIMURA, A., JHENG, H. F., YULIANA, A., KITANO-OHUE, R., NOMURA, W., TAKAHASHI, N., KIM, C. S., YU, R., KITAMURA, N., PARK, S. B., KISHINO, S., OGAWA, J., KAWADA, T. & GOTO, T. 2017. Synthesized enone fatty acids resembling metabolites from gut microbiota suppress macrophage-mediated inflammation in adipocytes. *Mol Nutr Food Res*, 61.
206. YASUKAWA, H., SASAKI, A. & YOSHIMURA, A. 2000. Negative regulation of cytokine signaling pathways. *Annu Rev Immunol*, 18, 143-64.
207. YONEYAMA, M., KIKUCHI, M., NATSUKAWA, T., SHINOBU, N., IMAIZUMI, T., MIYAGISHI, M., TAIRA, K., AKIRA, S. & FUJITA, T. 2004. The RNA helicase RIG-I has an essential function in double-stranded RNA-induced innate antiviral responses. *Nat Immunol*, 5, 730-7.
208. YONEYAMA, M., SUHARA, W., FUKUHARA, Y., FUKUDA, M., NISHIDA, E. & FUJITA, T. 1998. Direct triggering of the type I interferon system by virus infection: activation of a transcription factor complex containing IRF-3 and CBP/p300. *EMBO J*, 17, 1087-95.
209. YORIMITSU, T. & KLIONSKY, D. J. 2005. Autophagy: molecular machinery for self-eating. *Cell Death Differ*, 12 Suppl 2, 1542-52.
210. YOSHIURA, S., OHTSUKA, T., TAKENAKA, Y., NAGAHARA, H., YOSHIKAWA, K. & KAGEYAMA, R. 2007. Ultradian oscillations of Stat, Smad, and Hes1 expression in response to serum. *Proc Natl Acad Sci U S A*, 104, 11292-7.
211. YU, D., NGUYEN, S. M., YANG, Y., XU, W., CAI, H., WU, J., CAI, Q., LONG, J., ZHENG, W. & SHU, X. O. 2021. Long-term diet quality is associated with gut microbiome diversity and composition among urban Chinese adults. *Am J Clin Nutr*.
212. YUE, Z., JIN, S., YANG, C., LEVINE, A. J. & HEINTZ, N. 2003. Beclin 1, an autophagy gene essential for early embryonic development, is a haploinsufficient tumor suppressor. *Proc Natl Acad Sci U S A*, 100, 15077-82.

213. ZHANG, C., SHANG, G., GUI, X., ZHANG, X., BAI, X. C. & CHEN, Z. J. 2019. Structural basis of STING binding with and phosphorylation by TBK1. *Nature*, 567, 394-398.
214. ZHANG, J. M. & AN, J. 2007. Cytokines, inflammation, and pain. *Int Anesthesiol Clin*, 45, 27-37.
215. ZHANG, X., SHI, H., WU, J., SUN, L., CHEN, C. & CHEN, Z. J. 2013. Cyclic GMP-AMP containing mixed phosphodiester linkages is an endogenous high-affinity ligand for STING. *Mol Cell*, 51, 226-35.
216. ZHAO, B., SHU, C., GAO, X., SANKARAN, B., DU, F., SHELTON, C. L., HERR, A. B., JI, J. Y. & LI, P. 2016. Structural basis for concerted recruitment and activation of IRF-3 by innate immune adaptor proteins. *Proc Natl Acad Sci U S A*, 113, E3403-12.
217. ZIERHUT, C. & FUNABIKI, H. 2020. Regulation and Consequences of cGAS Activation by Self-DNA. *Trends Cell Biol*, 30, 594-605.